QATAR UNIVERSITY

COLLEGE OF ENGINEERING

SUSTAINABLE DESIGN AND ANALYSIS FOR GASOLINE PRODUCED FROM

GTL AND MTG PROCESSES: PROCESS SIMULATION, TECHNO-ECONOMIC,

AND ENVIRONMENT ASSESSMENT

BY

NOUR MUSTAFA YACOUB NASR

A Thesis Submitted to

the College of Engineering

in Partial Fulfillment of the Requirements for the Degree of

[Master of Science in Environmental Engineering]

January   2023

# COMMITTEE PAGE

The members of the Committee approve the Thesis of
Nour Mustafa Yacoub Nasir defended on 15/11/2022.

_____
Prof. Saad Al-Sobhi
Thesis/Dissertation Supervisor


_____
Prof. Fares Almomani
Co-Supervisor


_____
Dr. Sabla Yahya Ali Alnory
Committee Member


Approved:

_____
Khalid Kamal Naji, Dean, College of Engineering

# ABSTRACT

NASR, NOOR, M., Masters : January : [2023:], Masters of Science in Environmental Engineering

Title: SUSTAINABLE DESIGN AND ANALYSIS FOR GASOLINE PRODUCED FROM GTL AND MTG PROCESSES: PROCESS SIMULATION, TECHNO-ECONOMIC, AND ENVIRONMENT ASSESSMENT

Supervisor of Thesis: Prof. Saad Al-Sobhi.

The global energy demand will continue to expand as the world population grows. Energy and environmental concerns are closely related since it is nearly difficult to create, transfer, or consume energy without having a significant environmental impact. Thus, the use of clean and effective energy resources such as Natural gas (NG) shows less environmental impact, contributes to solving the global warming problem and reducing the emissions compared to the other conventional fossil fuels (Coal and Oil).

This thesis investigates the comparative analysis of gas to liquid (GTL) and methanol to gasoline (MTG) processes. The focus is to optimize the production of gasoline from both processes. Aspen HYSYS V.11 simulation software was used to simulate the MTG and GTL low and high-temperature configurations.

An equal amount of NG at 15372.37 Tonne/d is used in all cases. After performing the steady-state simulation, a sensitivity analysis was performed on the GTL process to maximize the gasoline production yield at different chain growth probability ($\alpha$) for both high Fischer Tropsch (HTFT) and low Fischer Tropsch (LTFT) processes. Moreover, the simulated flowsheets were examined from an environmental, and economic point of view . Results reveled that the maximum gasoline production was

achieved at $\alpha = 0.78$ for HTFT and $\alpha = 0.88$ for LTFT.

The study findings demonstrate a higher gasoline production from the MTG plant of 5345 Tonne/d compared 4798 Tonne/d from HTFT, whereas 2896 Tonne/d was produced from LTFT plant. In addition, the economic analysis revealed that the net profit per product for the MTG process is greater, at $1345/tonne of product compared to $981/tonne of product form the LTFT and $879/Tonne of product form the HTFT. Similarly, the $CO_2$ emissions/Tonne of product from the MTG plant was lower with 0.48 tons of $CO_{2\ equivelent}$/tonne of product compared with 1.76 and 1.50 tons of $CO_{2\ equivelent}$/product from LT-FT and HTFT. Moreover, the capital cost of LTFT, HTFT, and MTG were estimated as 74.7 million USD, 85.5 million USD and 109.2 million USD respectively. Moreover, the operating cost were valued as79.6 million USD, 102.5 million USD, and 47.8 million USD respectively.

# DEDICATION

*This thesis is dedicated to my parents, sisters, nephews and niece for their endless*

*support, love and encouraging.*

*To all my professors who have teach, support, guide, me and set a great example for*

*me to follow.*

# ACKNOWLEDGMENTS

# TABLE OF CONTENTS

# LIST OF TABLES

# LIST OF FIGURES

# Chapter 1 : Introduction

## 1.1. Natural gas Background

The global energy demand will continue to rise as the world increases and poverty decreases, according to the International energy agency (IEA) annual forecasts, The IEA has estimated that by 2040 the global population is projected to increase to over 9.7 billion pushing up the energy demand fourfold in reference to the recent amount [1]. Since it is almost impossible to generate, transport, or consume energy without having a major environmental effect, energy and environmental issues are inextricably linked. Air pollution, climate change, water pollution, thermal pollution, and solid waste disposal are all environmental issues directly related to energy production and use. With this growth in energy demand, the search for a cleaner energy source to minimize the environmental impacts is crucial [2].

Natural Gas (NG) emits 50 to 60 percent less carbon dioxide ($CO_2$) than other fossil fuels when burned in a new modern natural gas power plant compared to emissions from a conventional new coal power plant [1]. Table 1-1 represents the top reserves, production, and consumption countries of natural gas. Comparing the tailpipe emissions, NG emits 15 to 20% less heat-trapping gases than gasoline in today 's average vehicle [2]. In addition to high caloric value the availability, small environmental footprint, and accessibility allowed the NG to overtake other commercial fossil fuels. According to BP Worlds Energy, the global share of NG in 2019 was set at 24%, which is about 72% of global oil demand, 88% of coal used, and 1.5 folds higher than the combined renewable, hydro, and nuclear energy production as presented Figure 1-1 [3]. Oil is still leading the energy demand with 33%, while coal is 27%, and NG with 24%. However, there was a 5% decrease in the world NG demand

in 2020 due to the COVID-19 crisis, but the global NG consumption is estimated to grow with a rate of 0.8% from 2022-2025. Furthermore, following Russia's invasion of Ukraine NG demand has decline by 0.5% in 2022, before increasing gradually over the next years to reach 1.5% in 2025 [4]. Moreover, in 2020 the globe's primary energy production was estimated as 88391 barrels oil/day [5], 3853.7 billion cubic meters NG [6], 159.61 Exajoules  coal [5], 6475 MW from renewable [7], 4369 TWh from hydropower [8], and 2553 TWh from nuclear energy [9]. In 2020 the Globe's total NG proved reserves amounted to 188.1 Trillion cubic meters and production amounted to 3853.7 billion cubic meters. Moreover, the world's NG consumption was about 3822.8 billion cubic meters [6], the consumption was lower by 75 billion cubic meters compared to 2019 due to COVID-19 [10]. However, the NG consumption increase by 4.6% in 2021 [11].

Table 1-1: The top Natural Gas reserves, production, and consumption countries in the world [3].

| Country | Reserves<br>Size [Trillion cubic feet] | Production<br>Size [Billion cubic meters] | Consumption<br>Size [Billion cubic meters] |
|---|---|---|---|
| Russian | 1340.5 | 679 | 444.3 |
| Iran | 1130.7 | 244.2 | 223.6 |
| Qatar | 871.6 | 178.1 | 41.1 |
| Turkmenistan | 688.1 | 63.1 | 31.5 |
| United States | 454.6 | 920.9 | 846.6 |
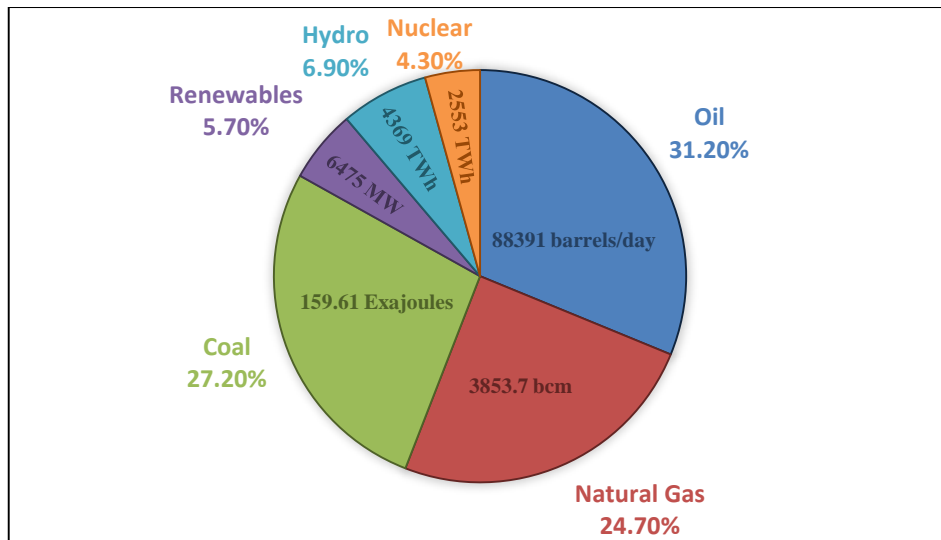
Figure 1-1:World primary source of energy in 2020 [5]–[9].

Storage and transportation are considered the main barriers to the production and utilization of NG on a large scale. Therefore, different technologies such as liquefied natural gas (LNG), Gas to hydrates conversion (GTH), compressed natural gas (CNG), natural gas liquid (NGL), and Gas to liquid (GTL) were employed to enable easy transportation of NG to different end users globally [12].

The liquefaction of NG reduces the volume by a factor of 600, making the production and transportation of LNG an attractive alternative and most feasible way of transporting over long distances [13]. On the other hand, GTL is proving to be one of the most significant innovations in the oil and gas industry in recent years. The method has made it possible to profit from NG, and businesses worldwide are adopting it for various reasons, including environmental, political, and financial.

Recently, there was growing attention to continue investing in GTL technology among other major energy-associated industries [14]. The conversion of gas to liquids (GTL) through the Fischer-Tropsch (FT) route to monetize stranded gas has gotten much attention. The use of GTL technology started in the middle of the 20th century,

3

and nowadays it stands on a strong footing of precise, intensive knowledge and industrial expertise. The FT technology involves rearranging carbon and hydrogen molecules to create a molten, heavier hydrocarbon molecule like Naphtha, Diesel, Wax, Gasoline, LPG, and other highly valuable products [15].

The production of these high fuel values involves the pretreatment stage where impurities such as Sulfides, Mercaptans and Mercury are removed from NG. Then the NG passed through three main unit, which is the reforming of NG to syngas ($H_2$/CO), Fischer Tropsch conversion and finally the upgrading of synthetic crude to yield product by different processes [16] will be discussed in detail in the next chapters.

Based on the information discussion, Gasoline is a petroleum-derived liquid that is used as a transportation fuel and a liquid fuel for industrial uses as cleaner drive fuel [17].

### 1.1.1. Gas to liquid (GTL) Background

Hans Tropsch and Franz Fischer German scientists at the Kaiser Wilhem Institute for Coal Research, which was founded in 1913 in Germany. They wanted to generate hydrocarbon (HC) from coal-derived syngas, However, it wasn't until the 1920s that it began to provide results [18]. Their goal was to meet the necessary demand for transportation fuel. The utilization of coal gasification resulted in a production of 600,000 tons per year [19]. Since the 1980s, there has been a resurgence in interest in FTS, owing to the desire for cleaner fuel. Most of oil corporations are currently contemplating, developing, or using Fischer-Tropsch Synthesis-based systems to convert natural gas into liquid yield [20]. NG has an attractive ability to reduce environmental impacts compared to other fossil fuels like coal and oil. Different processes such as gas to liquid (GTL) (Figure 1-2), have gotten a lot of interest in recent years because of their capacity to create a wide range of high-value products

that are sulfur-free. On a global scale. There are now five commercial-scale GTL units in operation as represented in Table 1-2. Four of the five plants were built in Qatar or South Africa. Qatar has the world's third-largest natural gas reserves, which is a natural player in the GTL industry, and it has recently been a focal point for the construction of next generation GTL facilities. The world largest GTL plant is the Pearl GTL in Qatar with a capacity of 260,000 barrels.

Table 1-2: World Gas to Liquid operating plant [21].

| Plant Name | Country | Capacity (bbl/d) | Start operation |
| --- | --- | --- | --- |
| Mossel Bay | South Africa | 36000 | 1992 |
| Bintulu | Malaysia | 14700 | 1993 |
| Oryx | Qatar | 34000 | 2007 |
| Pearl | Qatar | 140000 | 2011 |
| Escravos | Nigeria | 33000 | End of 2014 |

The outbreak of COVID-19 has resulted in a negative impact on the GTL demand globally, where the growth decreased by 27% in 2020. In addition, the GTL market is expected to grow by 2.97 billion USD from 2022 to 2026 with a compound annual growth rate (CAGR) of 4.58% [22]. The increase in CAGR related to the future growth and market demand to return to the pre-pandemic levels is connected to the ending of the pandemic crisis.

### 1.1.2. Methanol to gasoline (MTG) Background

The synthesis of hydrocarbons from methanol over the synthetic zeolite ZSM-5 was found by accident by Mobil scientists working on unrelated studies in the 1970s. Mobil Chemical in Edison, New Jersey, was trying to convert methanol to ethylene oxide, while Mobil Oil's Central Research Laboratory in Princeton was trying to methylate isobutene using methanol in the presence of ZSM-5. Neither reaction went

as planned, resulting in the formation of light olefins, which are then transformed into gasoline. As a result, the MTG process was discovered by chance [23]. MTG is a new method of producing fuel by converting methanol to gasoline, with gasoline accounting for 87% of the product weight, 13.6% as LPG and 1.4% fuel gas [24].
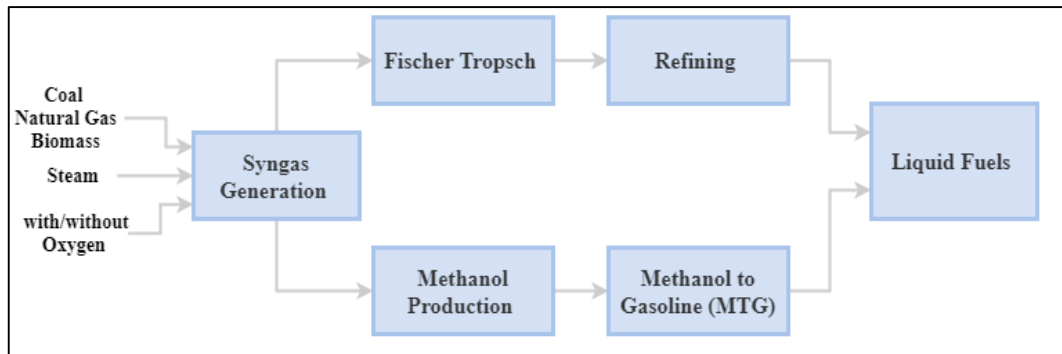


Figure 1-2: Gasoline production through Gas-to-Liquid and Methanol-to-Liquid.

Global Methanol demand has been increasing steadily in the past years from over 5 MMT (million metric tons) in 1975 to around 110 MMT in 2018 [25]. Moreover, the demand in 2020 decreased to 83.8 MMT due to the spread of COVID-19, China accounts for 63% of the methanol consumed in 2020. Furthermore in 2021, the worldwide methanol market growth from 35.3 billion USD in 2021 to 54.6 billion USD in 2030 with an CAGR of 5.03% between 2022 to 2030 [26], [27]. ExxonMobil's in Qatar has proven the MTG capacity to be increased up to 15 thousand barrels per day (KBD). Methanol has been used to derive the different types of products such as gasoline, formaldehyde, acetic acid, and other derivatives as shown in Figure 1-3.
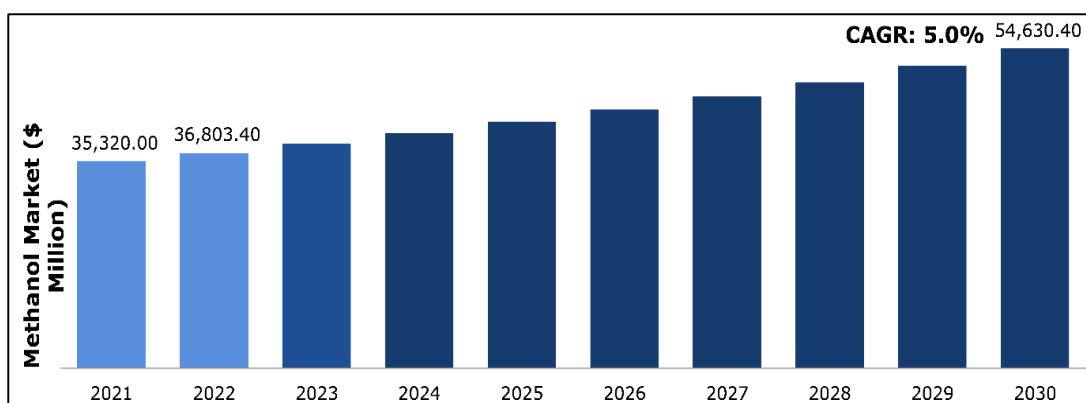
Figure 1-3: Global Methanol demand between the period of 2021 to 2030 [28].

The supply of MTG is connected to the availability of NG, and due to the pandemic crisis, which lead limited drilling and productions of the NG.

Methanol to gasoline is generated from different types of raw materials, natural gas, coal, and biomass. Moreover, around 87 wt% of the methanol produced from natural gas will be converted to gasoline [24]. In addition, there are presently 90 global methanol plants qualified to produce 110 MMT of methanol yearly [29]. Methanex Corporation is the largest world producer and seller the production sites are placed in Chile, New-Zealand, The United States, Egypt, and Trinidad [30].

## 1.2. Thesis Objective

The aforementioned background analysis reveals the importance of GTL (HTFT and LTFT) and MTG processes to the world energy sector. Although these processes are already in operation there still needs to develop a tool to optimize and improve efficiency as well as investigate the techno- economic, environmental and sustainability aspects of these processes. Therefore, this thesis focuses on optimizing and discovering strategies for improving gasoline yield through GTL (HTFT and LTFT) and MTG processes derived from natural gas. The aim is to raise the value of NG resources by identifying possible added- value products for future investments, to

7

develop simulation of these processes that would be used as tools to increase the gasoline yield, to evaluate the economic benefits from GTL (HTFT and LTFT) and MTG including capital and operating cost, total annual cost (TAC), net profit, and carbon emissions and to address the environmental consequences of such processes with considerations of the economic analysis and mitigation strategies. Lastly, the energy management and optimization using heat integration technique was developed for the proposed processes to minimize the total energy demand.

## 1.3. Thesis Structure

The structure of this thesis starts with the following sequence:

1- Thesis Abstract.

2- Chapter 1 Introduction and historical background on NG, MTG processes.

3- Chapter 2 Processes description.

4- Chapter 3 Literature Review.

5- Chapter 4 Methodology and procedures.

6- Chapter 5 is Process simulation.

7- Chapter 6 Economic evaluation.

8- Chapter 7 addressee the environmental analysis, an economic analysis, and mitigation strategies.

9- Chapter 8 energy demand management and optimization.

10- Chapter 9 conclusion and recommendation for future work.

# Chapter 2 : Process Description

## 2.1. Gas to Liquid (GTL) Process

As illustrated in Figure 2-1 The block flow diagrams (BFDs) corresponding to each block are described in the related plant sections. The reforming unit receives natural gas oxygen, and steam, which is processed to generate syngas, wastewater, and carbon dioxide. Before being fed into Fischer Tropsch production unit, the syngas mixture was adjusted to a 2:1 ratio of CO and $H_2$. In FT section, syngas is processed to produce a wide range of hydrocarbons. Hydrocarbons are subsequently fed into the cracking section, where it is further processed to generate gasoline, LPG, Diesel, and wax.
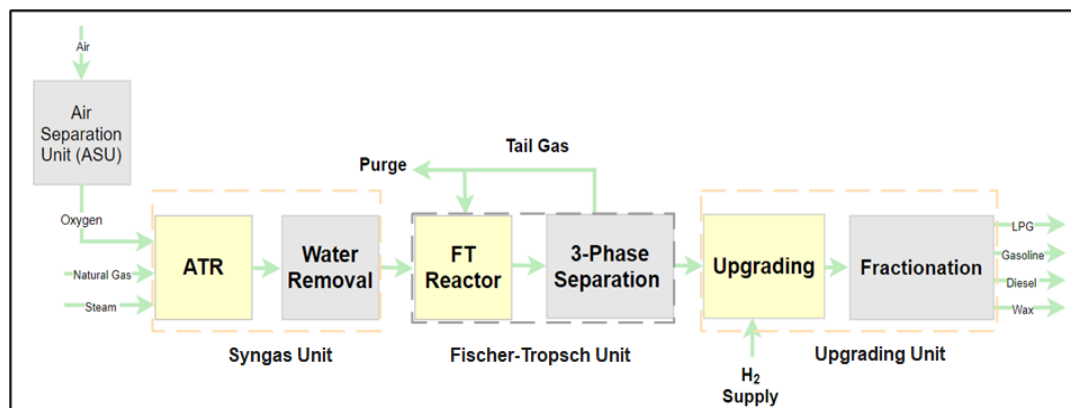


Figure 2-1: Gas to liquid Block flow-diagram.

There are several possible process pathways and combinations within each of these three components. The sections that follow will detail these alternatives, their primary features, and their uses.

## 2.1.1. Reforming unit in GTL

Synthesis gas, commonly known as syngas, is a combination of hydrogen and carbon monoxide that is utilized in the creation of a variety of compounds [31]. It is the

first and most important phase of the GTL process. Natural gas is turned into synthesis gas, which is a combination of hydrogen and carbon monoxide. The preparation of synthesis gas accounts for 50–75 percent of the total cost of capital [32]. The predominant component of natural gas feed is methane, but ethane, propane, and butane are also commonly present. A pre-reformer is frequently used as a preliminary step in the manufacture of syngas to prevent these heavier hydrocarbons from cracking and producing olefins in the reformer [33]. A pre-reformer is an adiabatic fixed bed reactor that uses a highly active nickel catalyst for steam reforming. Natural gas and steam are heated to 350-550°C before being supplied to the pre-reformer, which converts any hydrocarbons with more than one carbon atom in the chain to hydrogen and carbon monoxide as described in equation (1) [34]. The reactor is considered to be adiabatic in this work scenario, with the feed entering at 455°C [33] the reaction strategy is as follows, methanation and shift reactions, as detailed in equations (2) and (3) respectively, occur in addition to the cracking of heavier hydrocarbons. In the pre-reformer, these processes should reach equilibrium [35].

$$C_nH_m + nH_2O \leftrightarrow nCO + \left(n + \frac{m}{2}\right)H_2 \qquad \begin{array}{l} n \geq 2 \\ m \geq 3 \end{array} \qquad (1)$$

$$CO + 3H_2 \leftrightarrow CH_4 + H_2O \qquad (2)$$

$$CO + H_2O \leftrightarrow H_2 + CO_2 \qquad (3)$$
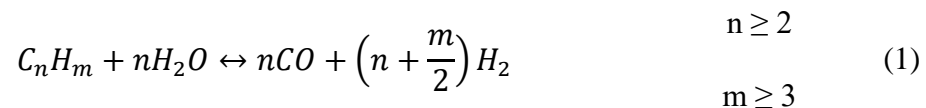
Natural gas, is converted to synthesis gas in a reformer using either steam methane reforming (SMR), partial oxidation (POX), or auto-thermal reformer (ATR) as discussed below in equations (4-(8) [36], [37].

### 2.1.1.1. Steam Methane Reforming (SMR):

The SMR as illustrated in Figure 2-2 is a catalytic method that involves reacting low-boiling hydrocarbons or NG with steam. For several years, this reactor has been used

to generate hydrogen fuel. As demonstrated in the endothermic reaction (4), the process involves the manufacture of synthetic gas by reforming natural gas in a catalytic process to create CO and $H_2$ [38]. The endothermic SMR reaction required a high ratio of $H_2O/CH_4$ around 3, a temperature in the range of 800-900 $^oC$ and a pressure in the range of 15-30 bar to achieve higher methane conversion [39].

$$CH_4 + H_2O \leftrightarrow CO + 3H_2 \tag{4}$$

SMR has two major advantages: it has vast industry experience, and it does not require expensive oxygen [40]. It does, however, generate syngas with an $H_2/CO$ ratio of 3-5. SMR is not suitable for this process since GTL production requires a ratio of roughly 2 [41].
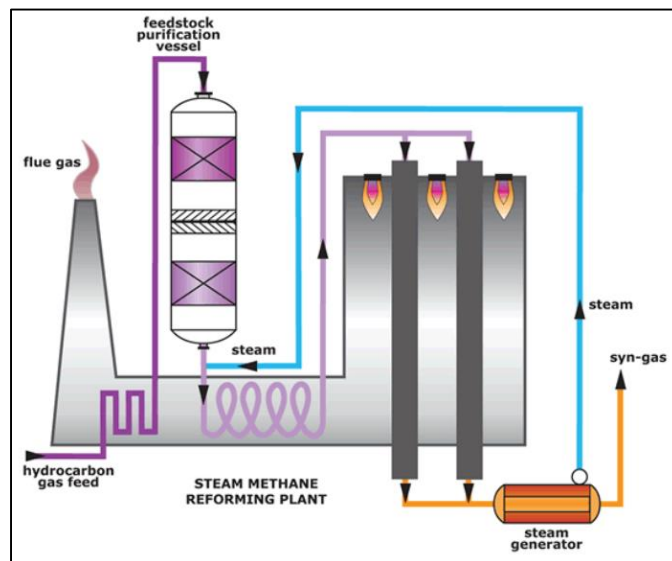


Figure 2-2: Illustration of steam methane reformer [35].

### 2.1.1.2. The partial oxidation (POX) process:

The POX as shown in Figure 2-3 has been utilized for nearly a century in the synthesis of syngas and the production of other variable products such as ammonia. The syngas is produced in POX with or without catalyst at a temperature ranging from 600-

900 °C, and 1 bar. The reaction between methane and oxygen, in POX reactor, varies with the air-to-fuel ratio as shown in equation (5) [42] and produces a synthetic gas of 1-1.8 or lower of $H_2/CO$ [43]. In addition, to the low syngas ratio and the requirement for a scrubber, POX consumes more oxygen than ATR [41].

$$CH_4 + \frac{1}{2}O_2 \leftrightarrow CO + 2H_2 \qquad (5)$$
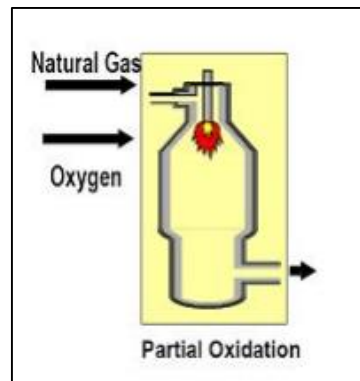


Figure 2-3:Illustration of partial oxidation reformer  [35].

### 2.1.1.3. Auto-thermal Reforming (ATR):

The ATR is an adiabatic reformer that was developed to enhance the reliability and the efficiency of the FT reaction intensified with SMR and POX. It is considered the most economical and attractive technology today for large FT applications [44], [45].

As shown in Figure 2-4, the ATR is separated into three primary sections: a burner section, a combustion section, and a catalyst bed [46]. Pre-reformed NG and oxygen enter the burner zone and is burnt with a sub-stoichiometric flame [46]. In the combustion unit, a portion of the methane is partly oxidized, and another portion has entirely combusted this oxidation shown in Equation (6). As stated in Equation (7), the

partial oxidation process and methane combustion are exothermic reactions, and the heat emitted acts as an energy source for the endothermic steam reforming reaction happening in the catalytic bed [47]. The ability to provide heat for the endothermic reactions by internal combustion of a part of the feed, causing the reforming reaction to occur "automatically," has given the process its name [35]. In addition to the steam reforming process, as stated in Equation (8), the shift reaction reaches equilibrium in the catalytic bed. Nickel is frequently the chosen catalyst in the other reformer applications discussed thus far when steam methane reforming is present, and this is also true for the ATR [35].

$$CH_4 + 1.5\ O_2 \leftrightarrow CO + 2H_2 \qquad\qquad (6)$$

$$CH_4 + H_2O \leftrightarrow CO + 3H_2 \qquad\qquad (7)$$

$$CO + H_2O \leftrightarrow CO_2 + H_2 \qquad\qquad (8)$$
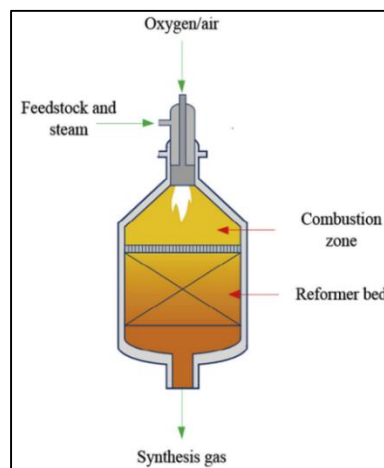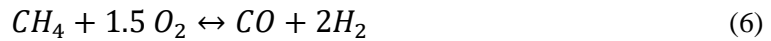


Figure 2-4: Illustration of auto-thermal reformer [48].

In addition, among all the reformer reactors to achieve the desired $H_2/CO$ value of 2 ATR has been selected as the more efficient in generating syngas. It is the most appropriate option for the large scale [40], [49].

### 2.1.2. Fischer- Tropsch synthesis unit

Fischer Tropsch was established more than 90 years ago by the German Chemists, Hans Tropsch and Franz Fischer [50]. It is considered the heart of the GTL method, it is known as a polymerization carbon-chain building up method to form a longer liquid, gaseous and solid hydrocarbon product [49]. A wide range of clean fuel products can be produced through the FT process as presented in Table 2-1 using a suitable catalyst [51].

Table 2-1: Fischer-Tropsch products.

| Carbon Number | Group name |
|---|---|
| $C_1$-$C_2$ | Synthetic natural gas (SNG) |
| $C_2$-$C_4$ | Liquefied petroleum gas (LPG) |
| $C_5$-$C_{11}$ | Gasoline/Naphtha |
| $C_{12}$-$C_{20}$ | Diesel |
| $C_{21+}$ | Soft wax |

This process is highly exothermic where synthetic gas is catalytically converted into long-chained hydrocarbons in the Fischer Tropsch reactor by a polymerization process in which methyl groups are successively added to the chain. This can be shown by the generalized reactions shown in Equations (9-(11) [52], [53], In addition to this reaction, if iron is used as the catalyst, the water gas shift reaction, illustrated in Equation (12), occurs [54], cobalt catalysts, on the other hand, have a minor effect, resulting in higher hydrocarbon yields. As a result, cobalt is a better catalyst for FTS [49].

Due to the FT reaction natural it is important to avoid the rise in the temperature to achieve the following [55]

- Maintain steady reaction conditions.

- Avoid the production of light hydrocarbons.

- Prevent the drop-in activity due to catalyst sintering.

$$1- \text{Paraffines} \qquad nCO + (2n + 1)\, H_2 \leftrightarrow C_nH_{2n+2} + nH_2O \qquad (9)$$

$$2- \text{Olefins} \qquad nCO + 2n\, H_2 \leftrightarrow C_nH_{2n} + nH_2O \qquad (10)$$

$$3- \text{Alcohol} \qquad nCO + 2nH_2 \leftrightarrow C_nH_{2n} + (n - 1)H_2O \qquad (11)$$

$$\text{WGS:} \qquad nCO + H_2O \leftrightarrow CO_2 + H_2 \qquad (12)$$
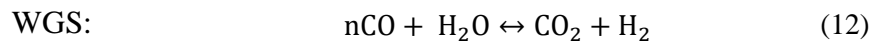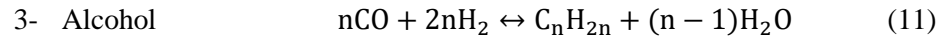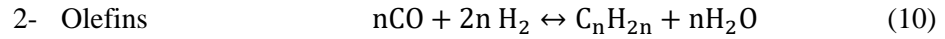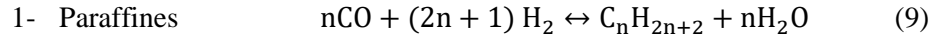
Fischer-Tropsch Synthesis:

Moreover, $\alpha$ value is known as the probability of chain growth is used to determine the carbon distribution in the FT process, and the probability of the hydrocarbon chain is described using the Anderson Schulz Flory (ASF) equation (13) [56], [57].

$$W_n = n(1 - \alpha)^2 \times \left(\alpha^{(n-1)}\right) \qquad (13)$$

n: Carbon number

α: is the chain growth probability as shown in Figure 2-5.

$W_n$: Weight fraction
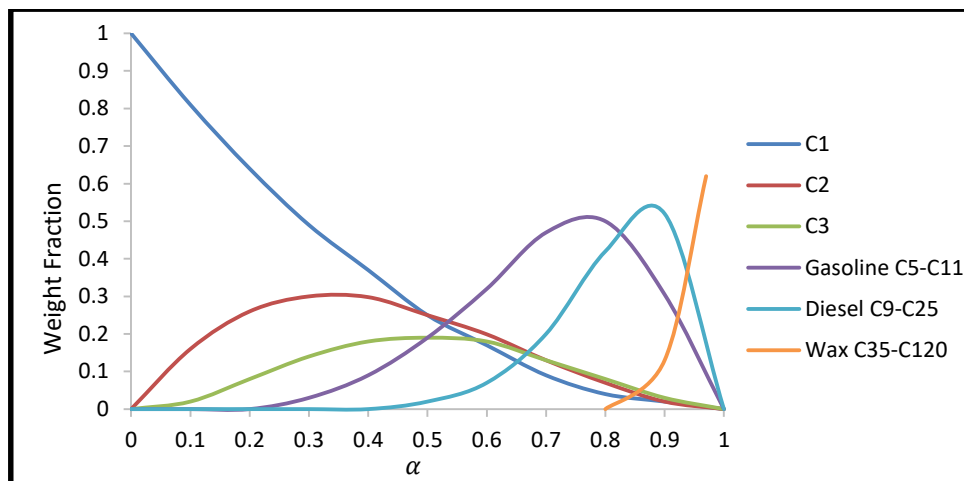


Figure 2-5: Fischer Tropsch Overall process [57].

In general, FT is divided into two approaches depending on the operating temperature, high temperature (HTFL) operates at 300-350 °C and low temperature (LTFT) ranges from 200-250 °C. Both procedures produce distinct products and use different reactor types as illustrated in Figure 2-6.

| High Temperature Processes<br>Gas phase reactions and products | Low Temperature Processes<br>Liquid phase reactor products<br>Products - mostly diesel |
|---|---|
| The Sasol Circulating<br>Fluidizing Bed<br>Reactor<br><br>1950 - present | The Tubular Fixed Bed<br>Reactor<br><br>Pre-WWll - present |
| The Sasol<br>Advanced Synthol<br>Reactor<br><br>1989 - present | The Sasol Slurry<br>Phase Distillate<br>Reactor<br><br>1993 - present |

Figure 2-6: Commercial use Fischer-Tropsch reactors [58].

For the HTFT the higher the temperature the lower the $\alpha$ value around 0.7 and it is preferred to produce gasoline and lower olefins. While, LTFT is preferred in producing log hydrocarbon chains such as diesel and wax with $\alpha$ value 0.88-0.95 [50], [59] as present in Figure 2-7.

In addition, one of the major parameters in the FT process is the amount of inlet gas that is converted to the required product known as carbon efficiency. Moreover, based on different studies showed that the GTL carbon efficiency ranges from 60 to 80 % [33], [47], [60].
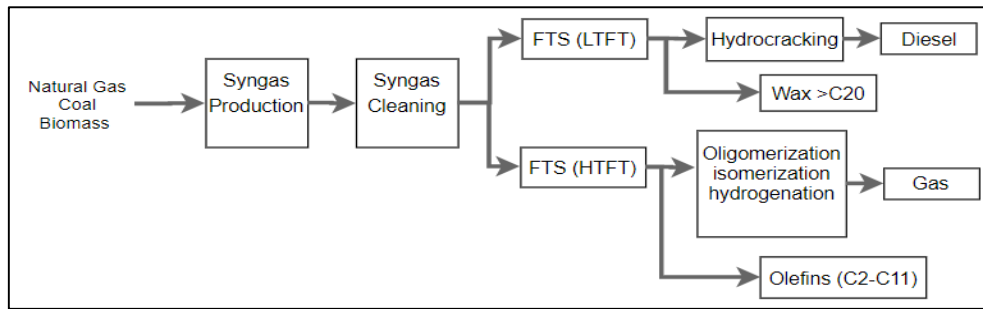
Figure 2-7: Product distribution in Fischer-Tropsch as a function of the chain growth $\alpha$ [61].

For FT processes different catalyst can be used in FT process, group 8 transition metals such as ruthenium (Ru), cobalt (Co), iron (Fe), and Nickel showed an optimum activity to generate hydrocarbon. However, platinum (Pt), iridium (Ir), palladium (Pd), and rhodium (Rh) showed higher selectivity than group 8 metals but were not industrially commercial due to their high cost. Overall, Fe and Co consider the most favorable catalyst to be used for the FT process due to their lowest cost. but Co considers more active than Fe [62]. Industrially, both iron and cobalt are used in the LTFT process, whereas only iron is used as a catalyst in the HTFT process. This is because an excessive amount of methane is created during the high-temperature process when cobalt is utilized as a catalyst [63].

And then the outlet of the FT reactor will pass through a 3-phase separator to separate oil, gas, and water. And the unreacted gas will be recycled back to the FTR to enhance the yield of the desired product.

### 2.1.3. Upgrading section unit

The upgrading unit, the third and final main part of a GTL plant, is the processing step that determines the composition of the final product pool [35].

### 2.1.3.1. Hydrocracking

In hydrocracking unit is used to crack the heavy hydrocarbon ($C_{21}$-$C_{100}$) in the presence of hydrogen gas at high temperature (T=345$^{o}$C) and high pressure (p=80bar) with 75% efficiency as shown in equation (14).

$$H_2(g) + \ C_nH_{2n+2} \rightarrow 2C_{\left(\frac{n}{2}\right)}H_{n+2} \qquad 21 \leq n \geq 100 \qquad (14)$$

### 2.1.3.2. Distillation column

Besides the hydrocracking this process involves distillation column, the Syncrude is fed to this column to obtain the desired separation to get the final products. The product will be distilled based on their boiling point differences [64].

### 2.2. MTG process

The synthesis of hydrocarbons from methanol over the synthetic zeolite ZSM-5 was found by accident by two teams of Mobil scientists working on separate topics [65], [66]. The gathering at Mobil Chemical in Edison, New Jersey, had been attempting to change methanol over to ethylene oxide, while laborers at Mobil Oil's Central Research Laboratory in Princeton were attempting to methylate isobutene with methanol in presence of ZSM-5. Neither reaction unfolded as expected, aromatic hydrocarbons were discovered instead. The Central Research team at Mobil investigated if methanol could be used as a precursor to a $C_1$ olefin in alkylating isobutane to produce, presumably, neopentane. ZSM-5 was the main impetus went after for this theoretical response. An equimolar combination of methanol and isobutane was passed over HZSM-5. Methanol was quantitatively converted, while only 27% of isobutane reacted. A full conversion of methanol was also demonstrated in an experiment using pure methanol. The entire reaction stoichiometry might be described as illustrated in equation (15) [23].

$$CH_3OH \rightarrow [CH_2] + H_2O \qquad (15)$$

Mobil's novel synthetic gasoline process, which uses zeolite catalysts to convert methanol to hydrocarbons, was the first major new synfuel breakthrough in the 50 years since the Fischer—Tropsch process was invented. The methanol-to-gasoline (MTG) process is the name for this procedure. It gave a new way to get high-octane gasoline from coal or natural gas [23].

### 2.2.1. Reforming unit in MTG section

Figure 2-8 presents the major unit operation in the MTG process. This process required the same procedure for the production of syngas where NG mainly methane oxidized steam, and with/without oxygen ($O_2$) to generate the syngas ($H_2$/CO) with a ratio of 2:1, by-products $CO_2$, wastewater, and energy. Then next unit will be the production of methanol by compressing the methane stream to 35bar and heated to $2016^oC$ before entering the reformer, while $O_2$ will be fed at an ambient temperature of $25^oC$ and pressure of 35 bar.
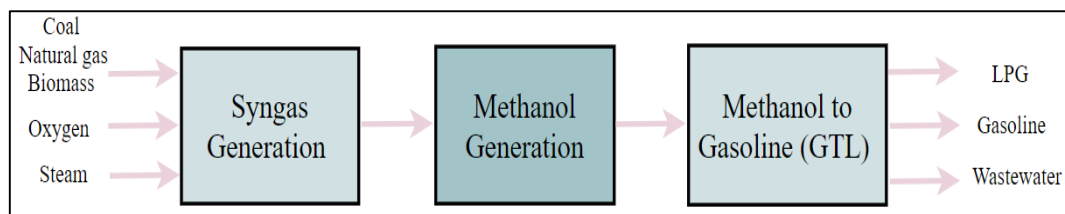


Figure 2-8: Methanol to Gasoline process block-diagram.

### 2.2.2. Methanol Production Section

Methanol is synthesized from syngas Equation (16) in the first stage of the MTG process. The process is mostly catalyzed by Cu/ZnO-based catalysts. One lucrative option to decrease global warming is to hydrogenate $CO_2$ and turn it into methanol as shown in Equation (17). When $CO_2$ is added to the CO/$H_2$ input, the production of

methanol increases dramatically. In addition, the energy balance has improved. Methanol is made directly from $CO_2$ without the need for $CO_2$ to be converted to CO [67]. In this unit, the syngas ($H_2$/CO) will be compressed to 65 bars through several compressors and then merged with a recycle stream and fed to the methanol reactor.

$$CO + 2H_2 \rightarrow CH_3OH \tag{16}$$

$$CO_2 + 2H_2 \rightarrow CH_3OH + H_2O \tag{17}$$
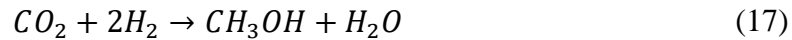
The outlet stream will enter a flash vessel where the generated methanol will be separated from the unreacted syngas will be recycled back to the methanol reactor. The produced liquid methanol will exit at 35°C and 63 bar. Next, the pressure of the methanol and by-product stream will pass through the valve to decrease the pressure to 2 bar before entering the distillation column to separate methanol from water.

### 2.2.3. Methanol to Gasoline Section

To handle the system's extremely exothermic reaction heat, the methanol-to-gasoline conversion was carried out in two independent adiabatic reactors. Where, 80% of methanol was dehydrated to obtain dimethyl ether (DME) acts as an intermediate, in the first reactor using a -alumina catalyst as shown in Equation (18). The generation of hydrocarbons from DME was then carried out in the second reactor using a HZSM-5 zeolite catalyst for the conversion of gasoline [68], [69] as shown in the Equations (19)-(22) [70].

$$2CH_3OH \rightarrow H_2O + CH_3OCH_3 \tag{18}$$

$$CH_3OCH_3 \rightarrow Light\ olefins + H_2O \tag{19}$$

$$Light\ olefins + CH_3OCH_3 \rightarrow Heavy\ olefins + H_2O \tag{20}$$

$$Heavy\ olefins \rightarrow Aromatics + Paraffins \tag{21}$$

$$Aromatics + CH_3OCH_3 \rightarrow Heavy\ Aromatics + H_2O \tag{22}$$
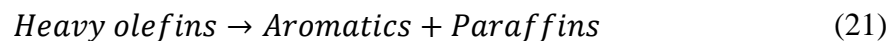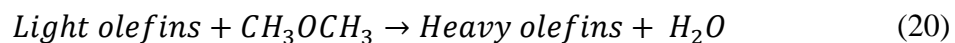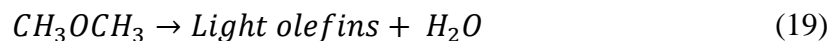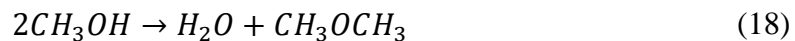
The contact period between the reactants and the catalyst is critical in the MTG process.

When the contact period is extremely short (3-10 hr), the major products produced are water and the DME. When the contact time is raised, the DME performance peaks but then begins to decline, where the DME has a greater probability of dehydrating to generate $C_2$-$C_5$ alkenes. With an increase in contact duration, alkanes, alkenes, $C_{6+}$, and aromatics are produced [71] as illustrated in Figure 2-9.
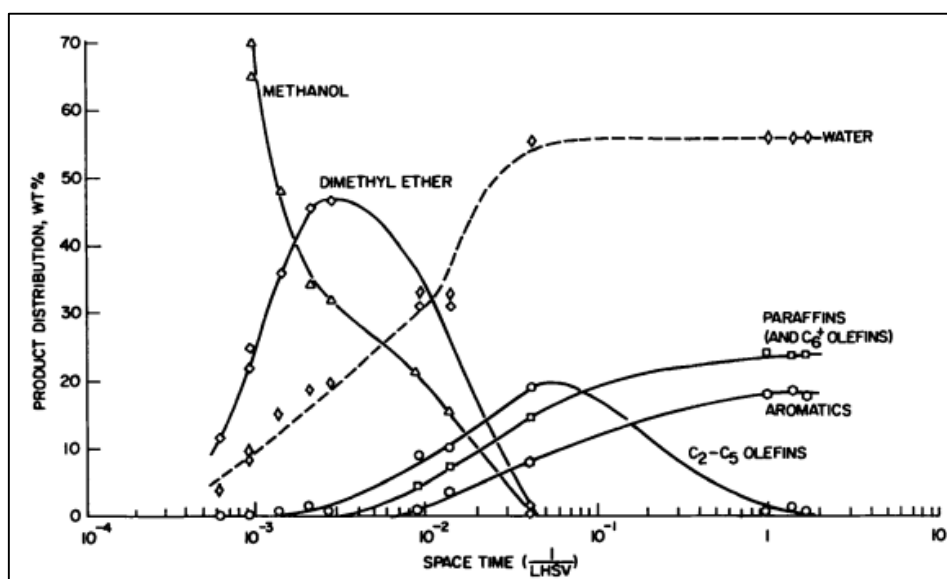


Figure 2-9: Methanol to gasoline reaction path [66].

### 2.2.4. Methanol to Gasoline Catalysts

Zeolite ZSM-5, which catalyzes the conversion of methanol to hydrocarbons, is a critical catalyst in the MTG process. The ZSM-5 structure features two types of intersecting channels: one roughly circular and one elliptical as shown in Figure 2-10. The size of the apertures has a significant impact on product dispersion. The MTG process relies on ZSM-5's strong hydrothermal stability and low coke selectivity to enable a long catalyst life. Because of the low coke selectivity, suitable cycle durations may be reached without requiring an excessive amount of catalyst [72].
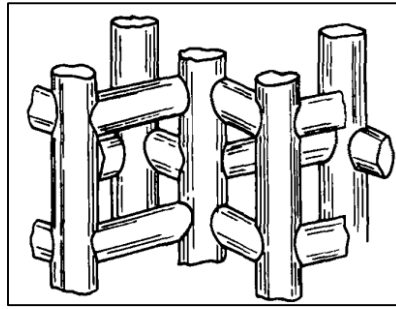
Figure 2-10: Zeolite-5 channel system [65].

The MTG technique has the following distinct advantages:

1- Hydrocarbons are produced in a relatively narrow compositional range; little methane and no hydrocarbons larger than $C_{11}$ are formed.

2- High methanol conversion can be combined with high selectivity for iso-paraffins and aromatics with higher octane value.

3- ZSM-5-based catalysts have a very low aging rate.

The MTG method was thought to be a novel and easier way to produce gasoline-range hydrocarbons from methanol. The gasoline produced by the MTG method is chemically conventional, has a limited boiling range ($C_4$–$C_{10}$, no $C_{11+}$), and outperforms traditional F–T processes in yield and quality, with RONs surpassing 90–95 [73].

# Chapter 3 : Literature Review

## 3.1. GTL Process

In the gas to liquid process, the typical syngas reactor used is ATR as proposed by a number of researchers, recommended as the most suitable and economical method to generate syngas [19], [74]–[76]. The production of syngas unit includes performer and reformer (ATR).

Makhura et al., [77] have shown that parameters such as temperature, catalyst, pressure, particle size, flowrate, bed height, and residence time affect the hydrocarbon output products in Fischer Tropsch process. Several experiments looked at the influence of the performance of FT efficiency in terms of yield, conversion, and selectivity. It has been discovered that increasing the residence time or lowering the feed concentration can boost conversion by up to 90% while not affect selectivity. The functioning of the fluidized bed reactor was investigated using mathematical models in polymerizing syngas, and simulation results suggested that iron catalyst is the best for optimizing liquid hydrocarbon products. High reactor pressure has a favorable influence on the reaction, resulting in an increasing in overall CO conversion and, as a result, the chain length of the products.

Another paper by Behroozsarand and Zamaniyan [62] presents an optimization and simulation framework using Aspen HYSYS V7.2. All GTL units have been optimized separately throughout the simulation process. The suitable recycling of light and unconverted gas ratio and a point has been investigated and optimized. Two recycling points has been investigated first, Amine and FT units, or syngas unit to maximize the yield. Results indicated the highest productivity around (4065 bbl./d) has been achieved with a split ratio of 13:87 between the Amine and

SMR (syngas) units.

In addition, simulation and optimization framework were carried by Al-Sobhi and Elkamel [78] for GTL and other facilities have been added to the natural gas processing and production network. ASPEN Plus v7.3 process simulator proved to be a valuable tool for simulating the processing network's core processing units to estimate mass and energy balances, operating conditions, and equipment specifications. The simulations' flowsheet is useful in several ways. The sensitivity analysis modeling tool, for example, allows us to adjust the $O_2$ flowrate between 70,000 to 72500 kmol/hr to obtain a syngas ratio of 2. To aid in the optimization of the processing network, the modeling program LINGO version 14.0 (LINGO) was employed. The simulation's product yields were used as beginning values for the model's variables. The most profitable flowrate values for both the network's feedstock and products shown in Table A 1 were discovered. Moreover, by processing more natural gas feedstock, the network's profit may be maximized, and intuitively, when the product's selling price rises. Furthermore, the model solves for lower values for all loss streams because they do not contribute to the processing network's profit. The loss stream from the GTL process has the greatest flowrate value where water and $CO_2$ are generated in large quantities as waste products. As a result, additional consideration of capturing $CO_2$ and using it inside the network, as well as including wastewater management, would greatly increase performance.

Zarandi et al., [60] simulated a GTL plant with a capacity of 6000 bbl/day through Aspen Hysys software, different α (0.9,0.92, and 0.95) along a multi-tubular Fischer Tropsch reactor (56 m$^3$) with cobalt catalyst to maximize the wax yield. The simulated Fischer Tropsch was divided into two sections to investigate the volume reduction versus wax yield. Results shows that staging the Fischer

Tropsch reactor enhances the reaction rates, increasing the reactor volume from 0-70% increase the wax yield to 7300.6 bbl/day at α value of 0.95.

Taghizadeh Damanabi and Bahadori [79] the GTL process has been improved by using tri-reforming of methane, FTR, and membrane separation units instead of the conventional reformer and FTR units. The process was built on Aspen HYSYS V.7.3, and the stream and units operation properties have been predicated by using the Peng-Robinson equation of state. The reforming reactor is replaced with a tri-reforming reactor to improve syngas output, with a reaction pressure of 1–10 bar and temperature of 500 °C–800 °C studied. It has been found that lowering the pressure and raising the temperature improves hydrocarbon conversion and the syngas ratio. $CO_2$ generation is shown to be reduced by regulating the oxygen input rate to the tri-reforming reactor. When a Pd/Ag membrane is used for separation and recycling syngas in a Fisher Tropsch reactor, the yield of light components such as methane decreases while the yield of heavy components increases. It has been demonstrated that using a tri reforming reactor and membranes increases gasoline and LPG output to 3337 bbl./day, more than twice as much as the conventional method, while reducing carbon dioxide selectivity in the Fisher Tropsch reactor by 15%.

Several literature studies have investigated the utilization of $CO_2$ as either a raw material or fed to FTR unit in the GTL plant to minimize the GTL emissions and maximize the production yield.

An integration study to maximize the wax by Rafiee et al. [80] was done to study the impacts of introducing $CO_2$ from the captured plant to the GTL plant and investigate the performance of ATR and SMR. Three different cases were studied, case 1 introduce $CO_2$ to ATR reactor, case 2 ATR reactor without $CO_2$ removal before Fischer Tropsch reactor, and the last case 3 ATR is replaced with SMR. The

25

optimization findings that for case 1 there is no need to add $CO_2$ to the standalone ATR, for case 2 there was a trivial improvement from removing $CO_2$ from the process while in case 3 the result shows that using all the captured $CO_2$ can be used in the SMR. The optimization results along with the wax production from each case in shown in Table A 2.

Nkemakolam Chinedu et al. [81] the study proposed a new GTL design process using steam/$CO_2$ as feed reactant instead of oxygen to optimize the syngas and minimize the cost as well as GHG emissions. The simulation of the conventional process with oxygen was simulated using Honeywell's Unisim software. The simulated GTL plant process involved the pre-treatment unit, syngas unit, the Fischer Tropsch unit and finally the upgrading unit. The technical analysis from the simulation showed that recycling and the reuse of $CO_2$ from-the purge stream instead of oxygen improved the syngas gas ratio by 1.8% bringing it close to 2 and increasing syngas production by 10.4%, while reducing $CO_2$ emission by 77%. The efficiency of steam/$CO_2$ method versus the conventional process is summarized in Table A 3.

Several scenarios have been studied by Al-Yaeeshi and AlNouss [82] to investigate the effectiveness ($H_2$/CO), recycle ratio on the process efficiency after $CO_2$ injection in ATR and SMR reformers. Three scenarios have been investigated first two for ATR with the different steam flows (6492 and 3223 Tonne/d), while the third is a single SMR. Moreover, the fed $CO_2$ was in the range of 500-4000 Tonne/d and study the effect on the product yield, and environmental and economic results, the study was simulated using Aspen HYSYS software. Besides, the amount of hydrogen carbon produced also emissions associated with each $CO_2$ fed was studied. Out of the simulation study, it was concluded that scenario two with

3223 Tonne steam/d, feeding $CO_2$ with a value of 1500 Tonne/d feeding directly to the FT reactor achieves higher hydrocarbon production and lower capital, utilities, and carbon emissions. This review was a comprehensive review where all conditions and parameters, and environmental and economic evaluations were investigated. However, the simulation study was limited to the use of commercial catalysts so, additional catalysts analysis along-with their possible limitations needs to be studied.

Greyling et. al. [83] applied a fault detection and isolation (FDI) technique for GTL process developed in Aspen HYSYS software. The GTL process is subjected to precisely selected defects while the exergy-based FDI approach is performed. The defects chosen are intended to influence numerous process units, with the consequent recycling stream of the GTL process being one of them. Pure methane ($CH_4$=8195 kgmol/hr) was used to represent the natural gas supply stream, also to alter the syngas composition, a carbon dioxide ($CO_2$) stream was supplied. The vapor outlet steam from the 3-phase separator is split into recycle fed to FTR and purge streams with a ratio of 0.8:0.2. The findings imply that when applied to PC processes of representative difficulty, the exergy-based FDI approach performs effectively. The technique described here is agnostic, allowing it to be quickly applied to different processes represented in Aspen HYSYS. Further research should include a comprehensive examination of the exergy-based technique's performance in noisy environments, a sensitivity analysis about the amount of detected faults, and an evaluation of the technique's performance in a dynamic simulation environment. Given the technique's sensitivity to ambient circumstances (which is considered to be static in this study), the influence of a constantly changing environment must be examined. A comparison of the exergy-based

scheme to other typical FDI strategies should also be examined.

When using process simulators for flowsheet optimization, high computational loads, slow convergence, and simulation crashes are prevalent. For time-consuming, simulation failures, and higher computational loads Panahi et.al., [84] proposed an alternative self-optimization using surrogate models for GTL simulation. The use of surrogate models in the self-optimizing control technique was examined to reduce the requirement for time-consuming and non-reliable thorough simulations for process optimization as illustrated in Figure A 1. There is four surrogate models' multilayer perceptron neural network (MLP-ANN), Radial basis function neural networks (RBF-ANNs), Support vector machine (SVM), and Adaptive neuro-fuzzy inference system (ANFIS). As a large-size process facility with several recycles, a natural GTL process was chosen. In terms of forecasting the output value as well as the best operating points, the surrogate models were evaluated. In virtually all circumstances, the MLP-ANN surrogate model outperformed the comprehensive GTL process flowsheet simulator and was determined to be a good alternative for it in the self-optimizing operation. The best self-optimizing control volume (CV) set derived using the MLP-ANN surrogate model was more trustworthy than the best set acquired using the comprehensive simulation-optimization technique, according to the findings.

### 3.1.1  Fischer Tropsch Catalysts.

Catalysts continue to have a huge influence on the chemical, energy, and environmental industries. Catalysts' activity, selectivity, and life-time are frequently used to describe their performance [85].

Jalama et, al., [86] tested the influence of process temperature on $CH_4$ selectivity and CO conversion using 10% cobalt on titanium dioxide support

(Co/TiO$_2$) in a fixed bed reactor at a pressure of 20 bar. The influence of temperature on CO conversion and methane selectivity is illustrated in Figure A 2**Error! Reference source not found.**, with an increase in temperature from 200-220$^o$C both CO conversion and methane selectivity rose from 13.2-19.4% and 6.1-19.4%, respectively. Also, increasing the operating temperature has a significant impact on the selectivity of C$_2$-C$_4$ and C$_{5+}$ hydrocarbons, the selectivity for C$_2$-C$_4$ increased from 3.4 to 13.5%, while the selectivity for C$_{5+}$ decreased from 90.5 to 67.1% as shown in Figure A 3.

F. K. Al-Zuhairi and W. A. Kadhim [87], studied the impact of Ce promotion and operation on Fe-based catalyst  pressures of 20 bar, H$_2$/CO ratio of =2, and varied reaction temperatures in the range 250 to 325 $^o$C. The addition of a promoter to an iron-based catalyst increased the reducibility of Fe$_2$O$_3$ by lowering the reduction temperature; additionally, conversion of CO and selectivity of undesired products like CO$_2$, C$_2$-C$_4$, and CH$_4$ were found to be increased for both catalysts, whereas selectivity of C$_{5+}$ decreases as the operation temperature increases from 55.87 to 35.65 percent and from 73.03 to 61.59 When a promotion catalyst were utilized, greater selectivities for high molecular weight hydrocarbons were discovered at a lower reaction temperature (250 $^o$C) with 73% selectivity.

Horáček et al., [88] provides an overview of Fischer–Tropsch synthesis (FTS) from a catalysis perspective. The importance of promoter type and amount loaded into the catalyst is detailed and addressed for both iron- (Cu, K, Na, S, Zr, Ni) and cobalt-based catalysts (Ru, Pt, Re, Zr, Ag, Rh, Ir, Au), as well as the significance of catalytic supports and reaction conditions. The reaction temperature for iron catalysts is described is between 508–613 K, whereas the reaction temperature for cobalt types is discussed as between 468–513 K with a pressure of 3 MPa for both

catalysts. FTS catalysts made of cobalt or iron have a wide range of applications and optimizations for the synthesis of necessary hydrocarbons. Noble metals such as Ru and Pt can be added to cobalt low-temperature catalysts to make them more stable and increase Fischer Tropsch production activity.

However, due to the cost associated with the gas to liquid (GTL) process especially the air separation unit (ASU) with 25-40% of the plant capital cost. In the coming section several innovation reactors, catalysts, and integration with other processes have been consider.

### 3.1.2  Syngas Generation Unit

Recently there has been growing attention toward the environment and reaching sustainability, several studies proposed Chemical looping reforming (CLR) as a promising technique, due to its higher efficiency, performance, and safety. The CLR process involves two steps, first methane is oxidized using oxygen carrier donated as OCs ($MO_y$), to generate the syngas. And step two the reduced oxygen carrier ($MO_{y-1}$) is recovered with dense air  or water to obtain hydrogen gas in the air reactor as shown in Figure A 4 [89].

However, a design of a suitable oxygen carrier is required to achieve high selectivity, activity, and redox strength. Li, Wang, and Wei [70], studied different oxygen carriers such as, $CeO_2$, and perovskite oxygen carriers. The oxidation of methane to syngas was first accomplished over $CeO_2$, and a syngas production with a ratio of 2 was indeed generated at a temperature of $700^oC$, it was also reported that using $Fe_{3+}$ along with Ce can enhance the redox due to the formation, $Fe_2O_3$ is the cheapest and most oxides metal available in flora. The combination of $CeO_2$-$Fe_2O_3$ has good selectivity, stability, and activity to generate syngas as shown in Figure A 5. However, Ce-Fe selectivity is highly affected by the oxygen carrier

surface area, so the higher the surface, resulting in complete methane oxidation to water and carbon dioxide. Moreover, perovskite with $ABO_3$ crystal structure sue to its high thermal stability, oxygen mobility, and outstanding redox property. It was reported that the reaction of methane with perovskite is controlled by the reaction temperature, a temperature higher than $800^oC$ is needed to achieve a high synthetic gas yield. In the end, more research need to be done in-order to solve these limitations. [90]

A recent study, by D. Li et al. [91] studied the new development of oxygen carrier materials, perovskite oxygen carriers were the most material studied due to their high oxygen mobility and thermo-stability. And the presence of Rn in perovskites reduce temperature by $300^oC$. However, optimization studies to balance the conversion of methane and synthetic gas selectivity at low temperature. In the end, chemical looping is promising technology with a cost saving of 25-40%, emitting fewer emissions, and indirect contact between methane and oxygen eliminates the risk of explosion at high temperatures. However, it is still very challenging to obtain definite information about reaction mechanisms and active sites under reaction conditions. Moreover, all the review studies on CLR were limited to investigating the performance of single or multi-oxygen carriers in terms of product yield, syngas ratio, CO, $H_2$ and Methane selectivity at different temperatures. But the unavailable information on environmental and economic evaluation, large-scale limitations, reactor type, and the need for more research on suitable OCs to be done makes it CLR economically not feasible.

Furthermore, more studies have been investigating the chemical looping reformer from different aspects all summarized in Table A 4.

However, over the past years, there has been an enormous increase in the

31

greenhouse gases in the atmosphere, affecting global warming, leading to the need for innovation technologies to reduce these emissions in the environment.

### 3.1.3 Fischer-Tropsch synthesis Unit

This unit considers the main unit where syngas is converted to a wide variety of hydrocarbon fuels with a large amount of $CO_2$ associated with the process. To minimize the emissions and to improve activity, selectivity, and productivity different type of reactors has been introduced.

Peacock et al. [92] shared a study on an advanced CANS$^{TM}$ catalyst carrier reactor, the proposed reactor enables high productivity, selectivity, and long catalyst operation stability. Employing the CANS reactor enhanced the selectivity to more than 90% for $C_{5+}$ with the use of powder catalysts, high heat transfer, and lower pressure drop 2-3m compared to 10-15 m conventional fixed bed. Moreover, FT and hydrocracking units can be combined by placing FT catalysts at the top of the CANS reactor and upgrading catalysts at the bottom thus, lowering the cost.

Huili and Xiaojin et al. [93] modeled mass and heat transfer in a microchannel reactor using MATLAB software. The performance of microchannel over cobalt catalysts achieves a CO conversion of 84% compared to 69% for the fixed bed reactor. However, thermocouples to detect the hot spots are difficult to be placed. more research needs to be done to solve this problem.

This new Fischer-Tropsch technology is a promise in terms of the environmental and economic point of view.

### 3.1.4 GTL integration technologies

A promise integration process was study by Ziaei et al. [37] the GTL plant was integrated with Ammonia and Urea plant, to maximize the profit and utilized the emissions associated with the GTL plant. The integration process is illustrated

in Figure A 6. The study shows that around 37 Tonne/h of the captured carbon dioxide was utilized in the urea plant, with a reduction of 52.8 Tonne/d of $CO_2$ emissions, and 35 million USD lower than the standalone GTL and ammonia-urea processes. This process is economically feasible in terms of environmental and economic perspectives.

The continuous growth of globe population has pushed up the energy demand leading to an increase in greenhouse gases to very high concentrations, so using renewable energy instead of fossil fuel is a must. A recent integrated study by Ghorbani et al. [94] weas done to generate one of the future sustainable fuel hydrogens beside a wide variety of hydrocarbon fuels. The production was done by generating $O_2$ and hydrogen through an electrolyzer as illustrated in Figure A 7. TRNSYS software was used to model both hydrogen liquefaction and alkaline electrolyzer, $CO_2$ cycle, and GTL process are simulated using Aspen HYSYS software. The integration of this process was linked using Aspen HYSYS and MATLAB program. The total energy produced from the integrated process was 195.2 MW, with a fuel efficiency of 94.73%. The Paris agreement setout framework to lower the earth's temperature below $2^oC$, the integrated grid and cleaner fuel which can be done using this integrated method where both liquid fuel and hydrogen fuel is produced. This integration is promising technology in terms of economic and environmental.

There are no innovation technologies in MTG process, moreover, all the founded reviews on GTL, have been limited to low-temperature Fischer- Tropsch simulation. Also, the economic, environmental, and heat integration, waste and mitigations strategies have not been evaluated. In this paper low and high Fischer Tropsch beside new promise technology to produce clean gasoline fuel known as

33

methanol to gasoline (MTG) process will be discussed in terms of environmental and economic evaluation, waste and mitigation strategies associated with this waste.

## 3.2. The MTG Process

Kulik et.al. [95] from the University of Akron, in collaboration with the Electric Power Research Institute, created a process comparison and analysis of Syngas-to-Methanol-to-Gasoline and Syngas-to-DME-to-Gasoline obtained from coal or natural gas-based syngas. It was demonstrated that the synthesis of gasoline using the direct DME route provides clear process benefits over the synthesis via the methanol route summarized below.

1. Syngas to DME conversion in a single step enhances per-pass conversion by 38% and reactor productivity by 8% over syngas to methanol conversion.

2. The copper-based $Cu/ZnO/Al_2O_3$) catalyst is used in the conversion of syngas to methanol. This catalyst is vulnerable to deactivation by crystal formation in methanol and water-rich liquid phase. However, the conversion of syngas to DME employs a dual catalytic system comprised of a $CU/ZnO/Al_2O_3$ catalyst and a gamma-alumina catalyst.

3. The one-step conversion of syngas to DME increases volumetric reactor productivity by up to 100% as compared to syngas to methanol conversion.

4. Methanol to gasoline conversion is extremely exothermic, having a heat of reaction of 398 cal/g of methanol converted. Thus, the conversion of DME to gasoline is approximately 25% less exothermic, with heat of reaction of around 300 cal/g of DME converted.

Galadima and Muraza [96] evaluated recent literature on the impact of catalyst structure, acidity characteristics, and reaction parameters on catalytic

34

activity, selectivity, and catalyst lifespan has been extensively discussed.

## 1. Catalyst modification and topology effect:

When compared to when the reaction was carried out with just the H-ZSM-5 catalyst, the reaction with the H-ZSM-5/H-MCM-48 composite catalyst yielded 34% better selectivity to gasoline range products "28 percent selectivity". The composite mixture reduces the likelihood of aromatic coke precursors and $C_2$ - $C_3$ hydrocarbon species being produced. The influence of zeolite nature was compared in another investigation. While the H-ZSM-5 "Si/Al =50" catalyst doubled the methanol conversion, it also had a 7% greater selectivity than the H-BEA catalyst. Under the reaction conditions used, the H-ZSM-5 catalyst created a superior system. At equivalent conversion, oxalic acid treatment of ZnO/CuO/HZSM-5 improved the selectivity of the parent catalyst by 4%. As a result, careful catalyst modification might be quite useful for the generation of gasoline hydrocarbons. The H-UZM-12 and H-SSZ-13 zeolites exhibited diverse behavior. The former catalyst converts 60 percent of methanol and is stable for just 4 hours. The H-SSZ-13, on the other hand, resulted in a 100 percent conversion to a longer lifetime (8 h). The H-UZM-12 catalyst, on the other hand, was more selective for the desired hydrocarbon products all results are shown in Table A 5.

## 2. Catalyst acidity effect:

During acidity-dependent reactions, the density and strength of either Lewis's acid or Brønsted sites play an essential impact. To increase catalytic activity, zeolite acidity can be desilicated using 0.05-0.20 M NaOH. The most severely desilicated catalyst achieved optimum conversion that was 3.3 times more stable than the untreated catalyst, according to the results. However, due to an increase in the speed of hydrogen transfer processes, the total selectivity to gasoline

35

hydrocarbons increased by 1.7. However, when the Brønsted to Lewis acidity ratio (B/L) increases, the selectivity for gasoline hydrocarbons improved.

## 3. Reaction parameters effect:

Temperature, space velocity, pressure, and perhaps reactor design are all reaction characteristics that must be chosen carefully. An experiment was carried out at a temperature ranging between 375-475ºC at 1.3 bar for 5 hours using a 0.2M NaOH modified H-ZSM-5 with Si/Al =38 catalysts. The optimal reaction temperature was found to be 425ºC. Under the same condition, the catalyst was more selective to the hydrocarbon products and had a longer lifetime. Even while increasing the temperature promotes methanol conversion and selectivity to desired hydrocarbons, there is a risk of a detrimental effect on selectivity above the ideal temperature. However, another research found that increasing the reaction pressure from 1 - 10 bar at 400 C resulted in an increase in methanol conversion from 93 to 98 percent. When the pressure was increased to 20 bar, however, the conversion rate decreases to 96%. While selectivity for gasoline range compounds improved with pressure, the scenario for light olefins was different. Propylene production dropped by half from 36 – 18%, whereas ethene production increased from 24% at low pressures to 37 percent at high pressures. H-MOR and Ca/H-MOR achieved equal conversion and selectivity under stable reaction conditions. The Ca-modified catalyst, on the other hand, was more stable, as conversion fell by 20% compared to 40% with the unmodified H-MOR zeolite. As a result, the change proved quite beneficial in this circumstance. Unfortunately, at identical reaction conditions and conversion rates, both conventional and mesoporous H-SSZ-13 (Si/Al =50) give very low selectivity to the required gasoline hydrocarbons. As a result, these catalysts are less favorable for the MTG reaction than, say, mordenite (H-MOR)

36

based zeolites.

Noor et. al. [97] worked on monitoring the methanol ($CH_3OH$) conversion and the product yield selectivity in the MTG process. The most common methods for determining these values are gas chromatography (GC) or other chromatographic-based procedures, which are both costly and time-consuming. To produce clean gasoline, a technique for determining $CH_3OH$ conversion and product selectivity to iso-paraffins and aromatics in the methanol-to-gasoline process was developed. As a process analytical technology tool, the approach can be used offline, online, or at-line. During the reaction, near-infrared and mid-infrared spectra of aqueous fractions and organic of MTG reactor is obtained. In comparison to existing chromatographic-based approaches, the suggested method can provide a cleaner, quicker, and less expensive way for measuring catalytic reaction parameters with excellent precision.

Liu et. al. [17] present an innovative superstructure for integrating the MTG process with the organic Rankine cycle (ORC), to improve energy productivity. The process was simulated in Aspen Plus coupled with MATLAB to simultaneously improve the flow-sheet structure, operating conditions, and the operating fluid. The proposed ORC-MTG integrated process saves 18.77 percent cooling water and has a return on investment (ROI) of 22.66 percent when compared to the present commercial equivalent method. The thermal efficiency of 18.3 percent is important for industrial applications, implying the need of bringing ORC to other heat-intensive industrial facilities that require better energy efficiency, especially when power is expensive.

Doluda et.al. [98] study is to use sodium hydroxide and oxalic acid to modify H-ZSM-5 samples to develop the zeolite's mesoporous structure and get the best

Si/Al ratio.

The treatment of H-ZSM-5 HKC zeolite with an aqueous solution of sodium hydroxide (NaOH) with 0.01 to 0.6 M concentration results in an increase in mesoporous volume and a decrease in micropore volume, which may be attributed to partial destruction of micropores with the creation of mesoporous. Mesoporous formation occurs as a result of the partial dissolution of silicon oxide, which also results in a drop in the Si/Al ratio. A drop in the Si/Al ratio leads to a reduction in the number of active cites. However, treating the zeolite with a concentrated solution of sodium hydroxide results merely in a reduction in micropore volume, which can be attributed to silica dissolution. Moreover, the transformation rate of dimethyl ether increased from $0.55\ kg\ DME/kg\ catalyst\ \times\ hr$ to $0.09\ kg\ DME/kg\ catalyst\ \times\ hr$ with an increase in sodium hydroxide concentration from 0.01 M - 0.2 M; however, an increase in sodium hydroxide concentration to 1.1 M resulted in a significant decrease in the transformation rate of dimethyl ether down to $0.02\ kg\ DME/kg\ catalyst\ \times\ hr$. The process selectivity for liquid hydrocarbons is 25 to 30% in the presence of zeolites modified with alkali solution, which is 5 to 10% lower than the original untreated zeolite.

Del Campo et.al. [99] tested the conversion of methanol-to- hydrocarbon over industrial and lab-made Zeolite catalyst (H-ZSM-22). The effects of post-synthesis treatments such as sodium hydroxide (NaOH) treatment, the mixture of CTAB with NaOH, and the mixture of TBAO with NaOH on catalytic lifespan and product dispersion were investigated. After treating the commercial material with acid and NaOH / CTAB, the overall methanol conversion capability increased by roughly tenfold compared to the untreated catalyst. The lab-made catalysts treated with acid and NaOH, on the other hand, saw a 17-fold growth in conversion capability. After the post-

synthetic treatments, the yield toward the aromatic-free $C_{5+}$ alkene fraction improved marginally, reaching 58 percent of the gasoline yield.

In the thermal catalytic cracking process, the zeolite catalyst plays a critical role. Zeolites-based and zeolite catalysts are the most acceptable candidates for the MTG process due to their unique structure and properties. Zeolites are good candidates for the thermal catalytic cracking process because of their stability, form selectivity, non-corrosion, and environmental friendliness. The most essential characteristics of these solid materials are their structure, high specific area, selective small particle absorption, and ion-exchange. The use of zeolites as a catalyst in the petrochemical industry has shown positive results [100].

Sanz-Martínez et. al [70] developed of catalysts suited for MTG operations in a fluidized bed reactor has been investigated, with a focus on increasing textural, physicochemical, morphological, structural, and mechanical qualities. To make the various catalysts, a combination of HZSM-5 zeolite (active material), boehmite or bentonite (binding), and alumina (inert filler) was utilized. Following preparation, characterization was performed using physical $N_2$ adsorption, XRF, XRD, and SEM-EDX methods. $N_2$ adsorption–desorption analysis was performed to assess the textural features of both fresh and used catalysts and their components shown in Table A 6. Because the agglomeration process is carried out using species of smaller specific area than the zeolite, the BET surface area of the fresh catalysts between 210.8–287.9 $m^2$ $g^{-1}$ was reduced in comparison to the HZSM-5 zeolite with the surface area of 319.9 $m^2$ $g^{-1}$.

The micropore size of the HZSM-5 zeolite and the three catalysts remained consistent, indicating that the zeolite is the sole source of the microporous contribution. After being used in a process, catalysts do not suffer from substantial

textural degradation. The surface area and volume of micropores have both decreased slightly less than 10%. Moreover, The SEM-EDX method was used to investigate the morphology and chemical content of the catalyst components. at 450°C the distribution of the three catalysts' products broken down into non-condensable "light HC", condensable "gasoline", and solid "coke" phases is illustrated in Figure A 8 .

The inquiry yielded the following results: The catalyst using boehmite as a binder was found to be the most suited, with a composition of 50 wt. percent HZSM5, 30 wt. percent boehmite, and 20 wt. percent alumina.

Moreover, gasoline is considered a primary driving fuel in the petroleum industry and transportation sector as a cleaner fuel. In this thesis, sustainable design and analysis for gasoline produced from lower, and higher Fischer Tropsch gas to liquid (GTL), and methanol to gasoline (MTG) processes, in terms of evaluation of profitability, environmental assessment, and process simulation has been performed.

## 3.3. Literature Gap

Several recent literature reviews studied the overall production yield from GTL process with low-temperature Fischer-Tropsch. However, research works that focused on process optimization, economic benefits and energy demand are limited.

Furthermore, there aren't many papers investigating the gasoline production from natural gas through HTFT, LTFT and MTG processes, there is only one recent published paper on 2021investigated the gasoline production only through GTL (LTFT) and MTG. Thus, it's important to address all the gasoline production possible production techniques to increase the value of natural gas resources in NG-

rich nations throughout the world by identifying potential downstream added-value

products to relevant investment decisions.

# Chapter 4 : Methodology

## 4.    Introduction

Gasoline is an important petroleum-derived liquid as a major commodity for transportation and liquid fuel for industrial applications. This study aim focuses on the evaluation and the comparative analysis of synthesis gasoline generation from different utilization possibilities such as GTL and MTG technologies.

This chapter will provide a detailed overview of the simulation methodology approach utilized to complete and complete this project. The designing model involves hierarchical procedure consisting of sequential steps illustrated in Figure 4-1. The first step is to identify all the information and requirement such as the process flowsheet shown in Figure B 1 and Figure B 2 which is based on widely used GTL and MTG technologies, and process specifications (e.g., temperature, pressure, feed flowrate), these data were collected from literature, and research papers. The second step is a steady-state simulation of the GTL and MTG process flowsheets was carried out using Aspen HYSYS V.11 simulation software, the stream and units' operation properties have been predicated by using the Peng-Robinson equation of state. Moreover, sensitivity analysis is carried out at this stage. Finally, the simulated flowsheets were examined from both economic and environmental perspectives. The capital and operational costs of the two models, as well as the environmental emissions in terms of $CO_2$ equivalent, were estimated using Aspen Process Economic and Process Energy Analyzers.
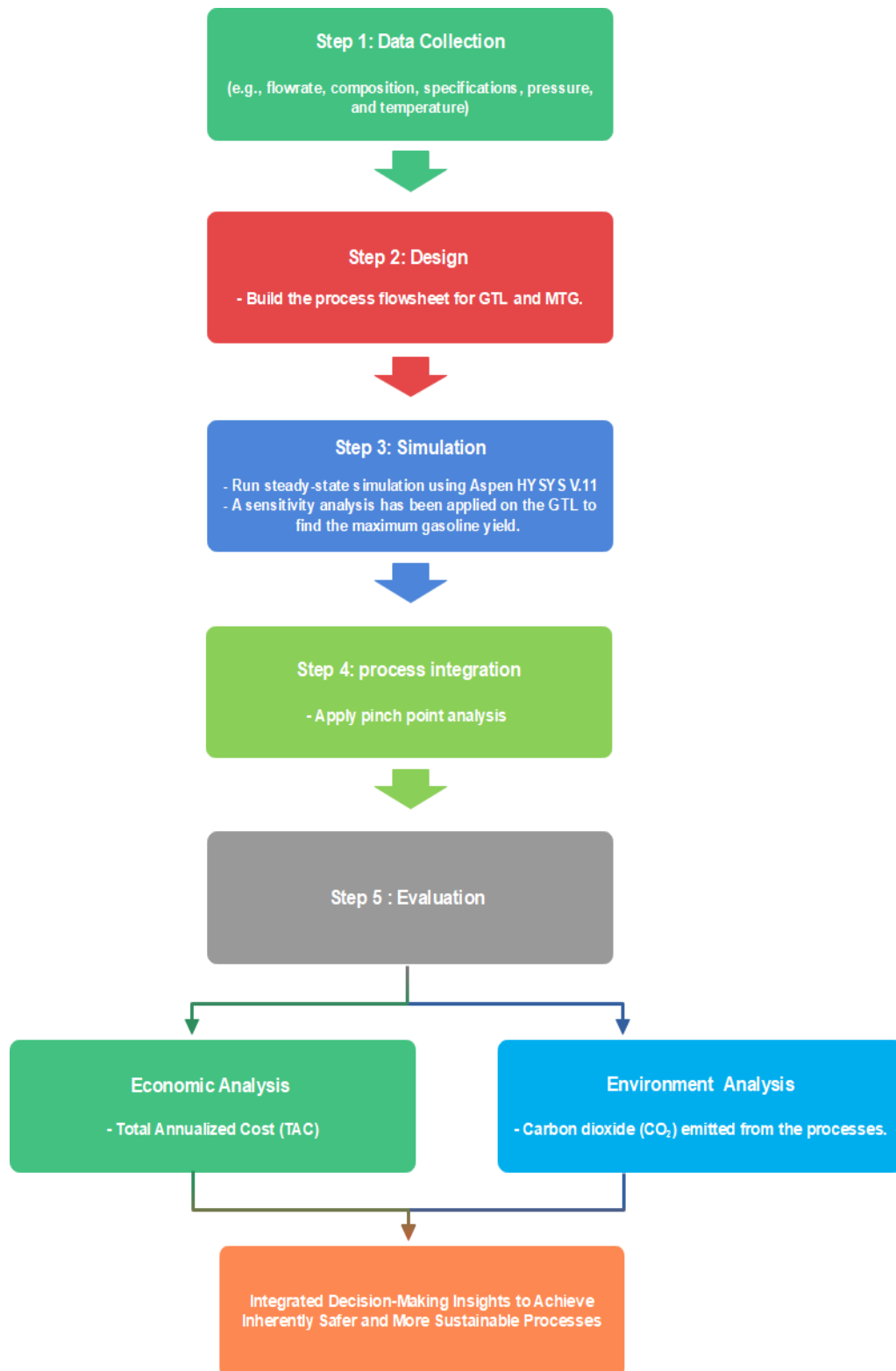
Figure 4-1: Overall methodology approach for gasoline production from GTL and MTG.

## 4.1. Data collection

Data collection is an important aspect in every field of study, The search was carried out across all three databases of IEEE Xplore, ScienceDirect, and Scopus. For analysis, the years 2015-2021 were chosen, with the search limited to articles and literature reviews. Research keywords such as GTL, Gas-to- Liquid, MTG, Methanol-to-Gasoline, sustainable, optimization, simulation, economic, environmental, Fisher Tropsch, low-temperature Fischer Tropsch, high-temperature Fischer Tropsch, and emissions.

Moreover, all the required specifications for both models such as temperature, pressure, steam to NG ratio and NG composition have been collected in this step as well shown in Table 4-1.

Table 4-1: GTL and MTG feed specifications [101].

| Input | Temperature (°C) | Pressure (kPa) | Molar flow (kmol/h) |
| --- | --- | --- | --- |
| | Gas-to-Liquid Specification | | |
| Natural Gas | 25 | | 37540 |
| Steam | 500 | 2500 | 7508 |
| Oxygen | 144 | | 21197 |
| | Methanol-to-Gasoline | | |
| Natural Gas | 25 | 2500 | 37540 |
| Steam | 500 | | 112620 |

## 4.2. Design

After collecting the data, a block flow diagram (BFD) for each system (MTG, HT-FT, and LT-FT) was designed as illustrated in Figure 2-1 and Figure 2-8. Also, the product distribution to evaluate the growth probability of hydrocarbons (α), was performed using Anderson– Schulz–Flory (ASF) equation.

### 4.3.   Simulation

A system simulation was run using Aspen HYSYS V.11 software to evaluate the system functionalities and examine the application consequences.

The Anderson-Schulz-Flory model was used to apply sensitivity analysis to the GTL process to chain growth probability ($\alpha$) on the product distribution to maximum gasoline.  Furthermore, a temperature of 350$^o$C and 240$^o$C for HT-FT and LT-FT was chosen to investigate the production of gasoline, results from the simulation reveal that the maximum gasoline production was at $\alpha$=0.78 for HTFT and $\alpha$= 0.88 for LTFT.

### 4.4.   Process integration

To minimize the amount of cooling and heating utilities in GTL and MTG plants, by enhancing the rate of heat transfer between several streams This strategy is created to make efficient use of the plant's energy to reduce utility costs and environmental effects. The minimal cooling and heating utilities required from the heat integration process are determined by graphical, and algebraic methods.

### 4.5.   Process Evaluation

The performance of the study can be assessed by conducting an economic, and environmental analysis using Aspen Process Energy and Economic Analyzers. Eventually, the simulation result will be the primary sources for determining the benefits in terms of sustainability and net profit.

# Chapter 5 : Process Simulation

## 5.1. GTL process simulation

Process simulation is a useful tool widely used to investigate the performance of the process. In this chapter, the GTL and MTG plants were simulated using ASPEN HYSYS © version 11 simulation software. This represents an important advancement in the engineering industry, providing an extremely powerful performance in predicting the outputs like, operating conditions, equipment sizes, stream properties and optimization [102].

In setting up the two models, the Peng-Robinson Equation of state (PR-EOS) was chosen as the fluid package since, it is the proposed thermodynamic property package for the hydrocarbon system. Hydrocarbon components with four C-atoms up to $C_{30}$ were added to the software [103]. The GTL simulation is represented in Figure 5-1.

## 5.1.1. Air Separation Unit

Table 5-1 represents the air composition fed to the ASU, Figure 5-2 shows a PFD for the air separation unit, in this process a two-stage compressors (C-01) and (C-02) with interstage cooling (E-01) are used to compress the air from 1.013 bar to 6.2 bar. The air is furthered cooled to -163.7 °C in (E-02) before entering the distillation column (T-01) to separate nitrogen and oxygen a pressure of 1.27 and 1.5 bar were set for the condense and the reboiler. Finally, nitrogen is further cool to -26 °C for further use and the oxygen is heated to 144°C and 25 bar in (E-04) and fed to ATR unit.

Table 5-1:Composition of Air.

| Composition | Mol fractions |
|---|---|
| Oxygen | 0.94 |
| Nitrogen | 0.06 |
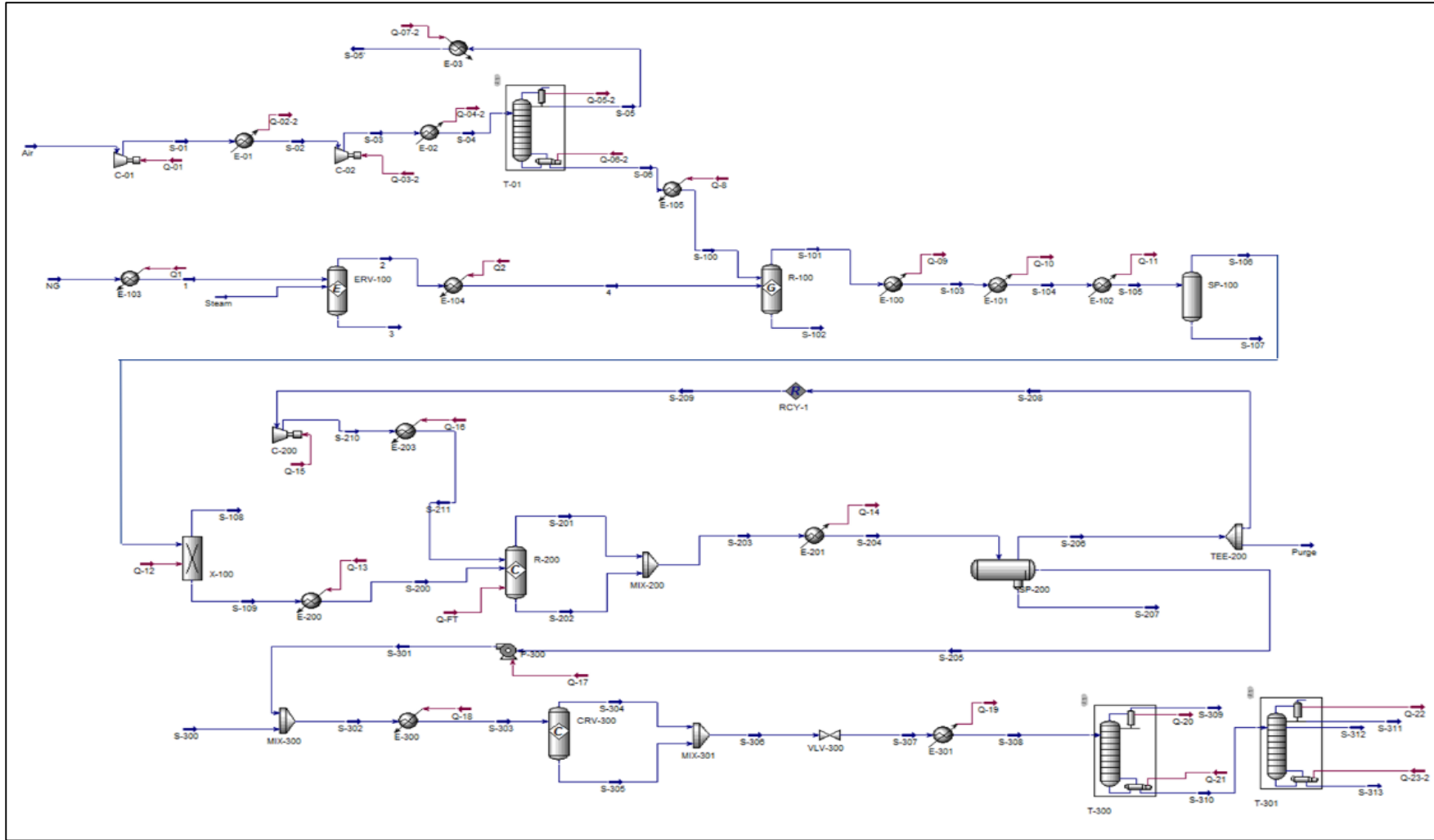
Figure 5-1: Aspen HYSYS process flow diagram of GTL process.
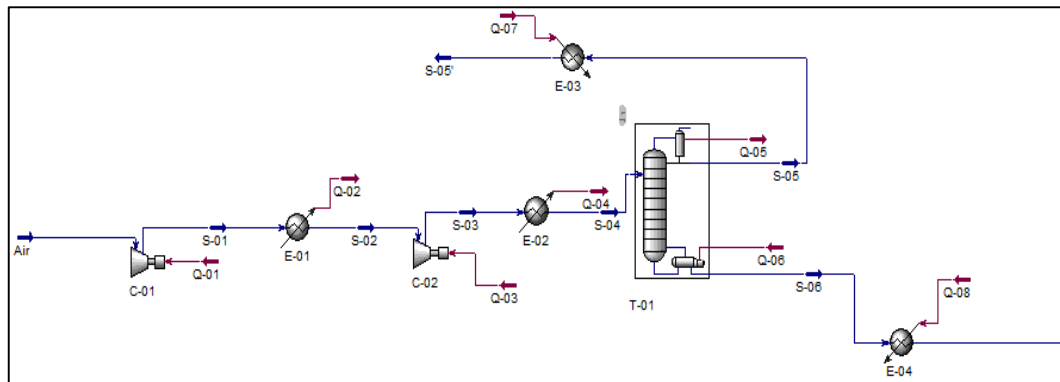
Figure 5-2:Flowsheet of Air Separation Unit (ASU) section in Aspen HYSYS.

### 5.1.2. Syngas section (100)

First, to avoid the formation of carbon in the autothermal reformer (ATR) the natural gas is heated and fed with steam to the pre-reformer to crack the heaver hydrocarbon $C_{2+}$ to $H_2$ and CO mixture (see Table 5-2). Then the output will be heated to and fed to the ATR section at 500 ºC and 25 bar with pure oxygen stream (Oxygen) coming from the air separation unit (ASU).

Table 5-2: Composition of Natural Gas [82].

| Composition | Mol fractions |
|---|---|
| Methane | 0.92 |
| Ethane | 0.03 |
| Nitrogen | 0.05 |

In this equilibrium reactor (R-100) the natural gas stream (NG) will be oxidized with the pure oxygen stream (oxygen) to produce the syngas which are hydrogen ($H_2$) and carbon dioxide (CO) besides other by-products such as water ($H_2O$) and carbon dioxide ($CO_2$). The inlet conditions for the three inlet streams are summarized in Table 5-3 [82]. The reactor temperature will increase to 1050ºC as a result of the complete and partial combustion reactions of methane with oxygen to production

48

syngas as shown in reactions (23-(25) below along with their corresponding enthalpies [75].

Table 5-3: Gas-to-Liquid feedstock conditions [101].

| Input | Temperature ($^o$C) | Pressure (KPa) | Molar flow (kmol/h) |
|---|---|---|---|
| Natural Gas | 25 | | 37540 |
| Steam | 500 | 2500 | 7508 |
| Oxygen | 144 | | 21197 |

$$CH_4 + 1.5\ O_2 \leftrightarrow CO + 2H_2 \qquad \Delta H = 519\ kJ/mole \qquad (23)$$

$$CH_4 + H_2O \leftrightarrow CO + 3H_2 \qquad \Delta H = -206\ kJ/mol \qquad (24)$$

$$CO + H_2O \leftrightarrow CO_2 + H_2 \qquad \Delta H = 41kJ/mol \qquad (25)$$

The outlet stream from this reactor (S-106) contain syngas, along with some side product and unreacted methane. The gas stream (S-106) will be cooled-down through two heat exchangers in series (E-102), (E-103) and (E-104) to reduce the syngas temperature from 1043°C to 38°C at 23 bars pressure to ensure that all produced water in this reactor is condensed. Then a two-phase separation (V-100) will be used separate the gaseous and liquid water. Then a two-phase separation (V-100) will be used separate the gaseous and liquid water. Then will go to $CO_2$ removal unit modeled as a component splitter (X-100).

The ATR was modeled as Gibb's reactor in Aspen HYSYS as represented in Figure 5-3. with a volume of 590 m$^3$ . The syngas ratio depends on the inlet composition of steam to carbon (S:C) where a ratio of 0.6 and even a ration down to 0.2 has been commercially used to obtain an H$_2$/CO ratio of 2 [49]. An S/C ratio of 0.2 was reported in the ATR feed unit and a syngas ration of 2.04. The next process unit in the GTL process is the Fischer-Tropsch reactor (FTR).
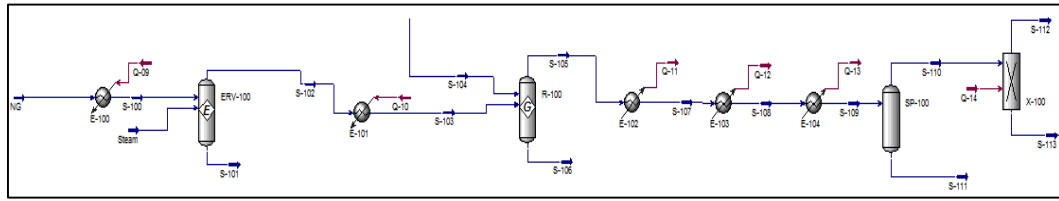
Figure 5-3: Flowsheet of Autothermal (ATR) reaction section (100) in Aspen HYSYS.

### 5.1.3. Fischer Tropsch Reactor Section (200)

The FT unit considers the heart of the GTL method, it is known as a polymerization carbon-chain building-up method to form a longer liquid, gaseous and solid hydrocarbon product [49]. A wide range of clean fuel is produced through the FT process presented in Table 2-1 using a suitable catalyst [51].

The inlet streams in this section (S-109) which is the main outlet stream from the Syngas section (100) and the recycled stream (S-211) from the (SP-200) as illustrated in Figure 5-4. This stream contains mainly syngas ($H_2$ and CO) with a ratio of 2.04 at a T=250 ºC P=20 bar. In the Fischer-Tropsch unit, syngas will be converted in (R-200) using a proprietary catalyst into a wide range of long-chain hydrocarbons as represented in Table 2-1.

This reactor operates adiabatically at a high temperature of 350 ºC to maximize the gasoline yield.

Moreover, the Fischer-Tropsch hydrocarbons are generated in a series of extremely exothermic reactions in which steam will be produced as by-products as shown in the reaction below (26) [50].

$$nCO + (2n)\,H_2 \leftrightarrow \{-CH_2-\}n + nH_2O \qquad (26)$$
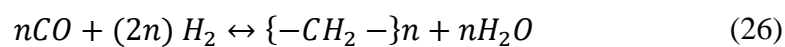
Furthermore, the outlet streams (S-201) and (S-202) will be mixed in the mixer (MIX-

200), and the combined stream (S-203) enters (E-201) to reduce the stream to T=38°C

and P =18bar, before entering the three-phase separator (gas/oil/water) (SP-200). The

unconverted gas stream (S-206) will be compressed in (C-200) to P=20bar and then

will be heated up in (E-203) to T=250°C. Whereas, the water outlet stream (S-207) will

be sent to the treatment unit to remove any dissolved alcohol, to be used later for heating

or cooling application in the plant. Finally, the light hydrocarbons (S-206), will be fed

to the next section for furthered treatment.
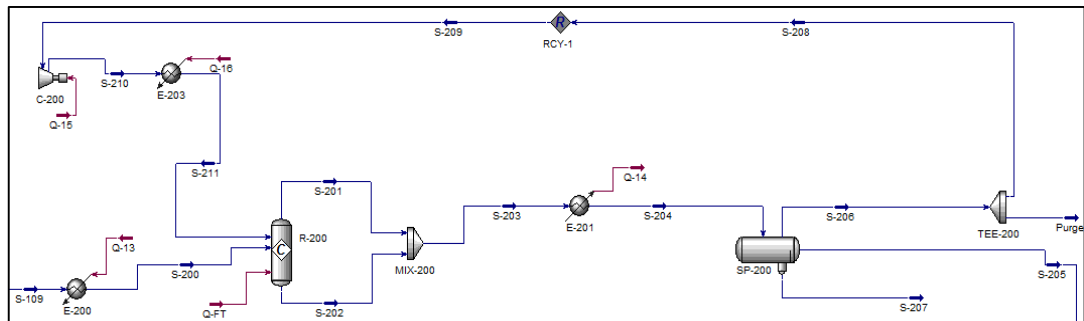


Figure 5-4: Flowsheet of Fischer-Tropsch (FT) reaction section (200) in Aspen

HYSYS.

The probability of the hydrocarbon chain is described using the Anderson Schulz Flory

(ASF).

$$W_n = n(1 - \alpha)^2 \times \left(\alpha^{(n-1)}\right)$$

Where, n is carbon number, $W_n$ is the weight fraction of hydrocarbon and, $\alpha$ value is

known as the probability of chain growth is used to determine the carbon distribution

in th FT process [56].

In addition, one of the major parameters in the FT process is the amount of inlet gas

that is converted to the required product known as carbon efficiency. Moreover, based

on different studies showed that the GTL carbon efficiency ranges from 60 to 80 %

[60].

### 5.1.4. Upgrade Section (300)

In this final section in the Gas-to- Liquid (GTL) plant the Fischer- Tropsch final and intermediate products will be further treated, separated, and refined into high-quality products. The First step is to crack the heavy hydrocarbons (e.g., Wax) which then will be fed to the distillation column to separate the products.

Additionally, the hydrocracking reactor (CRV-300) has two main inlets, stream (S-205) which will be pumped and mixed in (MIX-300) with stream (S-300), then preheated to $T=354^{\circ}C$ and P=80bar in (E-300).

### 5.1.4.1. Hydrocracking Reactor (CRV-300)

The main-stream (S-302) will be cracked and upgraded over a proper catalyst in the present of hydrogen. The reactor (CRV-300) will operate adiabatically at $T=354^{\circ}C$ and P=80bar. In this reactor the heavy hydrocarbons ($C_{21}$-$C_{100}$) in the stream (S-301) will be cracked with hydrogen stream (S-300) as shown in equation (27) and illustrated in Figure 5-5.

$$H_2(g) + C_nH_{2n+2} \rightarrow 2C_{\left(\frac{n}{2}\right)}H_{n+2} \qquad (27)$$
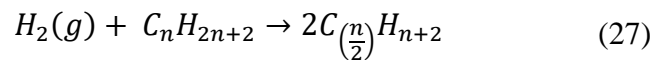
### 5.1.4.2. Refinery Distillation Column (T-300)

This column has only one inlet stream (S-308), the streams (S-304) and (S-305) prior f being fed to the distillation column have been well mixed in (MIX-301), reducing their pressure using the control valve (VLV-300) from 80 bar to 1.01bar, and cooled down in (E-301) from $345^{\circ}C$ to $70^{\circ}C$ to have more liquid fraction. Thus, achieving a degree of separation between the products across this column. However, there is a fundamental difference between the LTFT and HTFT processes are that the HTFT synthesis does not form a bulk liquid phase at synthesis conditions due to the

low α-value. Moreover, in this column the in-flowed hydrocarbons will be distilled into various fractions based on different boiling points and then separate into a valuable product where in this report the aim is to find if LT-FT or HT-FT will maximize gasoline.

For low-temperature Fischer-Tropsch (LT-FT) the simulation was done using a T=240°C, P= 20bar and alpha ($\alpha$) value of 0.88 were selected to find the weight percent fraction represent in Table 2-1 and shown in Figure 5-5.

However, the same procedures were done for the high-temperature Fischer-Tropsch (HT-FT) with a T= 350°C, P=20 bar with alpha ($\alpha$) value of 0.78.
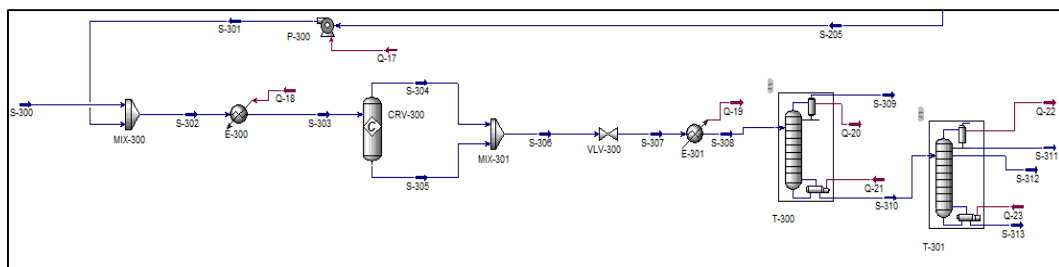


Figure 5-5: Upgrading product Section (300) in Aspen HYSYS for LT-FT.

The following Table 5-4 represents the amount of produced liquids from both high and low-temperature Fischer Tropsch processes. And as shown in Figure 5-6 the selectivity of gasoline is higher at a low $\alpha$ value while, low $\alpha$ value preferred in producing log hydrocarbon chain such as diesel.

Table 5-4:High and Low temperature liquid products.

| Low Temperature (LT-FT) | | |
| --- | --- | --- |
| | kgmol/h | kg/h |
| *LPG* | 265.89 | 13220 |
| *Gasoline* | 1086.52 | 120665 |

Low Temperature (LT-FT)

| | | |
|---|---|---|
| *Diesel* | 1048.27 | 216109 |
| *Wax* | 106.04 | 41583 |
| *Total* | 2506.72 | 391577 |
| *Wastewater* | 42267.37 | 761451 |

High Temperature (HT-FT)

| | | |
|---|---|---|
| *LPG* | 1032.82 | 49471 |
| *Gasoline* | 1959.71 | 199900 |
| *Diesel* | 519.67 | 106107 |
| *Wax* | 24.55 | 9450 |
| *Total* | 3536.74 | 364929 |
| *Wastewater* | 42267.37 | 761451 |
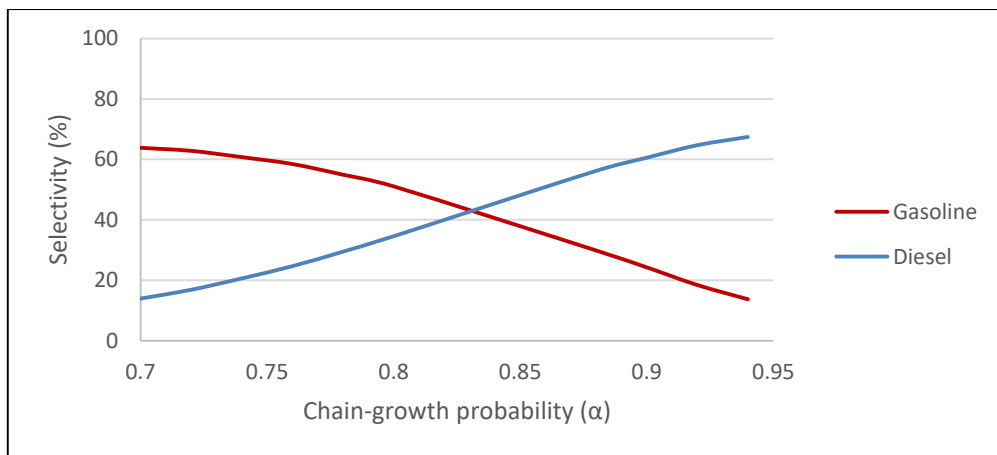


Figure 5-6: Fischer Tropsch Selectivity.

## 5.2. MTG process simulation
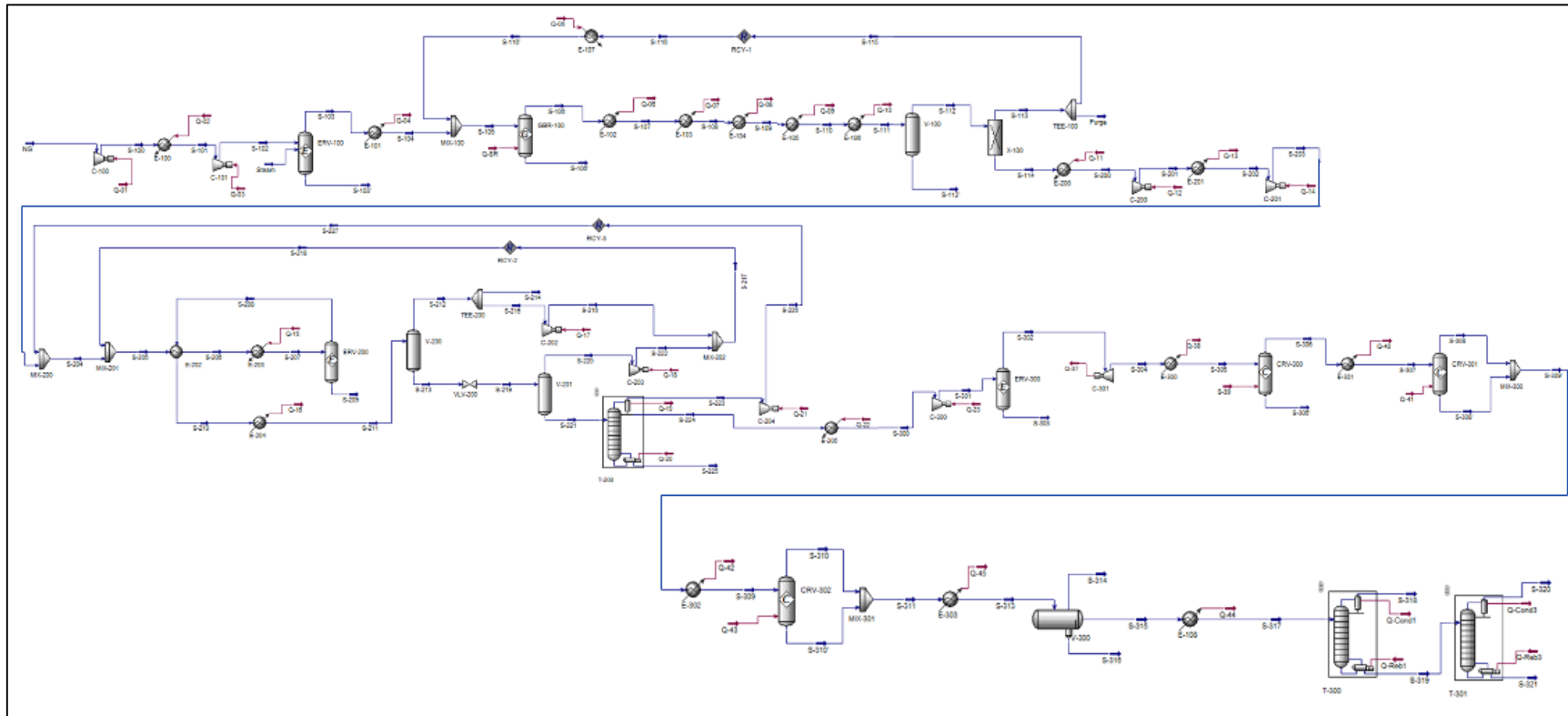


Figure 5-7: Aspen HYSYS process flow diagram of MTG process.

### 5.2.1. Synthesis gas generation section (100)

In this unit the same feed used in the GTL process was fed to the MTG process with different process parameters and with no oxygen shown in Table 5-5. NG stream would be compressed to 30 bar and heated to 345°C through 2 compressors C-100 and C-101 and heater E-100. While steam stream will enter 345°C and 30 bar as well then be fed to pre-former (ERV-100) to convert all HC to methane and then fed to reformer reactor (GBR-100), and a ratio of $H_2$/CO of 4.5:1 was obtained.

Table 5-5: Methanol-to-Gasoline feedstock conditions [101].

| Input | Temperature (°C) | Pressure (kPa) | Molar flow (kmol/h) |
|---|---|---|---|
| Natural Gas | 25 | 2500 | 37540 |
| Steam | 500 | | 112620 |

However, the effluent stream (S-108) from Reactor (GBR-100) will be cool in a series of heaters E-102, E-103, E-104, E-105, and E-106 to a temperature of 10°C. Then syngas will enter water vessel (V-100) to separate the water as illustrated in Figure 5-8. And the outlet stream (S-112) will enter the component splitter to adjust the syngas ratio to 2 before entering the methanol section.
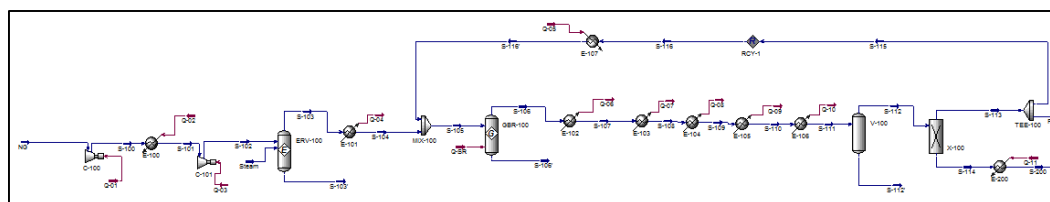


Figure 5-8: Aspen HYSYS process flow diagram of MTG syngas generation unit 100.

### 5.2.2. Methanol section (200)

As illustrated in Figure 5-9 the syngas (S-200) will enter the process at 160℃ and 30 bar and will be compressed in C-200 and C-201 to 110 bars and heated to 150 ℃ by (E-201) before being fed to the methanol reactor (ERV-200), where syngas will be converted to methanol using equations (25) and (26).

Moreover, the effluent stream (S-208) will be cool to 38 ℃ and fed to a separator (V-200) to separate unreacted syngas from methanol. The vapor products (S-212) are split into (S-214) and (S-215) with a ratio of (0.095:0.9050). The liquid stream (S-213) will be reduced to 2 bars before entering a second separator (V-201) to separate the by-product from methanol and water. Additionally, stream (S-215) and stream (S-220) will be compressed to 110 bar through (C-202) and (C-203) before being combined in (MIX-202) and recycled back to the methanol reactor (ERV-200). Furthermore, the outlet stream (S-221) is fed to the distillation column (T-200) at 36.45 ℃ and 2 bars to separate methanol from water and other by-products. Finally, the byproduct stream (S-223) will be compressed to 110 bars in (C-204) and recycled back to the methanol reactor to maximize the methanol production.
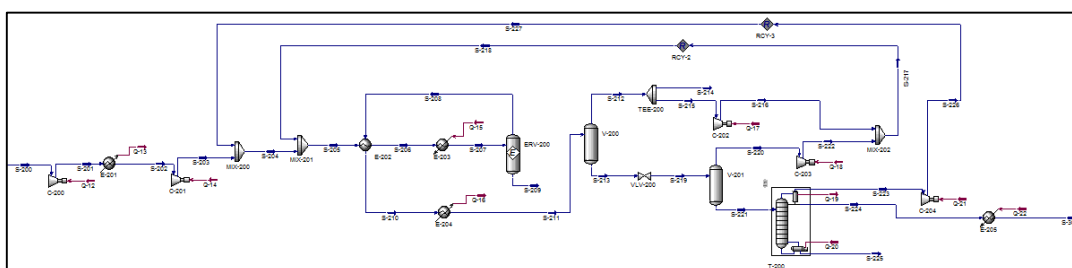


Figure 5-9: Aspen HYSYS process flow diagram of MTG Methanol unit 200.

### 5.2.3. Methanol-to- Gasoline section (300)

The MTG section is shown in Figure 5-10 methanol will be converted dehydrated to generate DME in the reactor (CRV-300) at 310°C and 27 bar, then it will pass through three reactors (CRV-301, CRV-302, and CRV-303) to produce light olefins, to heavy olefins then convert olefins to Paraffins, Naphthene's and Aromatics as shown in the below equation (28) [104].

$$2CH_3OH \underset{+H_2O}{\overset{-H_2O}{\leftrightarrow}} CH_3OCH_3 \xrightarrow{-H_2O} C_2^{2-} - C_5^{2-} \rightarrow \begin{matrix} Paraffins, Cyloparaffins \\ Aromatics \\ C_6^+ Olefins \end{matrix} \qquad (28)$$
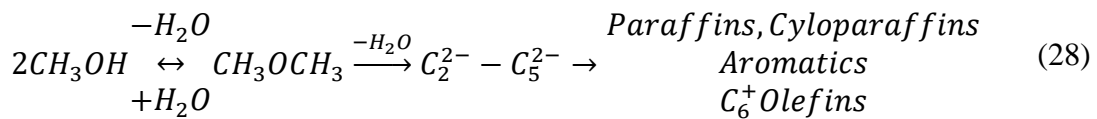
The reactor (CRV-301) will operate isothermally at a temperature of 350°C and 19 bar to generate light and heavy olefins. The reactor effluent (S-30) will be fed to (CRV-302) to convert olefins to paraffins and aromatic. Then naphthene's, durene (1,2,4,5-tetramethylbenzene) and more aromatics will be generated in the reactor (CRV-303) the outlets will be cool-down and enter as three-phase separator at 440°C and 17 bar. Finally, the aqueous stream (S-313) will be cooled down to 40oC and 20.7 bars through (E-304) and fed to distillation columns (T-300) to separate flue gas (S-318) from LPG and Gasoline (S-319). The liquid stream (S-319) will enter the second distillation column (T-301) to separate LPG from Gasoline. The following Table 5-6 represents the amount of produced liquids and wastewater from the MTG process.
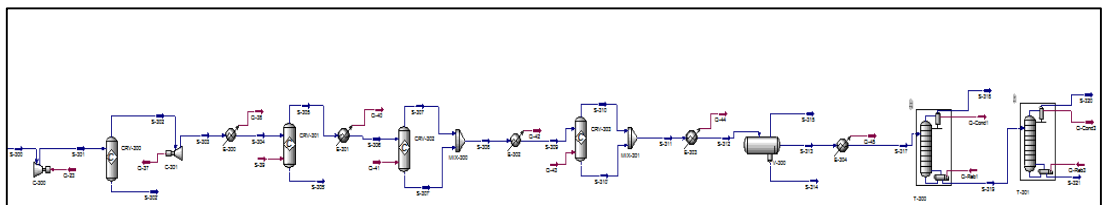


Figure 5-10: Aspen HYSYS process flow diagram of MTG Methanol-to-Gasoline unit 300.

Table 5-6: Methanol to Gasoline Products.

Methanol to Gasoline (MTG)

|  | kgmole/h | kg/h |
|---|---|---|
| Gasoline | 2701.6 | 222687.5 |
| Flue Gas | 251.5 | 7667.0 |
| *LPG* | 630.2 | 35382.4 |
| *Wastewater* | 98077.6 | 1766877.2 |

In this process 60% of the feed is converted to hydrocarbons, where 85% are gasoline, 2% gas and 13% LPG.

## 5.3. Results Discussion

The obtained results reveal that both GTL and MTG processes generate, a higher gasoline yield >5%. The gasoline yield from MTG process is 7% higher than GTL-HTFT process with 5% yield. Moreover, the MTG rout for gasoline production as an alternative to the GTL process is a promising option for NG-rich countries to make the best investing decision in the gas industry. To end the energy poverty, the demand growth in the next few years will be significant, and gasoline supplies is crucial to meet this growth.

The obtained result suggests that the proposed unit's operations have an advantage to enhance the product quality and produce more gasoline. It is believed that the process and the included reaction work in converting the hydrocarbons in the stream to gasoline. This is in agreement with Saad Al-Sobhi et al. [101] results which are presented in Table 5-7. It was observed that the higher yield from MTG is due to either light hydrocarbons was recycled and converted to $C_{5+}$ hydrocarbons or they were converted within the process, from the beginning to $C_{5+}$. Nevertheless, a large amount of wastewater is generated in the MTG process, which is generated from DME and

gasoline reactors, making the MTG process less attractive.

Table 5-7: Gasoline yield comparison with literature.

|  | Gasoline Yield from GTL HTFT | Gasoline Yield from MTG |
| --- | --- | --- |
| Simulation Results | 5% | 7% |
| Literature Results | 6% | 11% |

## 5.4. Conclusion

In conclusion, gasoline is a petroleum-derived liquid used as a transportation fuel and a liquid fuel for industrial applications as a cleaner driving fuel. And the growth in the energy demand imposes the need to establish an alternative route to generate sustainable fuels. Out from the simulation the overall gasoline yield was around 7% from MTG higher than GTL process with only 5% gasoline yield thus, MTG is considered as an alternative technology to GTL.

# Chapter 6 : Economic Evaluation

## 6.1. GTL and MTG Plant Costing

For the plans costing both capital and operating costs were calculated to classify the economic feasibility. The profit formulations are illustrated in the following equations ((29-(30):

$$\text{Net profit} = \frac{\text{Revenue} - \text{TAC}}{\text{Annual Natural gas input}} \qquad (29)$$

$$\text{TAC} = \text{CC}\,\frac{i(1+i)^n}{(1+i)^n - 1} + OC \qquad (30)$$

Where, TAC is the total annualized cost, CC is the capital cost, OC is the operating cost, i is the interest rate evaluated as 8% and n is the project life evaluated as 20 years. Two simulation scenarios have been studied, the first scenario with an air separation unit (ASU) and the second one without ASU. Both economic and environmental and evaluation of both scenarios have been investigated. Where, results indicate that ASU is economically and environmentally not feasible.

Table 6-1, Table 6-2 and Table 6-3 present the economic evaluation for Fischer-Tropsch at Low-Temperature and High-Temperature as well as economic evaluation for Methanol to Gasoline process.

Table 6-1: Results of economic evaluation for Fischer-Tropsch Low Temperature.

| | WITHOUT ASU | WITH ASU |
|---|---|---|
| Feed Amount | | |
| NG (Tonne/d) | 15372 | 15372 |
| Steam (Tonne/d) | 3246 | 3246 |
| $O_2$ (Tonne/d) | 16279 | 16260 |
| Product Amount | | |
| LPG (Tonne/d) | 317.3 | |
| Gasoline (Tonne/d) | 2896.0 | |
| Diesel (Tonne/d) | 5186.6 | |
| Wax (Tonne/d) | 998 | |
| TOTAL PRODUCTS (Tonne/d) | 9397.8 | |
| Feed And Product Prices | | |
| NG ($/Tonne)[82] | 163.73 | 163.73 |
| Steam ($/Tonne)[82] | 4.34 | 4.34 |
| $O_2$ ($/Tonne)[82] | 40 | 0 |
| LPG ($/Tonne)[82] | 338 | 338 |
| Gasoline ($/Tonne)[82] | 1003 | 1003 |
| Diesel ($/Tonne)[82] | 972 | 972 |
| Wax ($/Tonne)[82] | 1411 | 1411 |
| Total Capital Cost ($) | $7.4726 \times 10^7$ | $1.011 \times 10^8$ |
| Total Operating Cost ($/Y) | $7.9648 \times 10^7$ | $1.997 \times 10^8$ |
| Total Raw Materials Cost ($/Y) | $1.1615 \times 10^9$ | $9.2379 \times 10^8$ |
| Total Products Cost ($/Y) | $3.4534 \times 10^9$ | $3.4534 \times 10^9$ |
| Total Utilities Cost ($/Y) | $6.969 \times 10^7$ | $1.784 \times 10^8$ |
| Equipment Cost ($/Y) | $2.827 \times 10^7$ | $6.084 \times 10^7$ |
| Total Installed Cost ($) | $4.234 \times 10^7$ | $7.747 \times 10^7$ |
| Total Annualized Cost ($/Y) | $8.7259 \times 10^7$ | $2.1004 \times 10^8$ |
| Desired Rate of Return [Percent/Year] | 20 | |
| Net Profit Per Input ($/T) | 600 | 578 |
| Carbon Emissions [Tonne/d] (Process) | $8.162 \times 10^4$ | $2.707 \times 10^4$ |
| Net emissions per input | 1.09 | 9.40 |
| Net emissions per output | 1.76 | 15.17 |

Table 6-2: Results of economic evaluation for Fischer-Tropsch High Temperature.

| | WITHOUT ASU | WITH ASU |
|---|---|---|
| Feed Amount | | |
| NG (Tonne/d) | 15372 | 15372 |
| Steam (Tonne/d) | 3246 | 3246 |
| $O_2$ (Tonne/d) | 16279 | 16260 |
| Product Amount | | |
| LPG (Tonne/d) | 1187.3 | |
| Gasoline (Tonne/d) | 4797.6 | |
| Diesel (Tonne/d) | 2546.6 | |
| Wax (Tonne/d) | 226.8 | |
| TOTAL PRODUCTS (Tonne/d) | 8758.3 | |
| Feed And Product Prices | | |
| NG ($/Tonne)[82] | 163.73 | |
| Steam ($/Tonne)[82] | 4.34 | |
| $O_2$ ($/Tonne)[82] | 40 | 0 |
| LPG ($/Tonne)[82] | 338 | |
| Gasoline ($/Tonne)[82] | 1003 | |
| Diesel ($/Tonne)[82] | 972 | |
| Wax ($/Tonne)[82] | 1411 | |
| Total Capital Cost ($) | $8.5468 \times 10^7$ | $1.779 \times 10^8$ |
| Total Operating Cost ($/Y) | $1.0252 \times 10^8$ | $2.730 \times 10^8$ |
| Total Raw Materials Cost ($/Y) | $1.1615 \times 10^9$ | $9.2379 \times 10^8$ |
| Total Products Cost ($/Y) | $2.9231 \times 10^9$ | $2.9231 \times 10^9$ |
| Total Utilities Cost ($/Y) | $8.9699 \times 10^7$ | $2.427 \times 10^8$ |
| Equipment Cost ($/Y) | $3.3881 \times 10^7$ | $9.536 \times 10^7$ |
| Total Installed Cost ($) | $4.9957 \times 10^7$ | $1.396 \times 10^8$ |
| Total Annualized Cost ($/Y) | $1.1123 \times 10^8$ | $2.9108 \times 10^8$ |
| Desired Rate of Return [Percent/'Year] | 20 | |
| Net Profit Per Input ($/T) | 501 | 469 |
| Carbon Emissions [Tonne/d] (Process) | $2.274 \times 10^4$ | $2.707 \times 10^4$ |
| Net emissions per input | 0.75 | 8.65 |
| Net emissions per output | 1.50 | 17.28 |

Table 6-3: Results of economic evaluation for Methanol to Gasoline.

| Feed Amount | |
|---|---|
| NG (Tonne/d) | 15372 |
| Steam (Tonne/d) | 48693 |
| Product Amount | |
| Flue gas (Tonne/d) | 117.4 |
| Gasoline (Tonne/d) | 9336.7 |
| LPG (Tonne/d) | 1483.8 |
| TOTAL PRODUCTS (Tonne/d) | 10938 |
| Feed And Product Prices | |
| NG ($/Tonne)[82] | 163.73 |
| Steam ($/Tonne)[82] | 4.34 |
| LPG ($/Tonne)[82] | 338 |
| Gasoline ($/Tonne)[82] | 1003 |
| Flue-Gas($/Tonne) | - |
| Total Capital Cost ($) | $1.0919 \times 10^8$ |
| Total Operating Cost ($/Y) | $4.7764 \times 10^7$ |
| Total Raw Materials Cost ($/Y) | $9.9579 \times 10^8$ |
| Total Products Cost ($/Y) | $5.4736 \times 10^9$ |
| Total Utilities Cost ($/Y) | $2.6123 \times 10^9$ |
| Equipment Cost ($/Y) | $4.1415 \times 10^7$ |
| Total Installed Cost ($) | $6.6256 \times 10^7$ |
| Total Annualized Cost ($/Y) | $1.0362 \times 10^8$ |
| Desired Rate of Return [Percent/'Year] | 20 |
| Net Profit Per Input ($/T) | 929 |
| Carbon Emissions [Tonne/d] (Process) | $5.743 \times 10^{10}$ |
| Net emissions per input | 0.20 |
| Net emissions per output | 0.48 |

## 6.2. Results Discussion

MTG method has higher capital costs compared to the GTL process, which is balanced by the higher gasoline production and sale cost. As a consequence, the MTG process has a greater net profit per product, with $1345/tonne of product compared to $981/tonne of product form the (LTFT) and $879/tonne of product form the (HTFT) in the GTL example. Similarly, $CO_2$ emissions per-output are lower for the MTG process, with 0.48-ton $CO_2$-equivalent emitted per product against 1.75 (LTFT)

and 1.50 (HTFT) for the GTL process. Furthermore, economic and environmental result from [101] indicates higher NPV from MTG process, with lower carbon emissions.

## 6.3. Conclusion

To Summarize, the LTFT has the lowest capital cost at 74.7 million USD compared to 85.5 million USD for the HTFT, and 109.2 million USD for the MTG process. Furthermore, the MTG is more environmentally friendly than GTL process where $CO_2$ is converted to methanol, reducing climate change, and improving the efficiency of the process. The $CO_2$ emissions emitted per input were measured at around 0.2 out of the MTG compared to 0.75 from HT and 1.09 from LT processes. However, still more research needs to be performed to investigate the.

# Chapter 7 : Environmental Assessment and Mitigation Strategies

This chapter will provide a detailed outcome from GTL and MTG processes on the following environmental aspects.

1. Greenhouse gas (GHG's) contribution.

2. Air pollutants

3. Wastewater Generation

## 7.1.    Greenhouse gaseous (GHGs) contribution

In the natural gas and petroleum industry, the main GHGs that are relevant are carbon dioxide ($CO_2$), methane ($CH_4$) and nitrous oxide ($N_2O$). where these gaseous are emitted at any stage of GTL process from, production, transporting, transferring to GTL, distribution and fuel uses. However, $CO_2$ is the major combustion-related emissions, and because the combustion equipment are not 100 percent efficient methane and other unburned hydrocarbons at emitted into the environment. And last nitrous oxide is a result of both nitrogens in the environment and fuel-bound nitrogen.

## 7.1.1.  For GTL

The GHG emissions from GTL  account for a small percentage of $CO_2$ since 93% of the carbon dioxide is captured in order to minimize the emissions, cost, and equipment size [105].  Shell companies use Well to Wheels (WtW) or the Life Cycle to evaluate the GHG emissions with other industries. And according to the WtW the GTL plant produces 94.3 g eq/ MJ of $CO_2$ from GTL versus 95.1 g eq/ MJ of $CO_2$ from conventional fuel. Shell gas to liquid fuel has two main advantages over conventional fuel, first, GTL has a higher specific energy content which means

that less mass is required to produce the same amount of conventional fuel. Secondary, GTL fuel contains less carbon ratio with a ratio of 2.1 for hydrogen to carbon compare to 1.85 for conventional fuel, leading to shifting the ratio toward $CO_2$ rather than water [106].

### 7.1.2. For MTG

Carbon dioxide (CO) emissions are 0.63 g/ gallon of gasoline equivalent GGC while, $CO_2$ emissions from the MTG is 1466.74 lb/hr [107].

### 7.2. Air Pollutants

### 7.2.2. For GTL

Air pollutants such as nitrogen oxides ($NO_x$) are the contributor to the photochemical smog while, sulfur oxides ($SO_x$) and $NO_x$ are the main reason for acid rain and other environmental problems which can harm human health along with the environment. and The GTL fuels are non-toxic, colorless, odorless and have several beneficial environmental properties. They have a higher octane number (75-80) compare to 50-57 for the conventional fuel, the negligible volume of aromatic compounds, biodegradable, no sulfur and no polycyclic aromatic hydrocarbons (PAH) [108], [109]. Studies show the GTL emits less $SO_x$, $NO_x$, and particulate matter (PM) in a range of 10 to 20%, and also reduces the engine noise [106]. The GTL properties over the conventional are summarized in Table 7-1.

Table 7-1: Gas to Liquid Air Pollutant properties [110].

| GTL properties | Effect | Business Value |
| --- | --- | --- |
| Sulfur free | Improve combustion | Reduce the noise engine. |
| High Cetane number | White smoke | Can support environmental reputation |
| Aromatics free | Odorless and Non-toxic | Safe to handle, with no unpleasant smell. |

| GTL properties | Effect | Business Value |
|---|---|---|
| Biodegradable | Disperses easily | Safe and easy to handle |

### 7.2.3. For MTG

The Air pollution in the MTG fuel is non-toxic, contain no sulfur, and benzene content is very low around 0.3% by volume and high octane number between 82-92% [111]. while $NO_x$ account for 0.09 g/ GGE, $SO_x$ emissions are around 0.2 g/GGC [112]. In general MTG has low pollutant emissions with no soot (PM) no $SO_x$, low $NO_x$ and low $CO_2$ [113].

### 7.3.   Greenhouse Gases Mitigation

Despite the environmental awareness, greenhouse gases in the atmosphere have majorly increased and the impacts associated with the enormous increment caused a significant issue such as global warming. Thus, the level of $CO_2$ in the environment needs to be lower in-order to reach the sustainability vision by 2030. Several strategies have been used to remove $CO_2$. In any process, the emissions start from the source production, during the process, shipping, distribution, and the use of the produced fuel.

A large amount of gas flaring is released into the atmosphere, and according to the world bank around 150-170 billion $m^3$ of gases are vented annually. Thus, many countries have set a regulation in order to reduce these greenhouse gases sources, capturing and using these gases can be predeveloping. So, in the case of large, flared volume it is captured and converted to the more valuable product through GTL and LNG conversion.

While In Norway, the flared gas is injected back in-to the reservoir instead of water which can enhance the production gas. The technique of capturing was

also used in Qatargas and reduced the carbon footprint and emissions by 70% between the years 2004-2011 as illustrated below Figure 7-1 [109]. Beside utilizing the capture $CO_2$, the flue gases produced from the combustion of NG and coal it can be captured and stored in many scenarios for purified industries [114]. However, other strategies could be implemented such as gas renewable and clean energy and increasing energy efficiency by recycling part of unreacted gas is reformer and Fischer-Tropsch unit to reduce the emissions [115].
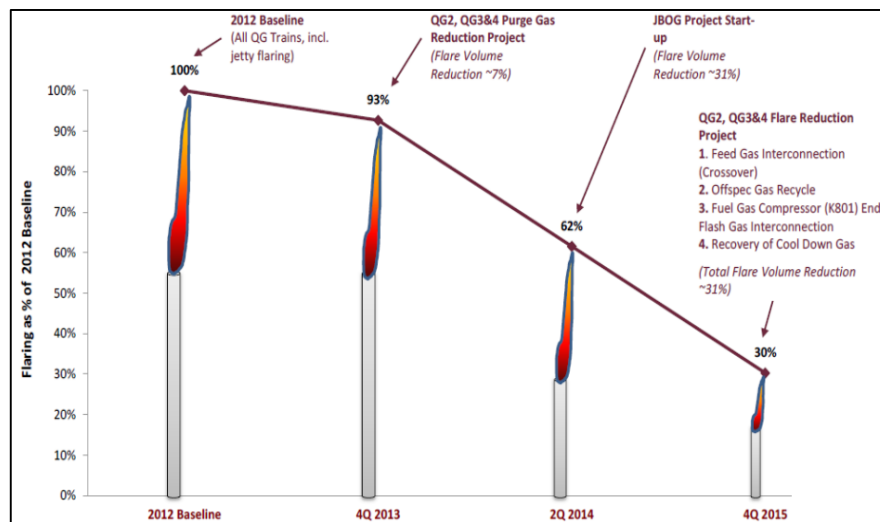


Figure 7-1: Flare Gas Reduction in Qatargas.

## 7.4. Wastewater generation

### 7.4.1. For GTL

The wastewater generated from the GTL process generally contains high constants of total organic carbon (TOC) around 28,910.6-31,530.8 mg/L and chemical oxygen demand (COD) around 118,533-13,116.9 mg/L due to the present of organic acids, ketones, and alcohol and a number of inorganic mixtures such as dissolved gases, bicarbonate acetate, and $CO_2$. Fischer Tropsch process is the main unit result in the

production of the large quantity of oxygenated hydrocarbons and inorganic compounds in wastewater in addition to a small contribution from boilers, syngas units and cooling towers with high-level minerals and dissolved solids. Every ton of GTL fuel results in the production of 1.1-1.3 tons of water however, the amount of water produced in HT-FT is lower compare to the LT-FT [116]. Discharging this huge amount of toxic contaminant water as shown in Table 7-2 can negatively effects the aquatic co-system and human health.

Due to water security, Qatar Shell research and Technology Center (QSETC) and Texas A\$M university in Qatar are doing a pilot-scale research on developing supports of QNV-2030 on water security challenges. With this huge amount of liquid produced from the GTL plant. In a treatment plant with a capacity of 45000 m$^3$/day, wastewater will be treated by reverse osmosis and ultrafiltration. The reverse osmosis brine treatment will be passed through evaporation and

crystallization in this process only crystal salt will be produced [117].

Table 7-2: F-T wastewater composition for different operation conditions.

| Component | Cobalt Catalyst (LTFT) Mass% | Iron Catalyst (HTFT) Mass% |
|---|---|---|
| Non-acidic oxygenated hydrocarbons | 1 | 3.57 |
| Acidic oxygenated hydrocarbons | 0.09 | 0.71 |
| Other hydrocarbons | 0.02 | 0.02 |
| Inorganic compounds | <0.005 | <0.005 |

### 7.4.2. For MTG

The MTG contains TOC and COD as in GTL except that the MTG contains

no alcohol as in GTL and for each yield of gasoline 56% of the product will be associated to wastewater [118].

## 7.5. Wastewater Mitigation

Several technologies have been used in treating the produced wastewater, with different level of success. These treatments include membrane bioreactor, membrane filtration like micro-filtration, nano-filtration ultra-filtration, and reverse osmosis, advance oxidation processes and thermal evaporation. These are used depending on the produced water characteristics [119]. The wastewater in GTL is treated mainly using an-aerobic digestion. The conventional process consists of coarse screening to remove the larger particles, followed by a biological unit using coagulation to remove the soluble materials, a clarifier unit is used next to settle the colloidal particles. Next, the wastewater is sent to the disinfection unit to decrease the biological oxygen demand (BOD) level by adding dis-infection agents and oxidation. A final unit is reducing to reduce the micro-organisms in water by adding chlorine and acid such as sulfuric acid is added to adjust the pH to the desired quality. Sulfuric acid is a very expensive and corrosive chemical so it required special equipment and handling [120].

The wastewater in GTL process is characterized by high total organic carbon (TOC), chemical oxygen demand (COD), ketones, organic acids, and alcohol. So, there is necessary to reduce the wastewater out of the plant, zero liquid discharge (ZLD) illustrated in Figure 7-2 can play a major role in minimizing wastewater discharge and producing high purity water to be reused. The ZLD contains a centrifugal separator, brine filtration, evaporators and dryers as illustrated in the Figure 7-2.
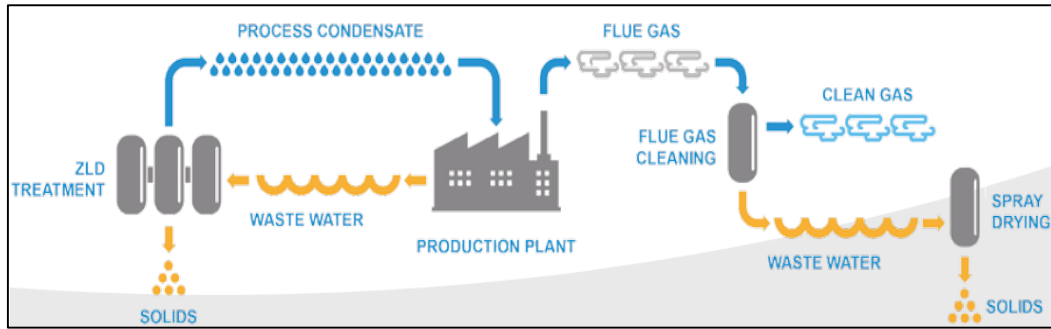
Figure 7-2: Zero Liquid Discharge Process.

The ZLD technology offers an Environmentally friendly and efficient process effluence that improves water reused in the plant, improves product recovery, and converts the discharge liquid to non-liquid waste using the ZLD offers the listed benefits [121].

- Meet the strict discharge regulations.

- Recover and treat valuable products from waste effluence.

- Offer better management.

- Lower the need to use fresh water.

- Minimize energy consumption.

As the climate change action continues to increase, the impact of the $CO_2$ emissions from energy industries, wastewater and catalyst mitigations needs to be considered. Equation (31) has been used to calculate the carbon dioxide emissions from each simulated process. The following section contains the mitigation needed for each simulated case.

$$Net\ Emission = \frac{Stream\ Emissions + Utility\ Emissions}{Hourly\ natural\ gas\ input} \qquad (31)$$

The CO2 emission from utilities $= Q \times EF \times \eta$

Q is the energy for each utility, EF is the emission factor for each utility and $\eta$ is the

efficiency factor for each utility illustrated in Table 7-3.

Table 7-3: Efficiency and emission factors associated with the used utilities.

| Utility | Emission Factor (kg $CO_2$/J NG) | Efficiency factor |
|---|---|---|
| Electricity | $5.589 \times 10^{-5}$ | 0.58 |
| Refrigerant | $5.589 \times 10^{-5}$ | 1 |

## 7.6. Gas to liquid/ Methanol to gasoline emissions

Gas to liquid emissions for both cases low temperature and high temperature with both ASU and with no ASU scenarios were determined. Also, emissions from methanol to gasoline simulation were studied all environmental results are shown in Table 7-4.

Table 7-4: GTL and MTG plant emissions.

| Emissions | Gas to liquid low temperature | |
|---|---|---|
| | With ASU | Without ASU |
| Net emissions | 1.09 | 9.40 |
| Wastewater (tonne/day) | $7.737 \times 10^5$ | $7.728 \times 10^5$ |
| | Gas to liquid high temperature | |
| | With ASU | Without ASU |
| Net emissions | 0.75 | 8.65 |
| Wastewater (tonne/day) | $7.512 \times 10^5$ | $7.506 \times 10^5$ |
| | Methanol to gasoline | |
| Net emissions | 0.20 | |
| Wastewater (tonne/day) | $1.92 \times 10^6$ | |

## 7.7. Gas to liquid/ Methanol to gasoline Mitigations.

The net emissions from both scenarios shown in Table 7-4 showed that the scenario with no ASU is more environmental. However, the emitted $CO_2$ from the

simulated plants can be captured and used in other industrial processes such as the urea plant whereas, mentioned in the literature review chapter that 37 Tonne/h of the captured carbon dioxide was utilized in the urea plant. Moreover, $CO_2$ can be fed to algae to generate biofuel, several commercial technologies such as membranes, amine solvent, and absorbents can be used to capture $CO_2$.

And for the wastewater, the new zero liquid discharge technology can be implemented to treat the huge amount of wastewater.

## 7.8.    Catalysts.

The Fischer Tropsch is an extremely exothermic reaction that will deactivate and reduce the selectivity of the catalyst thus, FT reactor is designed to maximize heat removal. FT reactors are categorized as low and high Fischer Tropsch, the main different between these processes is that no liquid phase will be outside the catalyst particles in the HTFT. Cobalt (Co) and iron (Fe) are commercially used [122].

## 7.9.    Results discussion

| GTL process | MTG process |
| --- | --- |
| **-** Greenhouse gaseous (GHGs) contribution | |
| -  $CO_2$ emission 94.3 g eq/ MJ. <br> -Sulfur free <br> -High octane number (75-80%) <br> -Aromatics free <br> -Biodegradable | -$CO_2$ emission 1466.74 Ib/hr. <br> -Sulfur free <br> -High octane number (82-92%) <br> -Benzene content $< 0.3\%$ /V |
| Greenhouse Gases Mitigation <br><br> -  Captured CO2 and converted it to more valuable product through GTL and LNG conversion. <br> -  Injected back into the reservoir instead of water which can enhance the production of gas. <br> -  It can be captured and stored in many scenarios to purified industries. | |

- Wastewater generation

- High total organic carbon (TOC) around 28,910.6 - 31,530.8 mg/L
- High chemical oxygen demand (COD) around 118,533-13,116.9 mg/L
- GTL process results in the production of 1.1-1.3 tons of water.

- MTG contains TOC and COD as in GTL except that in MTG contains no alcohol.
- 56% of the product will be associated with wastewater.

Wastewater Mitigation

- Qatar Shell research and Technology Center (QSETC) and Texas A$M university at Qatar design a pilot scale with a capacity of 45000 m$^3$/day, to treat GTL wastewater using reverse osmosis and ultrafiltration.
- The necessary to reduce the wastewater out of the plant, zero liquid discharge (ZLD) can play a major role in minimizing wastewater discharge and produce high pure water to be reuse.

## 7.10. Conclusion

In conclusion, both GTL and MTG processes have several beneficial environmental properties over conventional fuel. However, it still contributes to emissions to the environment, with $CO_2$ emission of 94.3 g eq/ MJ and 1466.74 Ib/hr from GTL and MTG processes. Moreover, a massive amount of wastewater around $7.74\times10^5$- $7.51\times10^5$ tons/day was generated from the LT and HT GTL process. Furthermore, 56% of the MTG product about $1.92\times10^6$ tons/day is associated with wastewater. Furthermore, these wastewater contains a high TOC level of 28,910.6 - 31,530.8 mg/L and COD level of 118,533-13,116.9 mg/L is discharge from these processes. Thus, to support of QNV-2030 on water security and sustainability challenges, applying technologies such as injecting back the emissions in-to the reservoir or back into the plant itself shows an enormous enhancement in productivity. And to reduce the massive amount of water used and generated out of these processes, including, ZLD and reverse osmosis and ultrafiltration treatment technologies to reduce the wastewater and reuse it.  Apart from this, water security,

requires a deep study on applying the zero liquid discharge technologies on GTL and MTG.

# Chapter 8 : Energy Management and Optimization

## 8.1. Heat Integration

The objective of this chapter is to minimize the amount of cooling and heating utilities in GTL and MTG plants, by increasing the amount of heat exchange between different streams. This method is designed to use the energy produced from the plant in an economical way to minimize the cost of utilities and environmental impact. The determination of the minimum cooling and heating utilities required from the process of heat integration is done by two methods:

- Graphical method
    - Pinch analysis
- Algebraic method
    - Problem table algorithm

Heat integration is one of the most essential categories for process integration, and the purpose of heat integration is to get the optimum utilization of the energy that is either generated or consumed in types of heat, mechanical, and electrical. This will end to reduce the amount of required external sources and minimize the consumed energy as fuel or electricity.

There are many advantages to applying heat integration, these advantages are listed as follows:

- Process integration is applied while designing the plant at the beginning of the project to optimize the design and plant operational functions.
- Process integration is used to reduce environmental impacts and minimize waste by preventing pollution.
- It increases process flexibility.

- Reducing the operating cost.

- Saving energy, by reducing the use of energy in the plant.

- Reducing the overall energy consumption.

### 8.1.1. Heat integration methods

In heat integration, there are several tools that can be used to reach the desired heat integration for the plant such as the graphical approach, and algebraic approach.

### 8.1.1.1. Graphical Method

It is also known as pinch analysis. The main objective of pinch analysis is to explore the flow of energy within the process, and to find the most economical means to maximize the heat recovery while minimizing the using of external utilities. Pinch analysis is based on the minimum approach temperature definition which represents the capital trade-off energy between obtained energy saving by heat exchange and the investment of required heat exchangers as shown in Figure 8-1.
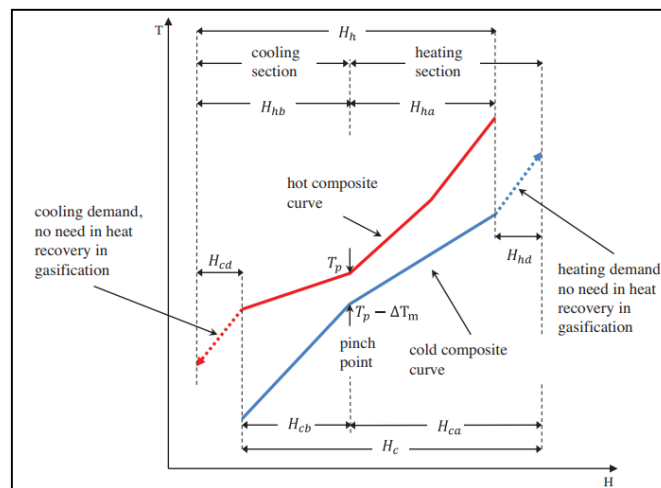


Figure 8-1: Graphic Pinch diagram method.

### 8.1.1.2. Algebraic Method

Also known as the cascade method and the problem table method as shown in

Figure 8-2. Also, it is used more than the graphical method in case there are a lot number of streams involved in the process and it needs to be solved manually using an equation. The algebraic method has a number of characters. These characters are listed below:

- It considers the minimum temperature difference to guarantee thermal feasibility in all temperature intervals by converting the actual temperature of each stream to a temperature interval.

- The algebraic method shows in the Temperature Interval Diagram (TID) any repeated interval temperatures as once.

- This method is thermodynamically viable when the heat extras are cascaded from one interval to the next one.

- This method overcomes negative cascaded values if any occur because it is not thermodynamically feasible since it happens when the temperature takes the wrong direction, and it can be done by adding enough heat to the top of the cascade.

- It removes the minimum cooling requirement as heat at the bottom of the cascade.

- This method is simply does an energy balance for each temperature interval as shown in the Figure 8-3.
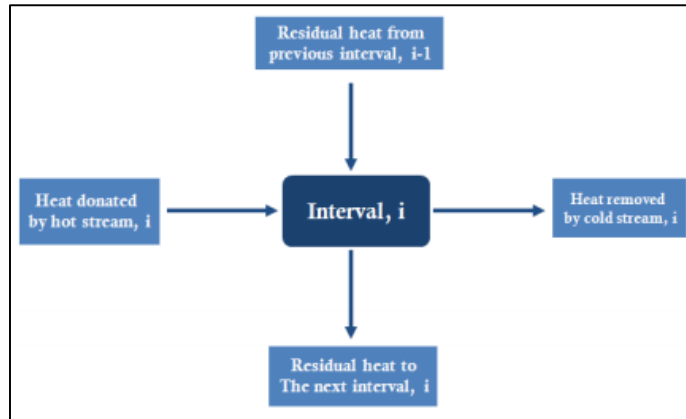
Figure 8-2: Algebraic Method schematic.

$$r_z = HH_z^{Total} - HC_z^{Total} + r_{z-1} \qquad (32)$$
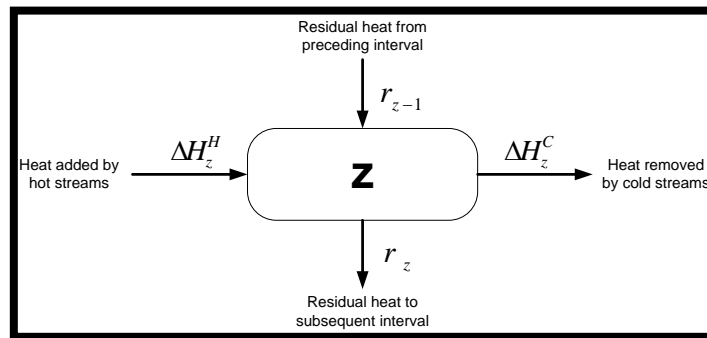


Figure 8-3: Cascade heat balance.

## 8.2. Heat Integration Methodology

To determine the maximum amount of heat that we can recover within the plant and to determine the minimum amount of cooling and heating utilities required. We need to find the pinch point and the excel spread sheet was used to achieve this goal [123].

The required data such as target and supply temperature, flow rate, Mass heat capacity (mCp = Cp) and the minimum allowable temperature $\Delta T_{min}$ for each stream were found using the energy balance and simulation done in Chapter 5.

## 8.3. Heat integration for GTL (LT-FT and HT-FT).

Table 8-1: Heat integration input data for LT-FT.

| Stream Name | Supply Temperature | Target Temperature | Heat Capacity Flowrate | Heat Flow | Stream Type | Supply Shift | Target Shift |
|---|---|---|---|---|---|---|---|
| | °C | °C | MW/K | MW | | °C | °C |
| *NG* | 25 | 455 | 0.500 | 215 | COLD | 30.0 | 460.0 |
| *S-102* | 379.6 | 500 | 0.702 | 85 | COLD | 384.6 | 505.0 |
| *S-105* | 1144 | 693.7 | 1.107 | 499 | HOT | 1139.0 | 688.7 |
| *S-107* | 693.7 | 293.7 | 1.040 | 416 | HOT | 688.7 | 288.7 |
| *S-108* | 293.7 | 38 | 1.056 | 270 | HOT | 288.7 | 33.0 |
| *S-113* | 38 | 240 | 0.848 | 171 | COLD | 43.0 | 245.0 |
| *S-203* | 240 | 38 | 1.079 | 218 | HOT | 235.0 | 33.0 |
| *S-210* | 48.91 | 240 | 0.198 | 38 | COLD | 53.9 | 245.0 |
| *S-302* | 41.19 | 345 | 0.339 | 103 | COLD | 46.2 | 350.0 |
| *S-307* | 309.9 | 70 | 0.303 | 73 | HOT | 304.9 | 65.0 |

Table 8-2: Heat integration input data for HT-FT.

| Stream Name | Supply Temperature | Target Temperature | Heat Capacity Flowrate | Heat Flow | Stream Type | Supply Shift | Target Shift |
|---|---|---|---|---|---|---|---|
| | °C | °C | MW/K | MW | | °C | °C |
| NG | 25 | 455 | 0.500 | 215 | COLD | 30.0 | 460.0 |
| S-102 | 379.6 | 500 | 0.702 | 85 | COLD | 384.6 | 505.0 |
| S-105 | 1144 | 743.7 | 1.111 | 445 | HOT | 1139.0 | 738.7 |
| S-107 | 743.7 | 343.7 | 1.048 | 419 | HOT | 738.7 | 338.7 |
| S-108 | 343.7 | 38 | 1.060 | 324 | HOT | 338.7 | 33.0 |
| S-113 | 38 | 350 | 0.855 | 267 | COLD | 43.0 | 355.0 |
| S-203 | 350 | 38 | 1.231 | 384 | HOT | 345.0 | 33.0 |
| S-210 | 46.36 | 350 | 0.369 | 112 | COLD | 51.4 | 355.0 |
| S-302 | 37.99 | 345 | 0.265 | 81 | COLD | 43.0 | 350.0 |
| S-307 | 308.3 | 70 | 0.226 | 54 | HOT | 303.3 | 65.0 |

The cooling and heating utilities required for the GTL and MTG plant were calculated using the following methods:

1- Graphical (Pinch) Analysis Method.

2- Algebraic Method.

### 8.3.1. Graphical Method



Figure 8-4: Shifted hot and cold composition curves for LT-FT.



Figure 8-5: Shifted hot and cold composition curves for HT-FT.

### 8.3.2. Algebraic Method

| Shift Temperature °C | Interval | $T_{(i+1)}-T_i$ °C | mCp net MW/K | dH MW | | Infeasible Cascade | Feasible Cascade |
|---|---|---|---|---|---|---|---|
| 1139 | | | | | PINCH | 0 | 0 |
| | 1 | 450.3 | 1.107 | 498.484 | surplus | 498.484 | 498.484 |
| 688.7 | | | | | | 498.48 | 498.5 |
| | 2 | 183.7 | 1.0398 | 191.0095 | surplus | 191.01 | 191.01 |
| 505 | | | | | | 689.49 | 689.5 |
| | 3 | 45 | 0.338 | 15.2109 | surplus | 15.2109 | 15.2109 |
| 460 | | | | | | 704.7 | 704.7 |
| | 4 | 75.4 | -0.1617 | -12.1913 | deman | -12.1913 | -12.1913 |
| 384.6 | | | | | | 692.51 | 692.5 |
| | 5 | 34.6 | 0.5401 | 18.6868 | surplus | 18.6868 | 18.6868 |
| 350 | | | | | | 711.2 | 711.2 |
| | 6 | 45.1 | 0.2012 | 9.0746 | surplus | 9.07459 | 9.07459 |
| 304.9 | | | | | | 720.27 | 720.3 |
| | 7 | 16.2 | 0.5043 | 8.1698 | surplus | 8.16976 | 8.16976 |
| 288.7 | | | | | | 728.44 | 728.4 |
| | 8 | 43.7 | 0.5204 | 22.7403 | surplus | 22.7403 | 22.7403 |
| 245 | | | | | | 751.18 | 751.2 |
| | 9 | 10 | -0.5264 | -5.2637 | deman | -5.26374 | -5.26374 |
| 235 | | | | | | 745.92 | 745.9 |
| | 10 | 170 | 0.5527 | 93.9528 | surplus | 93.9528 | 93.9528 |
| 65 | | | | | | 839.87 | 839.9 |
| | 11 | 11.09 | 0.2496 | 2.7677 | surplus | 2.76771 | 2.76771 |
| 53.91 | | | | | | 842.64 | 842.6 |
| | 12 | 7.72 | 0.4481 | 3.4591 | surplus | 3.45907 | 3.45907 |
| 46.19 | | | | | | 846.1 | 846.1 |
| | 13 | 3.19 | 0.7869 | 2.5103 | surplus | 2.51033 | 2.51033 |
| 43 | | | | | | 848.61 | 848.6 |
| | 14 | 10 | 1.6352 | 16.3519 | surplus | 16.3519 | 16.3519 |
| 33 | | | | | | 864.96 | 865 |
| | 15 | 3 | -0.4997 | -1.4991 | deman | -1.49913 | -1.49913 |
| 30 | | | | | | 863.46 | 863.5 |

Hot Pinch 1144 °C — Cold Pinch 1134 °C
Min Hot Utility 0.0 MW — Min Cold Utility 863.46 MW

Figure 8-6: Cascade diagram for LT-FT.

| Shift Temperature °C | Interval | $T_{(i+1)}-T_i$ °C | mCp hot kW/K | dH kW | | Infeasible Cascade | Feasible Cascade |
|---|---|---|---|---|---|---|---|
| 1139 | | | | | PINCH | 0 | 0 |
| | 1 | 400.3 | 1.1112 | 444.7965 | surplus | 444.7965 | 444.7965 |
| 738.7 | | | | | | 444.8 | 444.8 |
| | 2 | 233.7 | 1.0478 | 244.8668 | surplus | 244.8668 | 244.8668 |
| 505 | | | | | | 689.66 | 689.7 |
| | 3 | 45 | 0.346 | 15.5706 | surplus | 15.57059 | 15.57059 |
| 460 | | | | | | 705.23 | 705.2 |
| | 4 | 75.4 | -0.1537 | -11.5887 | demand | -11.5887 | -11.5887 |
| 384.6 | | | | | | 693.65 | 693.6 |
| | 5 | 29.6 | 0.5481 | 16.223 | surplus | 16.22297 | 16.22297 |
| 355 | | | | | | 709.87 | 709.9 |
| | 6 | 5 | -0.6751 | -3.3756 | demand | -3.37564 | -3.37564 |
| 350 | | | | | | 706.49 | 706.5 |
| | 7 | 5 | -0.9403 | -4.7016 | demand | -4.70156 | -4.70156 |
| 345 | | | | | | 701.79 | 701.8 |
| | 8 | 6.3 | 0.2906 | 1.8311 | surplus | 1.831057 | 1.831057 |
| 338.7 | | | | | | 703.62 | 703.6 |
| | 9 | 35.4 | 0.3026 | 10.7105 | surplus | 10.71051 | 10.71051 |
| 303.3 | | | | | | 714.33 | 714.3 |
| | 10 | 238.3 | 0.5282 | 125.8652 | surplus | 125.8652 | 125.8652 |
| 65 | | | | | | 840.2 | 840.2 |
| | 11 | 13.64 | 0.3026 | 4.1269 | surplus | 4.126876 | 4.126876 |
| 51.36 | | | | | | 844.32 | 844.3 |
| | 12 | 8.36 | 0.6712 | 5.6108 | surplus | 5.610822 | 5.610822 |
| 43 | | | | | | 849.94 | 849.9 |
| | 13 | 0.01 | 1.5258 | 0.0153 | demand | 0.015258 | 0.015258 |
| 42.99 | | | | | | 849.95 | 850 |
| | 14 | 9.99 | 1.7909 | 17.8915 | surplus | 17.89151 | 17.89151 |
| 33 | | | | | | 867.84 | 867.8 |
| | 15 | 3 | -0.4997 | -1.4991 | demand | -1.49913 | -1.49913 |
| 30 | | | | | | 866.34 | 866.3 |

Hot Pinch 1144 °C — Cold Pinch 1134 °C
Min Hot Utility 0.0 kW — Min Cold Utility 866.34 kW

Figure 8-7: Cascade diagram for HT-FT.

### 8.3.3. Heat Exchanger Network

The below Figure 8-8 and Figure 8-10 shows the hot and cold streams below the pinch at $\Delta T_{min} = 10°C$. Moreover, two important things point needs to be checked.

1- Number of cold streams more than hot streams $S_{cold} \geq S_{hot}$

2- $Cp_{hot} \geq Cp_{cold}$

Figure 8-8: Grid diagram for the LT-FT.



Figure 8-9: Heat exchanger network for LT-FT.

Table 8-3: Low Temperature FT Integration results.

| Utilities | Heating Utilities | Cooling Utilities |
|---|---|---|
| Before Integration (kW) | $6.12 \times 10^5$ | $1.48 \times 10^6$ |
| After Integration (kW) | 0 | $8.63 \times 10^5$ |
| Saving % | 100% | 41.70 % |

Figure 8-10:Grid diagram for the HT-FT.
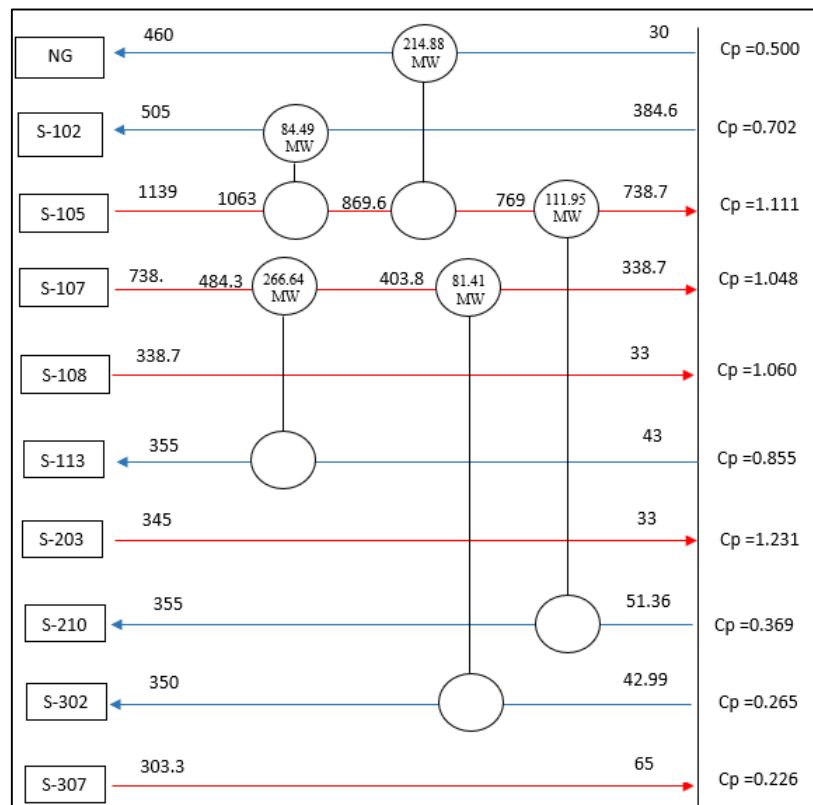


Figure 8-11:Heat exchanger network for HT-FT.

Table 8-4: High Temperature FT Integration results.

| Utilities | Heating Utilities | Cooling Utilities |
|---|---|---|
| Before Integration (kW) | $7.59 \times 10^5$ | $1.63 \times 10^6$ |
| After Integration (kW) | 0 | $8.66 \times 10^5$ |
| Saving % | 100% | 46.9 % |

## 8.4. Heat integration for MTG.

Table 8-5: Heat integration input data for MTG.

| Stream Name | Supply Temperature | Target Temperature | Heat Capacity Flow Flowrate | Heat Flow | Stream Type | Supply Shift | Target Shift |
|---|---|---|---|---|---|---|---|
| | °C | °C | MW/K | MW | | °C | °C |
| S-100 | 110.2 | 268.7 | 0.478 | 76 | COLD | 115.2 | 273.7 |
| S-103 | 321.1 | 345 | 1.792 | 43 | COLD | 326.1 | 350.0 |
| S-106 | 950 | 550 | 3.575 | 1430 | HOT | 945.0 | 545.0 |
| S-107 | 550 | 350 | 3.382 | 676 | HOT | 545.0 | 345.0 |
| S-108 | 350 | 170 | 3.266 | 588 | HOT | 345.0 | 165.0 |
| S-109 | 170 | 70 | 3.595 | 359 | HOT | 165.0 | 65.0 |
| S-110 | 70 | 10 | 3.981 | 239 | HOT | 65.0 | 5.0 |
| S-116 | 10.52 | 345 | 1.239 | 414 | COLD | 15.5 | 350.0 |
| S-114 | 10.52 | 160 | 0.830 | 124 | COLD | 15.5 | 165.0 |
| S-203 | 83.85 | 220 | 11.332 | 1543 | COLD | 88.9 | 225.0 |
| S-205 | 299.6 | 119.6 | 11.161 | 2009 | HOT | 294.6 | 114.6 |
| S-206 | 119.6 | 35 | 11.477 | 971 | HOT | 114.6 | 30.0 |
| S-212 | 76 | 148.2 | 0.815 | 59 | COLD | 81.0 | 153.2 |
| S-302 | 409.3 | 314.4 | 0.683 | 65 | HOT | 404.3 | 309.4 |
| S-306 | 367.9 | 50 | 0.842 | 268 | HOT | 362.9 | 45.0 |
| S-312 | 21.46 | 70 | 0.203 | 10 | COLD | 26.5 | 75.0 |

### 8.4.1. Algebraic Method

Figure 8-12: Cascade diagram for MTG.
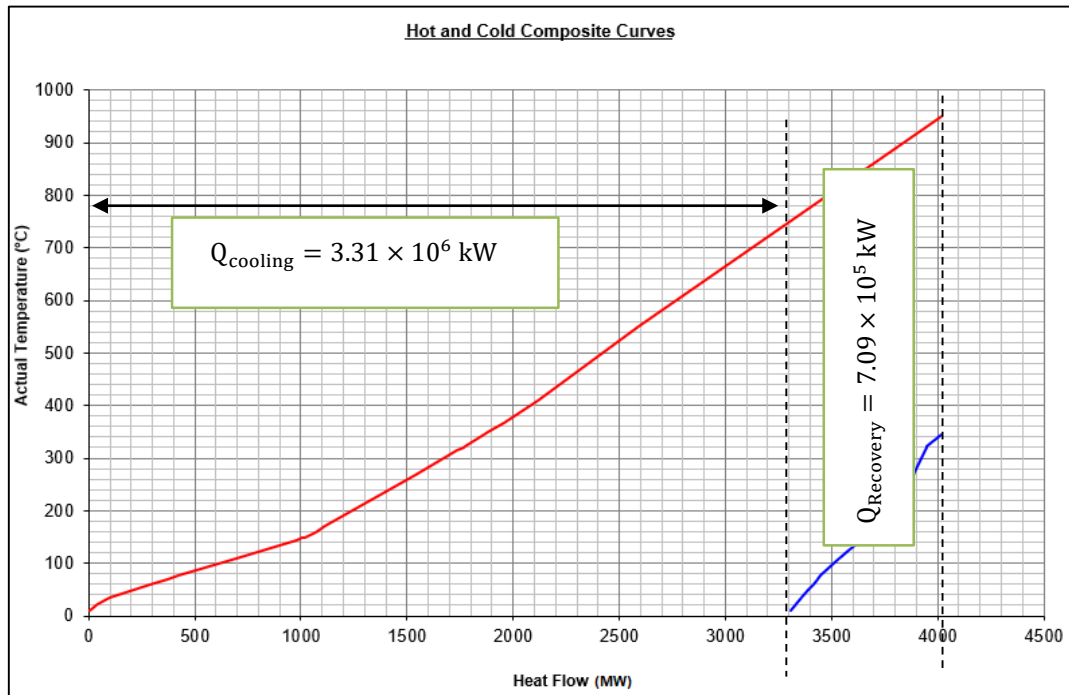


Figure 8-13:Shifted hot and cold composition curves for MTG.

## 8.4.2. Heat Exchanger Network
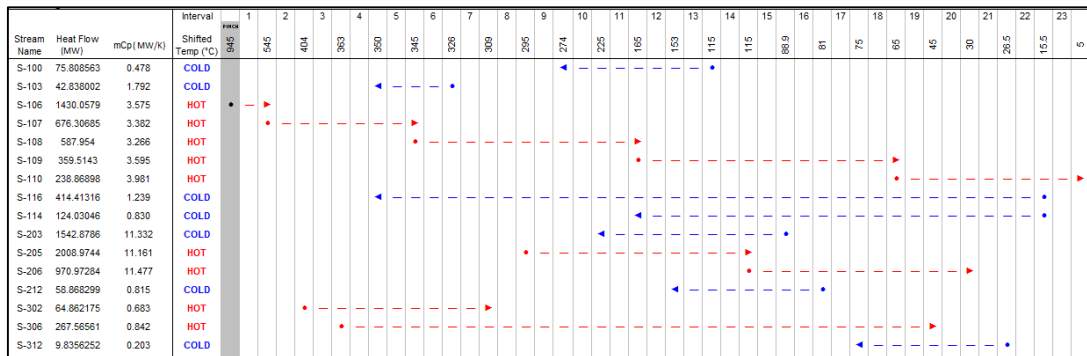


Figure 8-14:Grid diagram for the MTG.
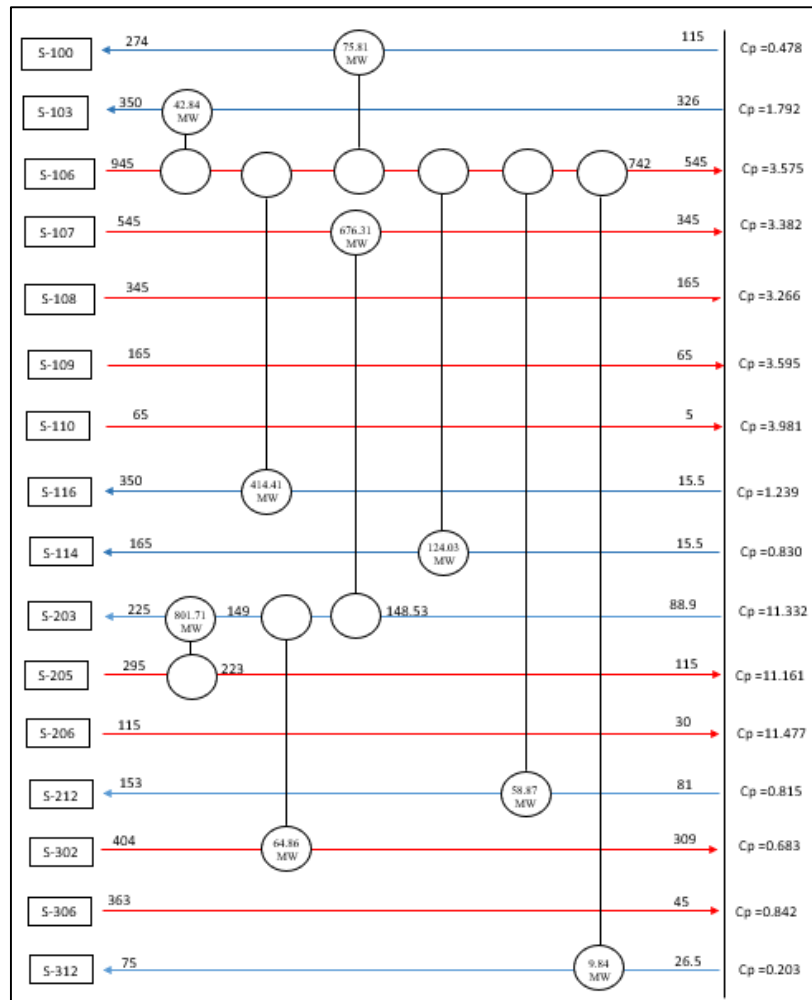
Figure 8-15:Heat exchanger network for MTG.

Table 8-6: Methanol to gasoline Integration results.

| Utilities | Heating Utilities | Cooling Utilities |
|---|---|---|
| Before Integration (kW) | $7.09 \times 10^5$ | $4.02 \times 10^6$ |
| After Integration (kW) | 0 | $3.31 \times 10^6$ |
| Saving % | 100% | 17.7% |

## 8.5. Results discussion

Heat integration (HI) is critical in energy-related applications for increasing energy efficiency and lowering operational costs. Both graphical method and the algebraic method were applied for each process. After performing the HI 100% of

88

heating utilities for MTG and GTL (HT and LT) processes were recovered while, around 42% of cold utilities for LT 47% for HT, and 18% of cold utilities for MTG were recovered.

## 8.6. Conclusion

Using HI is crucial to reduce the environmental impacts and minimize the waste by preventing pollution, saving energy by reducing the use of energy in the plant by reducing the overall energy consumption in the plant which reduces the operating cost, and increases the process flexibility. In addition, identifying the pinch point aided in determining the maximize energy recovery in the system. The heating utilities for MTG and GTL (HT and LT) processes were recovered by 100%, while the cooling utilities were recovered by 42%, 47%, and 18% for LT, HT, and MTG. As a result, reducing the external cooling and heating energy required.

Furthermore, the pinch analysis reduced the generated $CO_2$ emissions by 44%, 76%, and 3% from LT, HT, and MTG processes.

# Chapter 9 : Conclusion and Future Recommendations

## 9.1. Sustainable GTL

Since Paris agreement in 2015, all developing and developed countries adopted the international agreement to reduce the global emissions targets for 2030 [124]. One of the most pressing concerns facing the world today is the search for a sustainable carbon-free source of energy. The increasing threat of climate change is driving the development of innovative technologies for energy generation [125]. Thus, the world today needs to reduce its reliance on oil and coal and establish alternative clean fuels to meet future needs[126].

Natural Gas (NG) emits 50 to 60 percent less carbon dioxide ($CO_2$) than other fossil [1]. GTL, On the other hand, is proving to be one of the most significant oil and gas sector developments in recent years. The method has made it possible to profit from NG, and businesses worldwide are adopting it for a variety of reasons, including environmental, political, and financial. However, since the combustion equipment is 100% efficient CH4 and other unburned HC are emitted into the environment with a huge amount of wastewater to be treated.

Thus, several technologies have been discussed in the literature in-order to lower greenhouse gas emissions and increase product yield. some of these technologies such as the use of new syngas or FT reactor, new catalyst or integrating of the process with other plants which have been discussed in detail in Chapter 3 (literature review) and Chapter 8 (environmental assessment and mitigation strategies) Results as shown in Table 9-1.

Table 9-1: Sustainable Innovation technologies Comparison.

| Syngas unit | | |
|---|---|---|

**1- Chemical looping**

| Advantages | Disadvantages | References |
|---|---|---|
| ➤ Lower capital cost (25-40%) compares to conventional process.<br>➤ Smaller footprints.<br>➤ No air separator is needed.<br>➤ Low pressure is required for high conversion of syngas.<br>➤ High concentrations of $H_2/CO$ can be produced without the need for an excess amount of reactant to be co-fed with the NG.<br>➤ Does not require heat.<br>➤ Directly produce high-quality of hydrogen fuel.<br>➤ The indirect contact between O2 and CH4 eliminate the explosion risk at high temperature.<br>➤ catalyst should meet certain conditions to be feasible in industry application. | - Less research attention<br>- Limited experimental data for the novel CL-SMR and CLC coupling process | [90], [91], [127]–[129] |

**2- Gas-steam/CO2 reforming**

| Advantages | Disadvantages | References |
|---|---|---|
| ➤ Variety of commercialized products generated from CO2 such as syngas, building material, polymers, and chemicals.<br>➤ The lower capital cost compares to the conventional process.<br>➤ Smaller footprints.<br>➤ $CO_2$ is used to co-fed with NG instead of $O_2$.<br>➤ No air separator is needed.<br>➤ There are many advantages of using $CO_2$.<br>➤ $H_2/CO = 2.17$.<br>➤ Carbon efficiency = 92%, Methane conversion = 84%<br>➤ $CO_2$ reformer is 5.04 MMscfd.<br>➤ Steam/CO2 method vs. the conventional comparison process is summarized in Table 2-1. | | [80], [81], [103], [130], [131] |

| Advantages | Disadvantages | References |
|---|---|---|

**Fisher- Tropsch synthesis unit**

1- Advanced CANS Reactor

| Advantages | Disadvantages | References |
|---|---|---|
| ➢ The lower capital cost compares to the conventional process. <br> ➢ Reduce Pressure drop (ΔP). <br> ➢ Smaller catalyst is used to improve selectivity and productivity. <br> ➢ Loaded with a different type of catalysts at the top and bottom. <br> ➢ Combine FT unit and Cracking unit | The presence of water might affect catalyst performance | Error! Reference source not found.[92] |

2- Microchannel Reactor (MCR)

| Advantages | Disadvantages | References |
|---|---|---|
| ➢ Used for the production of syngas for small industrial application since the 1990s. <br> ➢ Enhancing the heat transfer, controlling the reactor temperature, and reducing the pressure drop. <br> ➢ Reduce the formation of the hot spot. <br> ➢ $H_2/CO$ value of 2 can be achieved. <br> ➢ Reduced the freshwater required for the process. <br> ➢ 72 % and 80 % CO conversion | -No commercial plants are yet available <br> - more research is needed to determine the role of CoO-Co. | Error! Reference source not found. [36], [93], [132]–[134] |

**GTL integration**

Integrated GTL with Ammonia and Urea synthesis

| Advantages | Disadvantages | References |
|---|---|---|
| ➢ Lower capital cost compares to standalone. <br> ➢ 37 Tonne/h of $CO_2$ captured from GTL is utilized in the Urea plant. <br> ➢ Minimize the $CO_2$ emissions by 52.8 Tonne/h. <br> ➢ Maximize the profit of both plants and the GHG emissions as well. <br> ➢ Ammonia capacity 576 Tonne/day and 12000bbl/day GTL products. <br> ➢ - 50% increase in the profitability. | | [37], [135] |

## 9.2. Future Work

This thesis provides comprehensive detailed evaluations of GTL both HT and LT also, and the MTG plants. Moreover, few future points need to be taken into consideration to helps to identify potential downstream value-added items and make relevant investment decisions.

Such as, improving solvent usage and wastewater management through implementing technology sch as ZLD. Strategies to reduce greenhouse gas (GHG) emissions from the GTL and MTG processes. And integration of GTL plants with other technology or the use of new reactors in-order to overcome some limitations with the GTL plant .

Furthermore, more research on MTG such as lowering the capital and operating cost, is to be wildly adopted.

## 9.3. Conclusion

This study has provided comprehensive detailed analysis of GTL and MTG plants. Gas to liquid and Methanol to gasoline plants were modeled and simulated using Aspen HYSYS v11. Different α has been performed and the highest gasoline for both high and low-temperature Fischer Tropsch was determined. Moreover, economic evaluation, environmental assessment and mitigation strategies, energy management and optimization and sustainability assessment. Both GTL and MTG processes from natural gas were studied and addressed throughout the thesis.

As a consequence, The results from the simulation showed that the MTG process has a greater net profit per product, with $1345 per tonne of the product against $981 per tonne of product from LTFT and $879 per tonne of product from HTFT in the GTL example. Similarly, $CO_2$ emissions per product are lower for the MTG process, with 0.2-ton $CO_2$-e emitted per product against 1.50 (HTFT) and 1.75 (LTFT) for the GTL process.

93

However, Fischer Tropsch (FT) has advantages over methanol to gasoline, where HC is directly produced from syngas rather than converting it to methanol and hydrocarbons.

# REFERENCES

[1]     ONU, *World population prospects 2019*, no. 141. 2019.

[2]     D. A. Wood, C. Nwaoha, and B. F. Towler, "Gas-to-liquids (GTL): A review of an industry offering several routes for monetizing natural gas," *J. Nat. Gas Sci. Eng.*, vol. 9, pp. 196–208, 2012, doi: 10.1016/j.jngse.2012.07.001.

[3]     BP, "Statistical Review of World Energy globally consistent data on world energy markets . and authoritative publications in the field of energy The Statistical Review world of World Energy and data on world energy markets from is The Review has been providing,"        p.        66,        2020,        [Online].        Available: https://www.bp.com/content/dam/bp/business-sites/en/global/corporate/pdfs/energy-economics/statistical-review/bp-stats-review-2020-full-report.pdf.

[4]     International Energy Agency, "Gas Market Report," *Gas Mark. Highlights 2021*, p. 8, 2022.

[5]     B.P. Statistical Review, "Statistical Review of World Energy globally consistent data on world energy markets . and authoritative publications in the field of energy," *BP Energy Outlook 2021*, vol. 70, pp. 8–20, 2021.

[6]     British Petroleum, "Statistical Review of World Energy 2021," *BP Energy Outlook 2021*, vol. 70, pp. 8–20, 2021.

[7]     F. G. Becker *et al.*, "No 主観的健康感を中心とした在宅高齢者における 健康関連指標に関する共分散構造分析Title," *Syria Stud.*, vol. 7, no. 1, pp. 37–72, 2021, [Online].                                                                       Available: https://www.researchgate.net/publication/269107473_What_is_governance/link/54817 3090cf22525dcb61443/download%0Ahttp://www.econ.upf.edu/~reynal/Civil wars_12December2010.pdf%0Ahttps://think-asia.org/handle/11540/8282%0Ahttps://www.jstor.org/stable/41857625.

[8]     R. Gill, "2021 Hydropower Status Report - International Hydropower Association

Reduced file size," 2020.

[9]     World Nuclear Association, "World Nuclear Performance Report 2022," pp. 6–15, 2022, [Online]. Available: http://world-nuclear.org/getmedia/b9d08b97-53f9-4450-92ff-945ced6d5471/world-nuclear-performance-report-2016.pdf.aspx.

[10]    "Global Energy Review 2019," *Glob. Energy Rev. 2019*, 2020, doi: 10.1787/90c8c125-en.

[11]    J.-B. Dubreuil, "Gas Market Report," *Gas, Coal Power Mark. Div.*, 2022.

[12]    E. Stanley Toochukwu *et al.*, "Economics of Gas-to-Liquids (GTL) Plants," *Pet. Sci. Eng.*, vol. 3, no. 2, p. 85, 2019, doi: 10.11648/j.pse.20190302.17.

[13]    M. A. Arefin, M. N. Nabi, M. W. Akram, M. T. Islam, and M. W. Chowdhury, "A Review on Liquefied Natural Gas as Fuels for Dual Fuel Engines: Opportunities, Challenges and Responses," *Energies*, vol. 13, no. 22, p. 6127, 2020, doi: 10.3390/en13226127.

[14]    W. Maqbool, S. J. Park, and E. S. Lee, "Gas-to-liquid process optimization for different recycling configurations and economic evaluation," *Ind. Eng. Chem. Res.*, vol. 53, no. 22, pp. 9454–9463, 2014, doi: 10.1021/ie500616j.

[15]    P. Balasubramanian, I. Bajaj, and M. M. F. Hasan, "Simulation and optimization of reforming reactors for carbon dioxide utilization using both rigorous and reduced models," *J. CO2 Util.*, vol. 23, no. December 2017, pp. 80–104, 2018, doi: 10.1016/j.jcou.2017.10.014.

[16]    H. Gai, K. Zheng, J. Lin, and H. H. Lou, "Process Simulation, Economic and Environmental Sustainability Assessment of a Gas-To-Liquids Process," *J. Chem. Eng. Process Technol.*, vol. 09, no. 01, pp. 1–10, 2018, doi: 10.4172/2157-7048.1000373.

[17]    S. Liu, J. He, D. Lu, and J. Sun, "Optimal integration of methanol-to-gasoline process with organic Rankine cycle," *Chem. Eng. Res. Des.*, vol. 154, pp. 182–191, 2020, doi: 10.1016/j.cherd.2019.11.036.

[18]    A. Rafiee and M. Panahi, "Optimal Design of a Gas-to-Liquids Process with a Staged

Fischer-Tropsch Reactor," *Chem. Eng. Technol.*, vol. 39, no. 10, pp. 1778–1784, 2016, doi: 10.1002/ceat.201600040.

[19] K. Moen, "Modelling and Optimization of a GTL Plant," no. June, 2014.

[20] R. M. de Deugd, *Fischer-Tropsch Synthesis Revisited; Efficiency and Selectivity Benefits from Imposing Temporal and/or Spatial Structure in the Reactor*. 2004.

[21] C. Us, F. Publications, A. Us, and F. Trial, "The future of Gas-To-Liquid ( GTL ) industry," pp. 2–3, 2018.

[22] G. Report, G. Type, and E. User, "Global Gas-to-liquid ( GTL ) Market 2022-2026 User license Our reports have been used by over 10K customers , including : Get Industry Insights . Simply . Generators Market Research Report by Fuel Type , Power Rating , Generator Type , End User , Region -," no. March, 2022.

[23] F. J. Keil, "Methanol-to-hydrocarbons: Process technology," *Microporous Mesoporous Mater.*, vol. 29, no. 1–2, pp. 49–66, 1999, doi: 10.1016/S1387-1811(98)00320-5.

[24] J. Nyari, "Techno-economic feasibility study of methanol plant using CO2 and H2," *Master Thesis*, p. 55+14, 2018, [Online]. Available: http://urn.fi/URN:NBN:fi:aalto-201811135745%0A[urn].

[25] S. S. Araya *et al.*, "A review of the methanol economy: The fuel cell route," *Energies*, vol. 13, no. 3, 2020, doi: 10.3390/en13030596.

[26] O. Chemical and E. Handbook, "Chemical Economics Handbook," *Text*, no. August, pp. 1–4, 2021.

[27] R. Store *et al.*, "Methanol Market by Feedstock (Coal, Natural Gas, Others), by End-use Industry (Automotive, Construction, Electronics, Appliances, Paints and Coatings, Insulation, Pharmaceutical, Packaging, Others): Global Opportunity Analysis and Industry Forecast, 2021-," vol. 5285, [Online]. Available: https://www.alliedmarketresearch.com/methanol-market-A16496.

[28] R. Only, "Methanol Market by Feedstock (Coal, Natural Gas, and Others), End-use Industry (Automotive, Construction, Electronics, Appliances, Paints & Coatings,

Insulation, Pharmaceutical, Packaging, and Others), and Regional Analysis (North America, Europe, Asia-Pa," vol. 4454, 2022, [Online]. Available: https://www.researchdive.com/8500/methanol-market.

[29]    Future Fuel Stategies, "Methanol: A Future-Proof Fuel," vol. 1072, no. February, p. 42, 2020.

[30]    T. O. F. Contents, "MethanexCorporation."

[31]    M. Curie, "PhD Thesis Novel catalysts for chemical CO 2 utilization," pp. 18–21, 2016.

[32]    I. Dybkjær and T. S. Christensen, "Syngas for large scale conversion of natural gas to liquid fuels," *Stud. Surf. Sci. Catal.*, vol. 136, no. 11, pp. 435–440, 2001, doi: 10.1016/s0167-2991(01)80342-6.

[33]    M. Panahi, A. Rafiee, S. Skogestad, and M. Hillestad, "A natural gas to liquids process model for optimal operation," *Ind. Eng. Chem. Res.*, vol. 51, no. 1, pp. 425–433, 2012, doi: 10.1021/ie2014058.

[34]    M. Panahi, S. Skogestad, and R. Yelchuru, *Steady State Simulation for Optimal Design and Operation of a GTL Process*, no. 2004. Elsevier B.V., 2010.

[35]    O. Of and W. E. Production, "Modelling and Optimization of Eurycoma," no. June, 2013.

[36]    G. R. S. Santos, O. M. Basha, R. Wang, H. Ashkanani, and B. Morsi, "Techno-economic assessment of Fischer-Tropsch synthesis and direct methane-to-methanol processes in modular GTL reactors," *Catal. Today*, 2020, doi: 10.1016/j.cattod.2020.07.012.

[37]    M. Ziaei, M. Panahi, M. A. Fanaei, A. Rafiee, and K. R. Khalilpour, "Maximizing the profitability of integrated Fischer-Tropsch GTL process with ammonia and urea synthesis using response surface methodology," *J. CO2 Util.*, vol. 35, pp. 14–27, Jan. 2020, doi: 10.1016/j.jcou.2019.08.019.

[38]    J. G. Speight, *Synthesis gas and the Fischer–Tropsch process*. 2020.

[39]    J. Baltrusaitis and W. L. Luyben, "Methane Conversion to Syngas for Gas-to-Liquids (GTL): Is Sustainable CO2 Reuse via Dry Methane Reforming (DMR) Cost

Competitive with SMR and ATR Processes?," *ACS Sustain. Chem. Eng.*, vol. 3, no. 9, pp. 2100–2111, 2015, doi: 10.1021/acssuschemeng.5b00368.

[40] G. A. Ozin, "Syngas production for gas-to-liquids applications: technologies, issues and outlook," *Joule*, vol. 1, no. 1, pp. 19–23, 2001, doi: 10.1016/j.joule.2017.08.010.

[41] a. a. El Shamy and a. M. Zayed, "Gas to liquids technology: a futuristic view," *Tesce*, vol. 30, no. 2, pp. 89–111, 2004.

[42] R. L. Keiski, S. Ojala, M. Huuhtanen, T. Kolli, and K. Leiviskä, *Partial oxidation (POX) processes and technology for clean fuel and chemical production*. Woodhead Publishing Limited, 2011.

[43] R. Copeland, Y. Gershanovich, and B. Windecker, "High Efficiency Syngas Generation," no. February, pp. 1–30, 2005, [Online]. Available: http://www.osti.gov/energycitations/product.biblio.jsp?osti_id=840258.

[44] P. K. Bakkerud, "Update on synthesis gas production for GTL," *Catal. Today*, vol. 106, no. 1–4, pp. 30–33, 2005, doi: 10.1016/j.cattod.2005.07.147.

[45] M. El-halwagi, M. S. Mannan, and F. Eljack, "MULTI-OBJECTIVE ANALYSIS OF A GAS-TO-LIQUID ( GTL ) PROCESS FROM ECONOMIC , SAFETY , AND ENVIRONMENTAL PERSPECTIVES," no. August, 2017.

[46] K. Aasberg-Petersen, T. S. Christensen, C. S. Nielsen, and I. Dybkjær, "Recent developments in autothermal reforming and pre-reforming for synthesis gas production in GTL applications," *Fuel Process. Technol.*, vol. 83, no. 1-3 SPEC., pp. 253–261, 2003, doi: 10.1016/S0378-3820(03)00073-0.

[47] X. Hao, M. E. Djatmiko, Y. Xu, Y. Wang, J. Chang, and Y. Li, "Simulation analysis of a gas-to-liquid process using aspen plus," *Chem. Eng. Technol.*, vol. 31, no. 2, pp. 188–196, 2008, doi: 10.1002/ceat.200700336.

[48] H. R. Shahhosseini, S. Saeidi, S. Najari, and F. Gallucci, "Comparison of conventional and spherical reactor for the industrial auto-thermal reforming of methane to maximize synthesis gas and minimize CO2," *Int. J. Hydrogen Energy*, vol. 42, no. 31, pp. 19798–

19809, 2017, doi: 10.1016/j.ijhydene.2017.06.192.

[49]   M. Jose and L. I. S. Arias, "Optimization Study of To-Liquid ( Gtl ) Process Using Aspen Hysys," no. June, 2019.

[50]   Y. Cheng, M. Qiao, and B. Zong, *Fischer-Tropsch Synthesis*, vol. 3. Elsevier, 2017.

[51]   J. G. Speight, *Production of syngas, synfuel, bio-oils, and biogas from coal, biomass, and opportunity fuels*. Elsevier Ltd, 2016.

[52]   S. Mehariya *et al.*, "Fischer–Tropsch synthesis of syngas to liquid hydrocarbons," in *Lignocellulosic Biomass to Liquid Biofuels*, Elsevier, 2020, pp. 217–248.

[53]   M. Martinelli, M. K. Gnanamani, B. Demirel, S. LeViness, G. Jacobs, and W. Shafer, "An Overview of Fischer Tropsch Process: Catalysts, Reactors and XtL Processes," *Appl. Catal. A Gen.*, p. 117740, 2020, doi: 10.1016/j.apcata.2020.117740.

[54]   R. Guettel, U. Kunz, and T. Turek, "Reactors for Fischer-Tropsch synthesis," *Chem. Eng. Technol.*, vol. 31, no. 5, pp. 746–754, 2008, doi: 10.1002/ceat.200800023.

[55]   J. G. Speight, "The Fischer−Tropsch Process," *Gasif. Unconv. Feed.*, pp. 118–134, 2014, doi: 10.1016/b978-0-12-799911-1.00005-4.

[56]   H. A. Choudhury, S. Chakma, and V. S. Moholkar, *Biomass Gasification Integrated Fischer-Tropsch Synthesis: Perspectives, Opportunities and Challenges*. 2015.

[57]   S. Saeidi, M. T. Amiri, N. A. S. Amin, and M. R. Rahimpour, "Progress in reactors for higherature fischer-tropsch process: Determination place of intensifier reactor perspective," *Int. J. Chem. React. Eng.*, vol. 12, no. 1, pp. 639–664, 2014, doi: 10.1515/ijcre-2014-0045.

[58]   A. P. Steynberg, M. E. Dry, B. H. Davis, and B. B. Breman, *Fischer-Tropsch reactors*, vol. 152. Elsevier B.V., 2004.

[59]   M. M. Martín, *Syngas*. 2016.

[60]   M. Zarandi, M. Panahi, and A. Rafiee, "Simulation of a Natural Gas-to-Liquid Process with a Multitubular Fischer-Tropsch Reactor and Variable Chain Growth Factor for Product Distribution," *Ind. Eng. Chem. Res.*, vol. 59, no. 43, pp. 19322–19333, 2020,

doi: 10.1021/acs.iecr.0c01951.

[61]   A. H. Sahir, Y. Zhang, E. C. D. Tan, and L. Tao, "Understanding the role of Fischer–Tropsch reaction kinetics in techno-economic analysis for co-conversion of natural gas and biomass to liquid transportation fuels," *Biofuels, Bioprod. Biorefining*, vol. 13, no. 5, pp. 1306–1320, 2019, doi: 10.1002/bbb.2035.

[62]   A. Behroozsarand and A. Zamaniyan, "Simulation and optimization of an integrated GTL process," *J. Clean. Prod.*, vol. 142, pp. 2315–2327, Jan. 2017, doi: 10.1016/j.jclepro.2016.11.045.

[63]   M. E. Dry, "The Fischer-Tropsch process: 1950-2000," *Catal. Today*, vol. 71, no. 3–4, pp. 227–241, 2002, doi: 10.1016/S0920-5861(01)00453-9.

[64]   S. Bachiller *et al.*, "No 主観的健康感を中心とした在宅高齢者における 健康関連指標に関する共分散構造分析Title," *Rev. Trab. Soc.*, vol. 11, no. 75, pp. 23–26, 2008, [Online]. Available: http://www.desarrollosocialyfamilia.gob.cl/storage/docs/Informe_de_Desarrollo_Social_2020.pdf%0Ahttp://revistas.ucm.es/index.php/CUTS/article/view/44540/44554.

[65]   C. D. Chang, "Hydrocarbons from Methanol," *Catal. Rev.*, vol. 25, no. 1, pp. 1–118, 1983, doi: 10.1080/01614948308078874.

[66]   C. D. Chang, "Catalysis Reviews Science and Engineering Methanol Conversion to Light Olefins Methanol Conversion to Light Olefins," *Catal. Rev.-Sci. Eng*, vol. 26, no. 4, pp. 323–345, 1984, [Online]. Available: https://www.tandfonline.com/action/journalInformation?journalCode=lctr20.

[67]   S. G. Jadhav, P. D. Vaidya, B. M. Bhanage, and J. B. Joshi, "Catalytic carbon dioxide hydrogenation to methanol: A review of recent studies," *Chem. Eng. Res. Des.*, vol. 92, no. 11, pp. 2557–2567, 2014, doi: 10.1016/j.cherd.2014.03.005.

[68]   J. P. V. A. N. D. E. N. Berg, "the Conversion of Methanol To Gasoline on Zeolite H-Zsm-5," no. 1981, 1981, doi: 10.6100/IR30334.

[69]   T. Rachman, "済無No Title No Title No Title," *Angew. Chemie Int. Ed. 6(11), 951–*

101

*952.*, pp. 10–27, 2018.

[70] A. Sanz-Martínez, J. Lasobras, J. Soler, J. Herguido, and M. Menéndez, "Methanol to Gasoline (MTG): Preparation, Characterization and Testing of HZSM-5 Zeolite-Based Catalysts to Be Used in a Fluidized Bed Reactor," *Catalysts*, vol. 12, no. 2, 2022, doi: 10.3390/catal12020134.

[71] J. Antonio and C. Garcia, "College of Petroleum Engineering Natural Gas and Petrochemicals Technical and Economic Feasibility for the Installation of an Industrial Plant for Producing High-Octane Gasoline from Methanol."

[72] S. Yurchak, *Developmbnt of mobil's H-IXBD-HKD methanol-to-gasoline (MTG) process*, vol. 36, no. C. 1988.

[73] M. R. Gogate, "Methanol-to-olefins process technology: current status and future prospects," *Pet. Sci. Technol.*, vol. 37, no. 5, pp. 559–565, 2019, doi: 10.1080/10916466.2018.1555589.

[74] Y. H. Kim, K. W. Jun, H. Joo, C. Han, and I. K. Song, "A simulation study on gas-to-liquid (natural gas to Fischer-Tropsch synthetic fuel) process optimization," *Chem. Eng. J.*, vol. 155, no. 1–2, pp. 427–432, 2009, doi: 10.1016/j.cej.2009.08.018.

[75] S. A. Al-Sobhi, A. Elkamel, F. S. Erenay, and M. A. Shaik, "Simulation-optimization framework for synthesis and design of natural gas downstream utilization networks," *Energies*, vol. 11, no. 2, pp. 1–19, 2018, doi: 10.3390/en11020362.

[76] M. Panahi, *Plantwide Control for Economically Optimal Operation of Chemical Plants*, no. December. 2011.

[77] E. Makhura, J. Rakereng, O. Rapoo, and G. Danha, "Effect of the operation parameters on the Fischer Tropsch synthesis process using different reactors," *Procedia Manuf.*, vol. 35, pp. 349–355, 2019, doi: 10.1016/j.promfg.2019.05.051.

[78] S. A. Al-Sobhi and A. Elkamel, "Simulation and optimization of natural gas processing and production network consisting of LNG, GTL, and methanol facilities," *J. Nat. Gas Sci. Eng.*, vol. 23, no. 2015, pp. 500–508, 2015, doi: 10.1016/j.jngse.2015.02.023.

[79] A. Taghizadeh Damanabi and F. Bahadori, "Improving GTL process by CO2 utilization in tri-reforming reactor and application of membranes in Fisher Tropsch reactor," *J. CO2 Util.*, vol. 21, no. August, pp. 227–237, 2017, doi: 10.1016/j.jcou.2017.07.019.

[80] A. Rafiee, M. Panahi, and K. R. Khalilpour, "CO2 utilization through integration of post-combustion carbon capture process with Fischer-Tropsch gas-to-liquid (GTL) processes," *J. CO2 Util.*, vol. 18, pp. 98–106, 2017, doi: 10.1016/j.jcou.2017.01.016.

[81] I. Nkemakolam Chinedu *et al.*, "Gas-to-Liquids (GTL) Plant Optimization Using Enhanced Synthesis Gas Reforming Technology," *Pet. Sci. Eng.*, vol. 3, no. 2, p. 94, 2019, doi: 10.11648/j.pse.20190302.18.

[82] A. A. Al-Yaeeshi, A. AlNouss, G. McKay, and T. Al-Ansari, "A simulation study on the effect of CO2 injection on the performance of the GTL process," *Comput. Chem. Eng.*, vol. 136, May 2020, doi: 10.1016/j.compchemeng.2020.106768.

[83] S. Greyling, H. Marais, G. van Schoor, and K. R. Uren, "Application of exergy-based fault detection in a gas-to-liquids process plant," *Entropy*, vol. 21, no. 6, pp. 1–19, 2019, doi: 10.3390/e21060565.

[84] M. Panahi, V. Khezri, E. Yasari, and S. Skogestad, "Application of surrogate models as an alternative to process simulation for implementation of the self-optimizing control procedure on large-scale process plants-a natural gas-to-liquids (gtl) case study," *Ind. Eng. Chem. Res.*, vol. 60, no. 13, pp. 4919–4929, 2021, doi: 10.1021/acs.iecr.0c05715.

[85] T. Xiao *et al.*, "The Catalyst Selectivity Index (CSI): A Framework and Metric to Assess the Impact of Catalyst Efficiency Enhancements upon Energy and CO2 Footprints," *Top. Catal.*, vol. 58, no. 10–11, pp. 682–695, 2015, doi: 10.1007/s11244-015-0401-1.

[86] K. Jalama, "Effect of temperature on CO Rate and Product Distribution during Fischer-Tropsch reaction over Co/Ti02 catalyst," *Lect. Notes Eng. Comput. Sci.*, vol. 2220, pp. 656–658, 2015.

[87] F. K. Al-Zuhairi and W. A. Kadhim, "Effect of Ce-promotion on iron catalysts activity through the synthesis of liquid fuels by the Fischer-Tropsch process," *IOP Conf. Ser.*

*Mater. Sci. Eng.*, vol. 579, no. 1, 2019, doi: 10.1088/1757-899X/579/1/012017.

[88] J. Horáček, "Fischer–Tropsch synthesis, the effect of promoters, catalyst support, and reaction conditions selection," *Monatshefte fur Chemie*, vol. 151, no. 5, pp. 649–675, 2020, doi: 10.1007/s00706-020-02590-w.

[89] Y. Kang *et al.*, "Promoted methane conversion to syngas over Fe-based garnets via chemical looping," *Appl. Catal. B Environ.*, vol. 278, no. June, p. 119305, 2020, doi: 10.1016/j.apcatb.2020.119305.

[90] K. Li, H. Wang, and Y. Wei, "Syngas generation from methane using a chemical-looping concept: A review of oxygen carriers," *Journal of Chemistry*. 2013, doi: 10.1155/2013/294817.

[91] D. Li, R. Xu, X. Li, Z. Li, X. Zhu, and K. Li, "Chemical Looping Conversion of Gaseous and Liquid Fuels for Chemical Production: A Review," *Energy and Fuels*, vol. 34, no. 5, pp. 5381–5413, 2020, doi: 10.1021/acs.energyfuels.0c01006.

[92] M. Peacock *et al.*, "Innovation in Fischer–Tropsch: Developing Fundamental Understanding to Support Commercial Opportunities," *Top. Catal.*, vol. 63, no. 3–4, pp. 328–339, Jul. 2020, doi: 10.1007/s11244-020-01239-6.

[93] C. Huili and T. Xiaojin, "Modelling of Microchannel Reactors for Fischer-Tropsch Synthesis," vol. 22, no. 2, pp. 93–101, 2020.

[94] B. Ghorbani, A. Ebrahimi, S. Rooholamini, and M. Ziabasharhagh, "Integrated Fischer-Tropsch synthesis process with hydrogen liquefaction cycle," *J. Clean. Prod.*, vol. 283, p. 124592, 2021, doi: 10.1016/j.jclepro.2020.124592.

[95] C. J. Kulik, M. Gogate, and C. J. Kulik, "Methanol-to-Gasoline Vs. DME-to-Gasoline II. Process Comparison and Analysis," *Fuel Sci. Technol. Int.*, vol. 13, no. 8, pp. 1039–1057, 1995, doi: 10.1080/08843759508947721.

[96] A. Galadima and O. Muraza, "From synthesis gas production to methanol synthesis and potential upgrade to gasoline range hydrocarbons: A review," *J. Nat. Gas Sci. Eng.*, vol. 25, pp. 303–316, 2015, doi: 10.1016/j.jngse.2015.05.012.

[97] P. Noor, M. Khanmohammadi, B. Roozbehani, F. Yaripour, and A. Bagheri Garmarudi, "Determination of reaction parameters in methanol to gasoline (MTG) process using infrared spectroscopy and chemometrics," *J. Clean. Prod.*, vol. 196, pp. 1273–1281, 2018, doi: 10.1016/j.jclepro.2018.05.288.

[98] V. Y. Doluda, V. G. Matveeva, N. V. Lakina, E. M. Sulman, M. G. Sulman, and R. V. Brovko, "Modified zeolites in methanol to hydrocarbons transformation," *Chem. Eng. Trans.*, vol. 74, no. May 2018, pp. 499–504, 2019, doi: 10.3303/CET1974084.

[99] P. del Campo, U. Olsbye, K. P. Lillerud, S. Svelle, and P. Beato, "Impact of post-synthetic treatments on unidirectional H-ZSM-22 zeolite catalyst: Towards improved clean MTG catalytic process," *Catal. Today*, vol. 299, no. November 2016, pp. 135–145, 2018, doi: 10.1016/j.cattod.2017.05.011.

[100] E. Kianfar and A. Razavi, "Zeolite catalyst based selective for the process MTG : A review Z EOLITE C ATALYST B ASED S ELECTIVE FOR THE P ROCESS MTG : A R EVIEW," no. September, 2020.

[101] S. A. Al-Sobhi, A. AlNouss, and M. Alhamad, "Techno-economic and environmental assessment of gasoline produced from GTL and MTG processes." 2021, doi: https://doi.org/10.1016/B978-0-323-88506-5.50283-7.

[102] O. Guide, "Hysys 200 4 .2 ®."

[103] S. Ekwueme, C. Izuwa, J. Odo, U. Obibuike, N. Ohia, and N. Nwogu, "Developments in gas-to-liquids technology plant optimisation for efficientutilisation of flared natural gas in the niger delta," *Soc. Pet. Eng. - SPE Niger. Annu. Int. Conf. Exhib. 2020, NAIC 2020*, 2020, doi: 10.2118/203668-ms.

[104] G. Alamsyah, M. Umar, M. Putra, and U. Al-azhar, "Preliminary Design of Methanol to Olefin Plant FINAL REPORT ' PRELIMINARY DESIGN OF METHANOL TO OLEFIN PLANT ' Group 6 Regular Members of Group Alan Try Putra Samad Ghandi Alamsyah Kameliya Hani Millati Umar Putra Syahruddin 1206247726 Uswatun Nur Khazana," no. March 2017, 2015, doi: 10.13140/RG.2.2.28634.54725.

[105] N. S. Prof. Ofira Ayalon , Dr. Miriam Lev-On , Dr. Perry Lev-On, "Assessment of Natural Gas Loss from the Well-to-Tank Supply Chain of Natural Gas Based Transportation Fuels," no. February 2020, 2020.

[106] Shell GTL fuel, "KNOWLEDGE GUIDE GTL Fuel."

[107] M. Jafari, S. Ashtab, A. Behroozsarand, K. Ghasemzadeh, and D. A. Wood, "Gas Processing Journal," vol. 6, no. 1, pp. 1–20, 2018.

[108] K. Choi, S. Park, H. G. Roh, and C. S. Lee, "Combustion and emission reduction characteristics of GTL-biodiesel fuel in a single-cylinder diesel engine," *Energies*, vol. 12, no. 11, 2019, doi: 10.3390/en12112201.

[109] E. A. Emam, "GAS flaring in industry: An overview," *Pet. Coal*, vol. 57, no. 5, pp. 532–555, 2015.

[110] S. Technology, F. O. R. Cleaner, W. Is, S. Gtl, C. Burning, and S. T. O. Use, "Your easy way to help reduce local emissions," 1970.

[111] M. L. Hindman, "Methanol to Gasoline technology," *Proc. Int. Offshore Polar Eng. Conf.*, pp. 38–41, 2013.

[112] M. C. J. Erick *et al.*, "No 主観的健康感を中心とした在宅高齢者における 健康関連指標に関する共分散構造分析Title," *Rev. CENIC. Ciencias Biológicas*, vol. 152, no. 3, p. 28, 2016, [Online]. Available: file:///Users/andreataquez/Downloads/guia-plan-de-mejora-institucional.pdf%0Ahttp://salud.tabasco.gob.mx/content/revista%0Ahttp://www.revistaalad.com/pdfs/Guias_ALAD_11_Nov_2013.pdf%0Ahttp://dx.doi.org/10.15446/revfacmed.v66n3.60060.%0Ahttp://www.cenetec.

[113] International Renewable Energy Agency (IRENA), *Innovation Outlook: Renewable Mini-Grids*. 2016.

[114] I. Panel and C. Change, *CARBON DIOXIDE CAPTURE*. .

[115] C. Zhang, K. W. Jun, R. Gao, G. Kwak, and S. C. Kang, "Efficient utilization of associated natural gas in a modular gas-to-liquids process: Technical and economic

analysis," *Fuel*, vol. 176, pp. 32–39, 2016, doi: 10.1016/j.fuel.2016.02.060.

[116]  R. Surkatti, M. H. El-naas, and M. C. M. Van Loosdrecht, "Treatment : A Review," 2020.

[117]  A. S. K. T. Network and R. Posts, "Shell collaborates to produce water in Quatar desert."

[118]  P. Borisut and A. Nuchitprasittichai, "Process Configuration Studies of Methanol Production via Carbon Dioxide Hydrogenation: Process Simulation-Based Optimization Using Artificial Neural Networks," *Energies*, vol. 13, no. 24, p. 6608, 2020, doi: 10.3390/en13246608.

[119]  U. Onwusogh, "Feasibility of Produced Water Treatment and Reuse – Case Study of a GTL Plant," 2015, doi: 10.2523/iptc-18354-ms.

[120]  O. Of, "I Nternational J Ournal of," *J. Energy*, vol. 1, no. 3, pp. 427–446, 2010, [Online]. Available:

http://ijee.ieefoundation.org/vol2/public_html/ijeeindex/vol2/issue4/IJEE_03_v2n4.pd f.

[121]  M. Chaubey, "Zero Liquid Discharge," *Wastewater Treat. Technol.*, pp. 184–203, 2021, doi: 10.1002/9781119765264.ch6.

[122]  J. A. Velasco, L. Lopez, M. Velásquez, M. Boutonnet, S. Cabrera, and S. Järås, "Gas to liquids: A technology for natural gas industrialization in Bolivia," *J. Nat. Gas Sci. Eng.*, vol. 2, no. 5, pp. 222–228, 2010, doi: 10.1016/j.jngse.2010.10.001.

[123]  S. M. H. Daghash, "Energy Saving and Recovery," pp. 1–31.

[124]  J. Foran, "The Paris agreement scam," *Nation*, vol. 302, no. 6, pp. 1–4, 2016.

[125]  P. Esmaili, I. Dincer, and G. F. Naterer, "Energy and exergy analyses of electrolytic hydrogen production with molybdenum-oxo catalysts," *Int. J. Hydrogen Energy*, vol. 37, no. 9, pp. 7365–7372, 2012, doi: 10.1016/j.ijhydene.2012.01.076.

[126]  M. K. Singla, P. Nijhawan, and A. S. Oberoi, "Hydrogen fuel and fuel cell technology for cleaner future: a review," *Environ. Sci. Pollut. Res.*, vol. 28, no. 13, pp. 15607–15626, 2021, doi: 10.1007/s11356-020-12231-8.

[127] W. W. Tso, A. M. Niziolek, O. Onel, C. D. Demirhan, C. A. Floudas, and E. N. Pistikopoulos, "Reprint of: Enhancing natural gas-to-liquids (GTL) processes through chemical looping for syngas production: Process synthesis and global optimization," *Comput. Chem. Eng.*, vol. 116, pp. 521–538, 2018, doi: 10.1016/j.compchemeng.2018.10.017.

[128] K. Kesehatan, "No TitleΕΛΕΝΗ," *Αγαη*, vol. 8, no. 5, p. 55, 2019.

[129] O. Vozniuk, N. Tanchoux, J. M. Millet, S. Albonetti, F. Di Renzo, and F. Cavani, *Spinel Mixed Oxides for Chemical-Loop Reforming: From Solid State to Potential Application*, 1st ed., vol. 178. Elsevier B.V., 2019.

[130] Q. Zhu, "Developments on CO2-utilization technologies," *Clean Energy*, vol. 3, no. 2, pp. 85–100, 2019, doi: 10.1093/ce/zkz008.

[131] S. Saeidi, M. K. Nikoo, A. Mirvakili, S. Bahrani, N. A. Saidina Amin, and M. R. Rahimpour, "Recent advances in reactors for low-temperature Fischer-Tropsch synthesis: Process intensification perspective," *Rev. Chem. Eng.*, vol. 31, no. 3, pp. 209–238, 2015, doi: 10.1515/revce-2014-0042.

[132] H. Becker, R. Güttel, and T. Turek, "Performance of diffusion-optimised Fischer-Tropsch catalyst layers in microchannel reactors at integral operation," *Catal. Sci. Technol.*, vol. 9, no. 9, pp. 2180–2195, 2019, doi: 10.1039/c9cy00457b.

[133] J. Chen and L. Li, "Mass transport limitations in microchannel methanol-reforming reactors for hydrogen production," *Int. J. Hydrogen Energy*, vol. 45, no. 51, pp. 26637–26654, 2020, doi: 10.1016/j.ijhydene.2020.07.010.

[134] N. C. Shiba, Y. Yao, R. P. Forbes, C. G. Okoye-Chine, X. Liu, and D. Hildebrandt, "Role of CoO-Co nanoparticles supported on SiO2 in Fischer-Tropsch synthesis: Evidence for enhanced CO dissociation and olefin hydrogenation," *Fuel Process. Technol.*, vol. 216, no. December 2020, p. 106781, 2021, doi: 10.1016/j.fuproc.2021.106781.

[135] A. A. Al-Yaeeshi, R. Govindan, and T. Al-Ansari, "Techno-economic-based dynamic

network design for optimum large-scale carbon dioxide utilisation in process industries," *J. Clean. Prod.*, vol. 275, p. 122974, 2020, doi: 10.1016/j.jclepro.2020.122974.

[136] D. Xiang, P. Li, and X. Yuan, "System optimization and performance evaluation of shale gas chemical looping reforming process for efficient and clean production of methanol and hydrogen," *Energy Convers. Manag.*, vol. 220, no. April, p. 113099, 2020, doi: 10.1016/j.enconman.2020.113099.

[137] S. Alam, J. P. Kumar, K. Y. Rani, and C. Sumana, "Comparative assessment of performances of different oxygen carriers in a chemical looping combustion coupled intensified reforming process through simulation study," *J. Clean. Prod.*, vol. 262, p. 121146, 2020, doi: 10.1016/j.jclepro.2020.121146.

[138] H. C. Mantripragada and G. Veser, "Chemical Looping Partial Oxidation of Methane for Co-Production of Syngas and Electricity: Process Modeling and Systems Analysis," *Energy Technol.*, vol. 8, no. 8, pp. 1–12, 2020, doi: 10.1002/ente.201900580.

[139] Z. Cheng *et al.*, "Effect of calcination temperature on the performance of hexaaluminate supported CeO2 for chemical looping dry reforming," *Fuel Process. Technol.*, vol. 218, no. April, p. 106873, 2021, doi: 10.1016/j.fuproc.2021.106873.

[140] Q. Yang *et al.*, "Thermodynamic analysis of chemical looping coupling process for coproducing syngas and hydrogen with in situ CO2 utilization," *Energy Convers. Manag.*, vol. 231, no. October 2020, p. 113845, 2021, doi: 10.1016/j.enconman.2021.113845.

[141] Z. Cheng *et al.*, "Effect of calcination temperature on the performance of hexaaluminate supported CeO2 for chemical looping dry reforming," *Fuel Process. Technol.*, vol. 218, no. December 2020, p. 106873, 2021, doi: 10.1016/j.fuproc.2021.106873.

[142] Y. He, L. Zhu, L. Li, and L. Sun, "Zero-energy penalty carbon capture and utilization for liquid fuel and power cogeneration with chemical looping combustion," *J. Clean. Prod.*, vol. 235, pp. 34–43, 2019, doi: 10.1016/j.jclepro.2019.06.325.

109

[143] J. Guerrero-Caballero, T. Kane, N. Haidar, L. Jalowiecki-Duhamel, and A. Löfberg, "Ni, Co, Fe supported on Ceria and Zr doped Ceria as oxygen carriers for chemical looping dry reforming of methane," *Catal. Today*, vol. 333, pp. 251–258, 2019, doi: 10.1016/j.cattod.2018.11.064.

[144] M. F. Mingchen Tang, Kuo Liu, Dean M. Roddick, "Enhanced Lattice Oxygen Reactivity over Fe2O3/Al2O3 Redox Catalyst for Chemical_Looping Dry (CO2) Reforming of CH4: Synergistic La-Ce Effect," pp. 1–33.

[145] A. Zaabout, P. I. Dahl, A. Ugwu, J. R. Tolchard, S. Cloete, and S. Amini, "Gas Switching Reforming (GSR) for syngas production with integrated CO2 capture using iron-based oxygen carriers," *Int. J. Greenh. Gas Control*, vol. 81, no. January, pp. 170–180, 2019, doi: 10.1016/j.ijggc.2018.12.027.

[146] M. Osman, A. Zaabout, S. Cloete, and S. Amini, "Internally circulating fluidized-bed reactor for syngas production using chemical looping reforming," *Chem. Eng. J.*, vol. 377, no. xxxx, pp. 0–1, 2019, doi: 10.1016/j.cej.2018.10.013.

[147] V. H. Collins-Martinez, J. F. Cazares-Marroquin, J. M. Salinas-Gutierrez, J. C. Pantoja-Espinoza, A. Lopez-Ortiz, and M. J. Melendez-Zaragoza, "The thermodynamic evaluation and process simulation of the chemical looping steam methane reforming of mixed iron oxides," *RSC Adv.*, vol. 11, no. 2, pp. 684–699, 2020, doi: 10.1039/d0ra08610j.

[148] A. Ugwu, A. Zaabout, and S. Amini, "An advancement in CO2 utilization through novel gas switching dry reforming," *Int. J. Greenh. Gas Control*, vol. 90, no. July, p. 102791, 2019, doi: 10.1016/j.ijggc.2019.102791.

# APPENDIX A: Literature Review

Table A 1: the optimal natural gas feedstock and products flowrate.

| | |
|---|---|
| Natural gas feedstock flowrate (kg/hr) | $1.55 \times 10^6$ |
| LPG (kg/hr) | $1.20 \times 10^5$ |
| Gasoline (kg/hr) | $2.30 \times 10^5$ |
| Diesel (kg/hr) | $1.80 \times 10^5$ |
| Wax (kg/hr) | $1.00 \times 10^5$ |

Table A 2: Integration of three different options using SMR and ATR.

| Cases | Case 1 | Case 2 | Case 3 |
|---|---|---|---|
| $H_2$/CO ratio | 0.73 | 0.96 | 1.15 |
| Carbon efficiency (%) | 62.41 | 68.24 | 63.15 |
| Wax (kg/h) | 77753 | 76691 | 65340 |

Table A 3: Performance result for conventional and proposed method.

| Parameter | Base Case (ATR) | Proposed method (Steam/$CO_2$) |
|---|---|---|
| $H_2$/CO ratio at FT inlet | 2.21 | 2.17 |
| Carbon efficiency (%) | 77.68 | 92.17 |
| Thermal efficiency (%) | 65.16 | 68.76 |
| Steam/carbon ratio at the reformer | 0.58 | 0.87 |
| Methane conversion (%) | 76.06 | 84 |
| Unreacted methane (%) | 23.94 | 16 |
| Unreacted carbon (%) | 28.91 | 16.01 |
| Liquid yield (b/d) | 5430 | 5730 |
| Gasoline (b/d) | 3025 | 3120 |
| Diesel (b/d) | 1380 | 1425 |
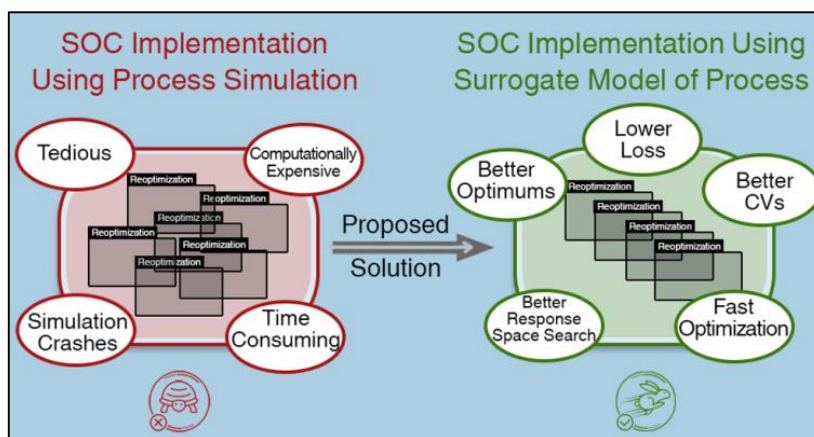
Figure A 1: Process Simulation Vs. proposed Surrogate model.
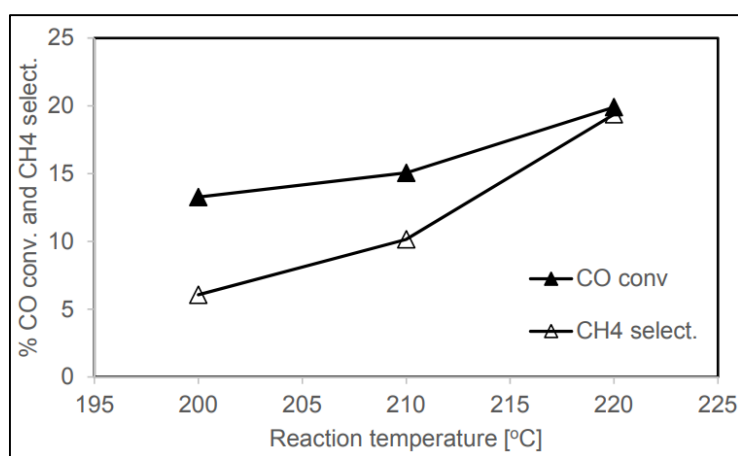


Figure A 2: GTL process temperature effect on CH4 selectivity and CO conversion.
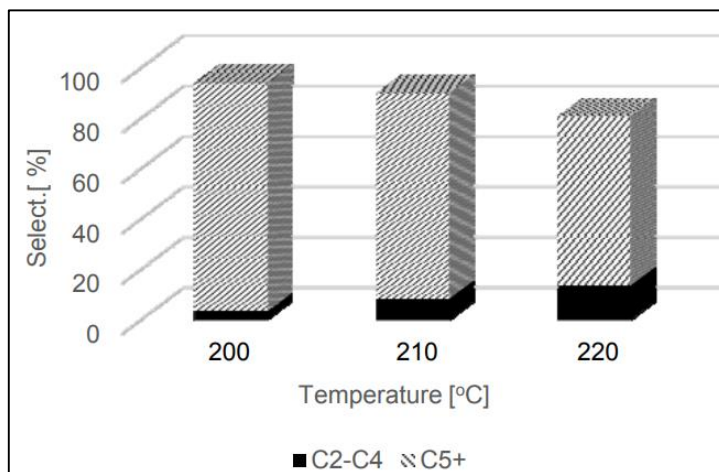


Figure A 3: Operating Temperature effect on the selectivity of $C_2$-$C_4$ and $C_{5+}$.

Table A 4: Summarize Chemical Looping Reforming studies.

| No | Capacity | conditions | Analysis Tool | Catalyst/Oxygen Carrier | Contribution | Results | Ref |
|----|----------|-----------|---------------|------------------------|--------------|---------|-----|
| 1 | 2000 kmol/h | P = 1 bar T=900 °C | N/A | Fe-Cu and $Al_2O_3$ | Optimize CLR to maximize the hydrogen and methanol | • NG conversion = 99.32%<br>• H2/CO = 1.85 (because of NG composition)<br>• $CO_2$ emissions (kmol/kmol) = 0.02<br>• $H_2$ production (kmol/kmol) = 0.777<br>• Gas (kmol/kmol) = 4.018<br>• Methanol (kmol/kmol) =1.079<br>• Energy efficiency = 77.5 % | [136] |
| 2 | N/A | N/A | ASPEN Plus | 15% SiC and 15% Al2O3 Support catalyst | Evaluating the role of different OCs, | Cupper with maximum yield production and environmentally feasible.<br>• Cheap and non-toxic<br>• $H_2$ yield purity = 98.97%<br>• $CO_2$ capture = 98.27%<br>• $CH_4$ conversion =98.85%<br>• Energy Efficiency = 52.74 %<br>• Power generated = 224.27 kW | [137] |
| 3 | plant scale 1,10,50, and 100 (kBPD) | N/A | Aspen Plus | NiO and $Fe_2O_3$ | Economical and $CO_2$ emissions | • Cost saving of 25-40% over the commercial processes.<br>• The CLR process emit less emissions over the commercial.<br>• CLR remain competitive even as natural gas cost rises. | [127] |
| 4 | 50,000 (BPD) | N/A | Aspen Plus HRSG | OC (Ni/Fe) | Comparison in terms of fuel and energy efficiency | • $CH_4$ conversion is 75% lower than ATR.<br>• 50% more fuel required to produce 1 kmol/s.<br>• Produces around 240 MW electricity | [138] |

| No | Capacity | conditions | Analysis Tool | Catalyst/Oxygen Carrier | Contribution | Results | Ref |
|---|---|---|---|---|---|---|---|
| 5 | N/A | N/A | COP<br>N/A<br>IM<br>SG, HTEM, WMK, COM and PEC | Ni-based/ $Al_2O_3$<br>Fe-based/ $Al_2O_3$<br>Ce-based/ $Al_2O_3$<br>Perovskite oxide | Optimize the CLR (OCs) | • Fe-base completely oxidize $CH_4$ to $H_2O$ and $CO_2$.<br>• Ce-base produce syngas at low temperature, the $O_2$ storage needs to be improved.<br>• perovskite oxides have very high redox stability and selectivity for synthesis gas production, at very high temperature only.<br>• More research needs to be optimized to satisfy the performance and economic aspects. | [91] |
| 6 | N/A | Atmospheric pressure<br>T= 700, 800, 900 and 1000 °C | N/A | $CeO_2/BF_3$ | Investigate the $CeO_2/BF3$ interaction at different T. | • Increasing the Temperature from 700 °C to 900 °C showed an increase in the interaction between $CeO_2$ and $BF_3$ which enhanced the diffusion of oxygen. | [139] |
| 7 | 1 kmol/h | P= 1 atm | Aspen Plus<br>Experiment | Iron Oxide | Study the production of syngas and hydrogen coupled with $CO_2$ utilization | • $H_2$ yield purity = 100%<br>• $CO_2$ capture = 93-99%<br>• $CH_4$ conversion =98-100%<br>• Energy Efficiency = 90.54% | [140] |
| 8 | N/A | T= 700, 800, 900 and 1000 °C | XRD<br>XPS | CeO2/BF3-T | Study the effect of temperature on hexa-aluminate ($BF_3$-T) supported $CeO_2$ | • $CH_4$ conversion =85% at T= 900°C<br>• Syngas ratio =2 | [141] |
| 9 | N/A | N/A | Aspen plus<br>Experiment | Fe-based | Study the environmental and energy efficiency of CO2-to-liquid ratio | • Higher energy efficiency 60.37% compared to conventional GTL process (49-56%).<br>• $CO_2$ Capture efficiency= 98.95% | [142] |

| No | Capacity | conditions | Analysis Tool | Catalyst/Oxygen Carrier | Contribution | Results | Ref |
|----|----------|-----------|---------------|-------------------------|--------------|---------|-----|
| 10 | N/A | N/A | XRD | Fe-based | Study novel garnet | • $CH_4$ conversion =94% | [89] |
| 11 | N/A | T= 600 ºC | ICP<br>XRD | Ni,Co and Fe/ Ce | Study the Ni,Co and Fe support on ceria as Oxygen carrier | • $Co/CeO_2$ displayed the best balance between surface reactions towards methane, $CO_2$, and bulk reactivity. | [143] |
| 12 |  | T= 1300 ºC | ICP-OES<br>DXR<br>XPS | lanthanum iron perovskite | Study the improvement of a perovskite-based OC | • High syngas selectivity > 99% | [37] |
| 13 | N/A | N/A | XPS<br>XRD | $La_xCe_{1-x-}Fe_2O_3/Al_2O_3$ | Investigate the recent developments in CLR | • $CH_4$ conversion =92.23% | [144] |
| 14 | N/A | N/A | SEM/EDS<br>XRD | Fe/ alumina<br>Fe/NiO<br>Fe/Ce | Investigate the Fe-based on three different OC (alumina, NiO and Ce) | • $CH_4$ conversion increase from 75% to 80% at 800ºC<br>• Ni containing OC outperformed the others with 40% improvement in methane conversion | [145] |
| 15 | N/A | P= 1.7 bara<br>T= 650 ºC | N/A | $NiO/Al_2O_3$ | Investigate the feasibility of the ICR idea for methane chemical looping reforming in an experimental study | • $CH_4$ conversion =98%<br>• Syngas purity and recovery = 95% and 81%.<br>• $CO_2$ purity and recovery = 91% | [146] |
| 16 | $CH_4$ = 4 kmol/h | P = 1 atm<br>T= 775 ºC | XRD<br>Aspen Plus | $FeMoO_4$<br>$Fe_2ZnO_4$<br>$Fe_2MnO_4$ | To overcome the present disadvantages of methane | • Among the investigated OCs, $Fe_2MnO_4$ had the best working conditions.<br>• Thermal efficiency over $Fe_2MnO_4$ = 89-93%<br>• H2/ fuel molar ratio = 2.98. | [147] |

| No | Capacity | conditions | Analysis Tool | Catalyst/Oxygen Carrier | Contribution | Results | Ref |
|----|----------|------------|---------------|-------------------------|--------------|---------|-----|
| | | | | | SMR and POX processes, the use of $FeMoO_4$, $Fe_2ZnO_4$, and $Fe_2MnO_4$ as oxygen carriers (OC) in the CL-SMR reaction scheme was proposed. | • Syngas yield = 87.4% | |
| 17 | N/A | P = 1bar $T= 850\ ^oC$ | N/A | $NiO/Al_2O_3$ | Experimental study of $CO_2$ utilization to generate syngas | • The high temperature lowers the syngas ratio. <br> • Reduce the OC utilization by 50%. <br> • CO2 and CH4 conversion negatively drop by 22%. | [148] |
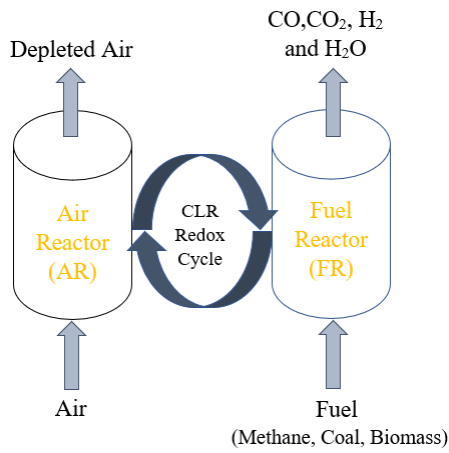
Figure A 4: Chemical Looping Reformer.
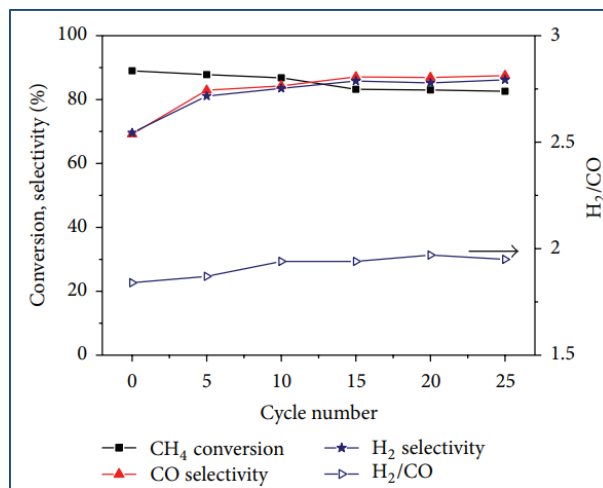


Figure A 5: $Ce_{0.7}Fe_{0.3}O_2$ OC, Selectivity, Stability, and syngas production Stability.
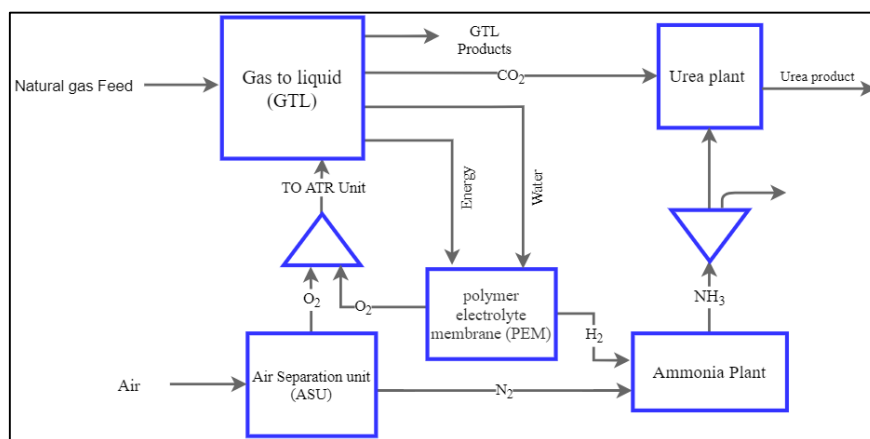


Figure A 6: GTL and Ammonia- Urea integration.

**Fig. 1.** Schematic of integrated the proposed integrated system.
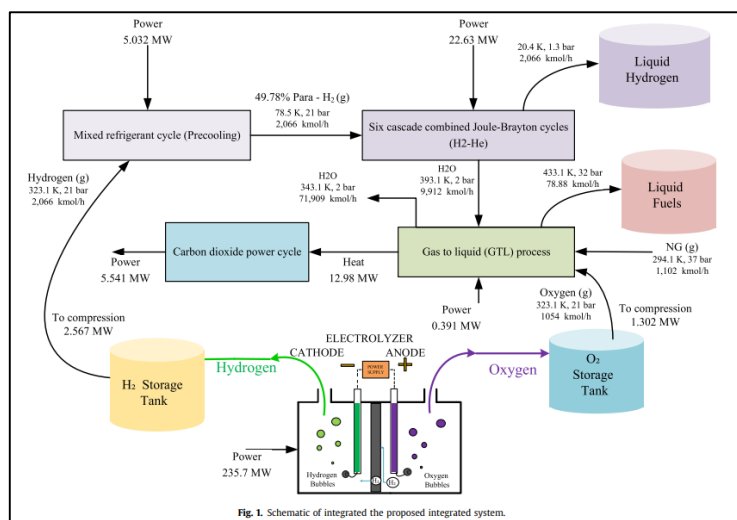
Figure A 7:GTL and hydrogen integration schematic.

Table A 5: Modification and topology zeolite effect.

| Catalyst | Reaction conditions | Methanol conversion, % | Selectivity/yield of gasoline range hydrocarbons ($C_5^+$), % |
|---|---|---|---|
| Nano-crystalline H-ZSM-5 | 1.0 g catalyst mixed with 1.0 g alumina, 380 °C, 2.0 h$^{-1}$ | 98, stable for 70 h | 45 |
| Nano-crystalline H-ZSM-5, treated with tetrapropyl ammonium hydroxide for 24 h | 1.0 g catalyst mixed with 1.0 g alumina, 380 °C, 2.0 h$^{-1}$ | 98, stable for 170 h | 46 |
| Nano-crystalline H-ZSM-5, treated with tetrapropyl ammonium hydroxide for 48 h | 1.0 g catalyst mixed with 1.0 g alumina, 380 °C, 2.0 h$^{-1}$ | 90, stable for 240 h | 45 |
| H-ZSM-5 | 1.40 g catalyst, 380 °C, 1.0 MPa, 2.0 h$^{-1}$ | 98 | 28 |
| H-ZSM-5/H-MCM-48 mixture | 1.40 g catalyst, 380 °C, 1.0 MPa, 2.0 h$^{-1}$ | 97 | 34 |
| H-ZSM-5 (Si/Al = 50) | 0.06 g catalyst, 350 °C, 7 h$^{-1}$, 15 min reaction | 95 | 47 |
| H-BEA | 0.06 g catalyst, 350 °C, 7 h$^{-1}$, 15 min reaction | 55 | 40 |
| ZnO/CuO/HZSM-5 | 400 °C, 0.1 MPa, 0.129 g of catalyst·h/g of methanol fed, 18 h | 95 | 08 |
| ZnO/CuO/HZSM-5, modified with oxalic acid | 400 °C, 0.1 MPa, 0.129 g of catalyst·h/g of methanol fed, 18 h | 94 | 12 |
| H-UZM-12 | 0.1 g of catalyst, 0.67 h$^{-1}$, 350 °C | 60, stable for 4 h | 50 |
| H-SSZ-13 | 0.1 g of catalyst, 0.67 h$^{-1}$, 350 °C | 100, stable for 8 h | 40 |
| Conventional H-SSZ-13 | 0.05 g of catalyst, 0.8 h$^{-1}$, 350 °C, 10 h | 100, stable for 3 h | 2 |
| Hierarchical H-SSZ-13 | 0.05 g of catalyst, 0.8 h$^{-1}$, 350 °C, 10 h | 100, stable for 8 h | 3 |

Table A 6: Textural properties of catalysts.

| Sample | Surface Area [m$^2$·g$^{-1}$] | | Pore Volume [cm$^3$·g$^{-1}$] | | Pore Diameter [nm] | |
|---|---|---|---|---|---|---|
| | BET | Micropores [*] | Pores | Micropores [*] | Pores | Micropores |
| HZSM-5 | 319.9 | 202.1 | 0.23 | 0.11 | 2.8 | 2.2 |
| Boehmite | 212.3 | - | 0.49 | - | 9.0 | - |
| Bentonite | 22.7 | 4.28 | 0.083 | 0.002 | 14.5 | - |
| Al$_2$O$_3$ | 179.4 | - | 0.37 | - | 8.1 | - |
| Fresh catalysts | | | | | | |
| HZ_Boeh | 287.9 | 113.4 | 0.40 | 0.06 | 5.5 | 2.1 |
| HZ_Bent | 210.8 | 57.9 | 0.35 | 0.03 | 6.6 | 2.1 |
| HZ_Bent+IE | 217.6 | 57.1 | 0.36 | 0.03 | 6.6 | 2.0 |
| Used catalysts | | | | | | |
| HZ_Boeh | 271.5 | 92.5 | 0.40 | 0.04 | 5.8 | 1.8 |
| HZ_Bent | 188.5 | 49.3 | 0.35 | 0.02 | 7.3 | 1.8 |
| HZ_Bent+IE | 200.6 | 48.4 | 0.36 | 0.021 | 7.2 | 1.7 |
| [*] t-plot method; [**] Straight cylindrical pores (4V/A method). | | | | | | |
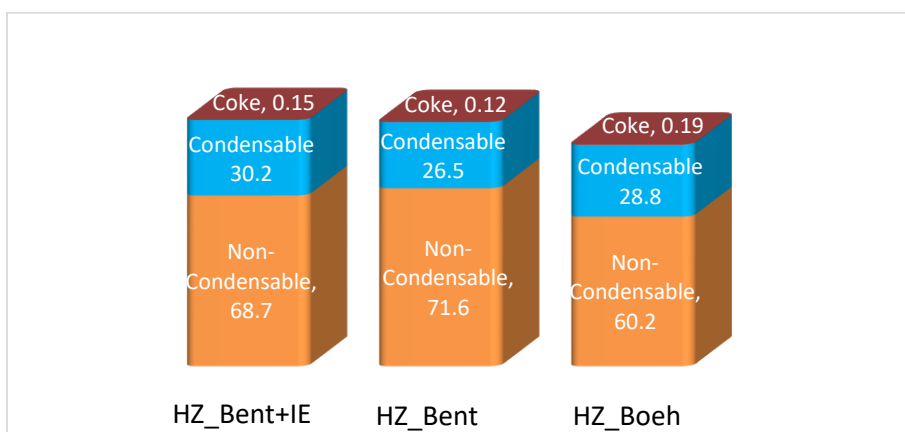
Figure A 8:Product yield distribution for the three catalysts.

# APPENDIX B: Process Flow Diagram
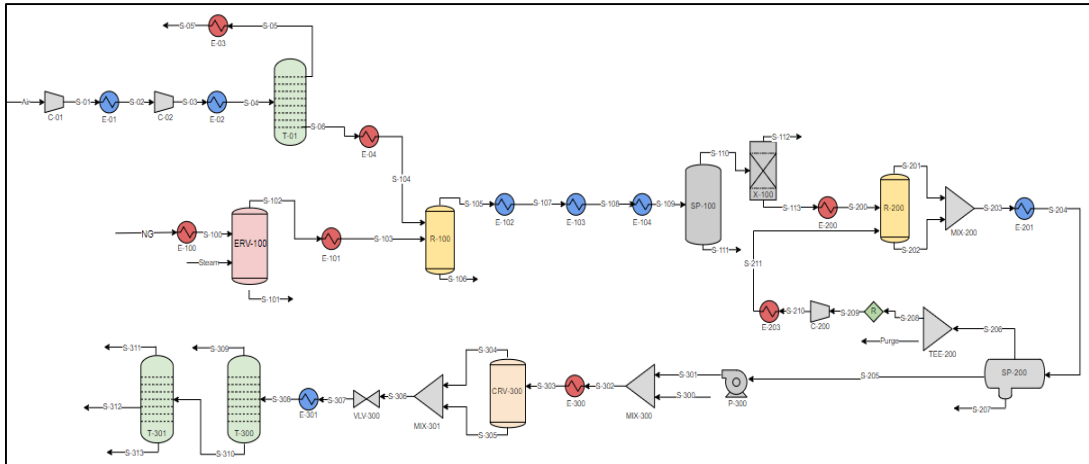


Figure B 1: Gas-to-Liquid process flow diagram.
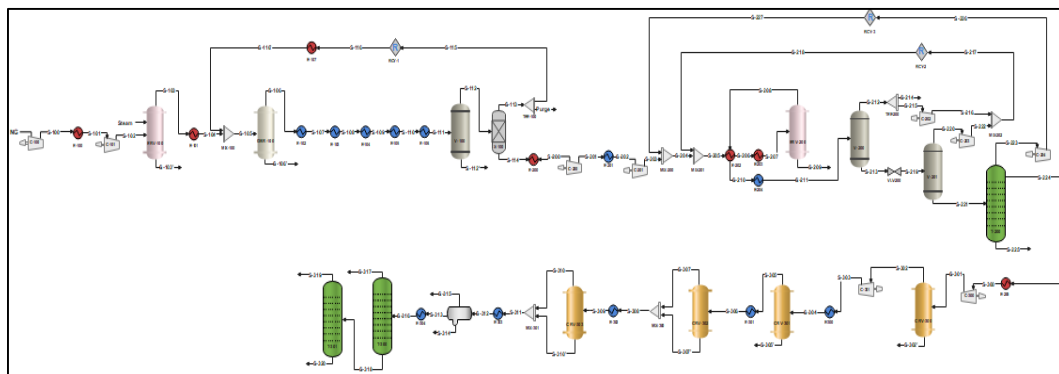


Figure B 2: Methanol-to-gasoline process flow diagram.
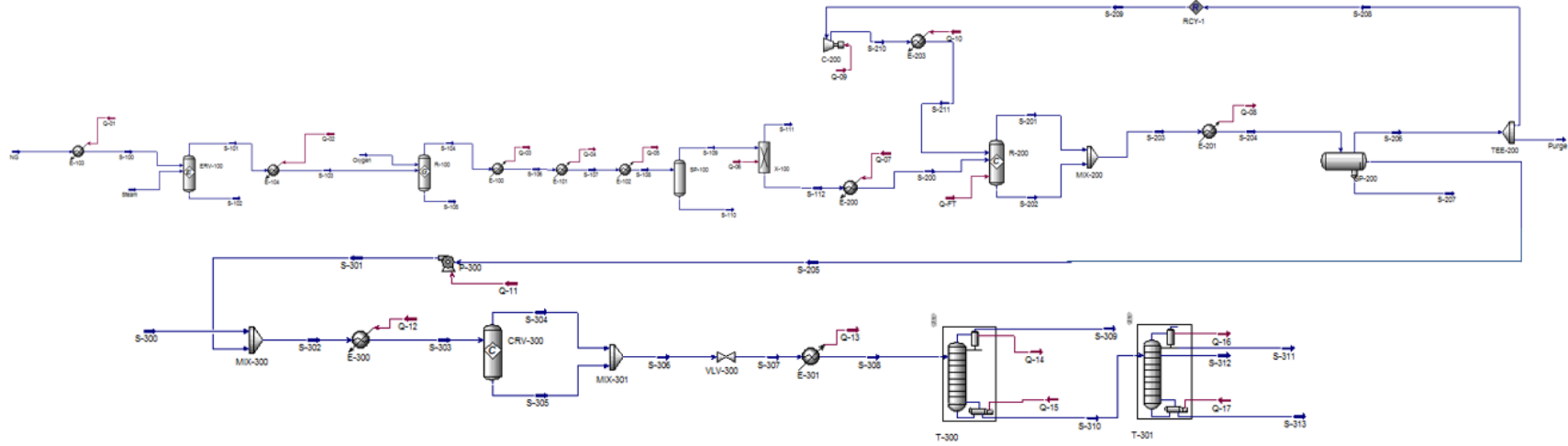
## APPENDIX C: High Temperature Fischer Tropsch material stream

Table C 1: High temperature Fischer Tropsch material stream.

| Name | NG | Steam | S-104 | S-105 | S-107 | S-110 | S-109 |
|---|---|---|---|---|---|---|---|
| Vapour Fraction | 1 | 1 | 1 | 0 | 1 | 0 | 1 |
| Temperature [C] | 25 | 500 | 1124.047 | 1124.047 | 324.0469 | 38 | 38 |
| Pressure [bar] | 25 | 25 | 25 | 25 | 24 | 23 | 23 |
| Molar Flow [MMSCFD] | 753.7081 | 150.7416 | 2349.89 | 0 | 2349.89 | 220.651 | 2129.239 |
| Mass Flow [kg/h] | 640515.6 | 135257.4 | 1454066 | 0 | 1454066 | 198037.5 | 1256029 |
| Liquid Volume Flow [m3/h] | 2011.056 | 135.5303 | 3555.154 | 0 | 3555.154 | 198.4644 | 3356.689 |
| Heat Flow [kJ/h] | -2.7E+09 | -1.7E+09 | -3.4E+09 | 0 | -6.5E+09 | -3.1E+09 | -4.8E+09 |
| Name | S-200 | S-206 | S-205 | S-207 | S-204 | S-202 | S-201 |
| Vapour Fraction | 1 | 1 | 0 | 0 | 0.433029 | 0 | 1 |
| Temperature [C] | 350 | 38 | 38 | 38 | 38 | 350 | 350 |
| Pressure [bar] | 20 | 18 | 18 | 18 | 18 | 20 | 20 |
| Molar Flow [MMSCFD] | 2077.774 | 535.327 | 72.84933 | 628.0619 | 1236.238 | 0 | 1236.238 |
| Mass Flow [kg/h] | 1143218 | 811076.3 | 377030.9 | 563567.3 | 1751675 | 0 | 1751675 |
| Liquid Volume Flow [m3/h] | 3220.004 | 1364.69 | 550.5942 | 564.7182 | 2480.002 | 0 | 2480.002 |
| Heat Flow [kJ/h] | -2.9E+09 | -2E+09 | -8.2E+08 | -8.9E+09 | -1.2E+10 | 0 | -9.2E+09 |
| Name | S-203 | S-209 | S-210 | S-211 | S-300 | S-302 | Purge |
| Vapour Fraction | 1 | 0.999997 | 1 | 1 | 1 | 5.27E-02 | 1 |
| Temperature [C] | 350 | 38 | 46.97493 | 350 | 320 | 38.33964 | 38 |
| Pressure [bar] | 20 | 18 | 20 | 20 | 20 | 20 | 18 |
| Molar Flow [MMSCFD] | 1236.238 | 401.6356 | 401.6356 | 401.6356 | 2.5 | 75.34933 | 133.8318 |
| Mass Flow [kg/h] | 1751675 | 608487.9 | 608487.9 | 608487.9 | 251.0277 | 377282 | 202769.1 |
| Liquid Volume Flow [m3/h] | 2480.002 | 1023.718 | 1023.718 | 1023.718 | 3.593343 | 554.1875 | 341.1725 |
| Heat Flow [kJ/h] | -9.2E+09 | -1.5E+09 | -1.5E+09 | -1.2E+09 | 1059928 | -8.2E+08 | -5E+08 |

| Name | S-303 | S-304 | S-305 | S-306 | S-307 | S-308 | S-208 |
|---|---|---|---|---|---|---|---|
| Vapour Fraction | 1 | 1 | 0 | 1 | 1 | 0.484614 | 1 |
| Temperature [C] | 345 | 349.7006 | 349.7006 | 349.7006 | 301.0436 | 70 | 38 |
| Pressure [bar] | 80 | 80 | 80 | 80 | 1 | 1.01 | 18 |
| Molar Flow [MMSCFD] | 75.34933 | 75.34933 | 0 | 75.34933 | 75.34933 | 75.34933 | 401.4953 |
| Mass Flow [kg/h] | 377282 | 377282.7 | 0 | 377282.7 | 377282.7 | 377282.7 | 608307.2 |
| Liquid Volume Flow [m3/h] | 554.1875 | 554.3428 | 0 | 554.3428 | 554.3428 | 554.3428 | 1023.517 |
| Heat Flow [kJ/h] | -4.7E+08 | -4.7E+08 | 0 | -4.7E+08 | -4.7E+08 | -7.6E+08 | -1.5E+09 |
| Name | S-106 | S-108 | S-111 | S-112 | Oxygen | S-301 | S-309 |
| Vapour Fraction | 1 | 0.906102 | 1 | 0.999898 | 1 | 0 | 0.998668 |
| Temperature [C] | 724.0469 | 38 | 38 | 38 | 144 | 38.08232 | -18.4539 |
| Pressure [bar] | 24 | 23 | 23 | 23 | 25 | 20 | 1 |
| Molar Flow [MMSCFD] | 2349.89 | 2349.89 | 51.46495 | 2077.774 | 425.5795 | 72.84933 | 23.93693 |
| Mass Flow [kg/h] | 1454066 | 1454066 | 112810.9 | 1143218 | 678300 | 377030.9 | 52484.38 |
| Liquid Volume Flow [m3/h] | 3555.154 | 3555.154 | 136.685 | 3220.004 | 596.2133 | 550.5942 | 101.3394 |
| Heat Flow [kJ/h] | -5E+09 | -8E+09 | -1E+09 | -3.8E+09 | 72583130 | -8.2E+08 | -1.3E+08 |
| Name | S-310 | S-311 | S-312 | S-313 | S-100 | S-101 | S-102 |
| Vapour Fraction | 0 | 0 | 0 | 0 | 1 | 1 | 0 |
| Temperature [C] | 95.74548 | 70.65234 | 254.019 | 417.0137 | 455 | 430.1144 | 430.1144 |
| Pressure [bar] | 1.5 | 1 | 1.5 | 1.5 | 25 | 25 | 25 |
| Molar Flow [MMSCFD] | 51.4124 | 39.35696 | 11.4681 | 0.587334 | 753.7081 | 937.5427 | 0 |
| Mass Flow [kg/h] | 324798.3 | 199993.5 | 114028.7 | 10776.17 | 640515.6 | 775773.3 | 0 |
| Liquid Volume Flow [m3/h] | 453.0034 | 290.6038 | 149.023 | 13.37667 | 2011.056 | 2203.884 | 0 |
| Heat Flow [kJ/h] | -6.4E+08 | -4.2E+08 | -1.6E+08 | -8259591 | -1.9E+09 | -3.6E+09 | 0 |
| Name | S-103 | ** New ** | | | | | |
| Vapour Fraction | 1 | | | | | | |

| Name | S-103 | ** New ** |
|---|---|---|
| Temperature [C] | 500 | |
| Pressure [bar] | 25 | |
| Molar Flow [MMSCFD] | 937.5427 | |
| Mass Flow [kg/h] | 775773.3 | |
| Liquid Volume Flow [m3/h] | 2203.884 | |
| Heat Flow [kJ/h] | -3.4E+09 | |

# APPENDIX C: High Temperature Fischer Tropsch stream composition

Table C 2: High temperature Fischer Tropsch stream composition.

| Name | NG | Steam | S-104 | S-105 | S-107 | S-110 | S-109 |
|---|---|---|---|---|---|---|---|
| Comp Mole Frac (Methane) | 0.9200 | 0.0000 | 0.0067 | 0.0067 | 0.0067 | 0.0000 | 0.0074 |
| Comp Mole Frac (Ethane) | 0.0300 | 0.0000 | 0.0000 | 0.0000 | 0.0000 | 0.0000 | 0.0000 |
| Comp Mole Frac (n-Octane) | 0.0000 | 0.0000 | 0.0000 | 0.0000 | 0.0000 | 0.0000 | 0.0000 |
| Comp Mole Frac (n-Hexane) | 0.0000 | 0.0000 | 0.0000 | 0.0000 | 0.0000 | 0.0000 | 0.0000 |
| Comp Mole Frac (n-Nonane) | 0.0000 | 0.0000 | 0.0000 | 0.0000 | 0.0000 | 0.0000 | 0.0000 |
| Comp Mole Frac (n-Heptane) | 0.0000 | 0.0000 | 0.0000 | 0.0000 | 0.0000 | 0.0000 | 0.0000 |
| Comp Mole Frac (n-Decane) | 0.0000 | 0.0000 | 0.0000 | 0.0000 | 0.0000 | 0.0000 | 0.0000 |
| Comp Mole Frac (n-C22) | 0.0000 | 0.0000 | 0.0000 | 0.0000 | 0.0000 | 0.0000 | 0.0000 |
| Comp Mole Frac (n-C21) | 0.0000 | 0.0000 | 0.0000 | 0.0000 | 0.0000 | 0.0000 | 0.0000 |
| Comp Mole Frac (n-C20) | 0.0000 | 0.0000 | 0.0000 | 0.0000 | 0.0000 | 0.0000 | 0.0000 |
| Comp Mole Frac (n-C19) | 0.0000 | 0.0000 | 0.0000 | 0.0000 | 0.0000 | 0.0000 | 0.0000 |
| Comp Mole Frac (n-C18) | 0.0000 | 0.0000 | 0.0000 | 0.0000 | 0.0000 | 0.0000 | 0.0000 |
| Comp Mole Frac (n-C17) | 0.0000 | 0.0000 | 0.0000 | 0.0000 | 0.0000 | 0.0000 | 0.0000 |
| Comp Mole Frac (n-C16) | 0.0000 | 0.0000 | 0.0000 | 0.0000 | 0.0000 | 0.0000 | 0.0000 |
| Comp Mole Frac (n-C15) | 0.0000 | 0.0000 | 0.0000 | 0.0000 | 0.0000 | 0.0000 | 0.0000 |
| Comp Mole Frac (n-C14) | 0.0000 | 0.0000 | 0.0000 | 0.0000 | 0.0000 | 0.0000 | 0.0000 |
| Comp Mole Frac (n-C13) | 0.0000 | 0.0000 | 0.0000 | 0.0000 | 0.0000 | 0.0000 | 0.0000 |
| Comp Mole Frac (n-C12) | 0.0000 | 0.0000 | 0.0000 | 0.0000 | 0.0000 | 0.0000 | 0.0000 |
| Comp Mole Frac (n-C11) | 0.0000 | 0.0000 | 0.0000 | 0.0000 | 0.0000 | 0.0000 | 0.0000 |
| Comp Mole Frac (n-Butane) | 0.0000 | 0.0000 | 0.0000 | 0.0000 | 0.0000 | 0.0000 | 0.0000 |
| Comp Mole Frac (Propane) | 0.0000 | 0.0000 | 0.0000 | 0.0000 | 0.0000 | 0.0000 | 0.0000 |
| Comp Mole Frac (i-Butane) | 0.0000 | 0.0000 | 0.0000 | 0.0000 | 0.0000 | 0.0000 | 0.0000 |

| Name | NG | Steam | S-104 | S-105 | S-107 | S-110 | S-109 |
|---|---|---|---|---|---|---|---|
| Comp Mole Frac (i-Pentane) | 0.0000 | 0.0000 | 0.0000 | 0.0000 | 0.0000 | 0.0000 | 0.0000 |
| Comp Mole Frac (H2O) | 0.0000 | 1.0000 | 0.0969 | 0.0969 | 0.0969 | 0.9998 | 0.0033 |
| Comp Mole Frac (Oxygen) | 0.0000 | 0.0000 | 0.0000 | 0.0000 | 0.0000 | 0.0000 | 0.0000 |
| Comp Mole Frac (Hydrogen) | 0.0000 | 0.0000 | 0.5728 | 0.5728 | 0.5728 | 0.0000 | 0.6321 |
| Comp Mole Frac (CO2) | 0.0000 | 0.0000 | 0.0219 | 0.0219 | 0.0219 | 0.0002 | 0.0242 |
| Comp Mole Frac (CO) | 0.0000 | 0.0000 | 0.2856 | 0.2856 | 0.2856 | 0.0000 | 0.3152 |
| Comp Mole Frac (1-Butene) | 0.0000 | 0.0000 | 0.0000 | 0.0000 | 0.0000 | 0.0000 | 0.0000 |
| Comp Mole Frac (n-Pentane) | 0.0000 | 0.0000 | 0.0000 | 0.0000 | 0.0000 | 0.0000 | 0.0000 |
| Comp Mole Frac (n-C30) | 0.0000 | 0.0000 | 0.0000 | 0.0000 | 0.0000 | 0.0000 | 0.0000 |
| Comp Mole Frac (n-C29) | 0.0000 | 0.0000 | 0.0000 | 0.0000 | 0.0000 | 0.0000 | 0.0000 |
| Comp Mole Frac (n-C28) | 0.0000 | 0.0000 | 0.0000 | 0.0000 | 0.0000 | 0.0000 | 0.0000 |
| Comp Mole Frac (n-C27) | 0.0000 | 0.0000 | 0.0000 | 0.0000 | 0.0000 | 0.0000 | 0.0000 |
| Comp Mole Frac (n-C26) | 0.0000 | 0.0000 | 0.0000 | 0.0000 | 0.0000 | 0.0000 | 0.0000 |
| Comp Mole Frac (n-C25) | 0.0000 | 0.0000 | 0.0000 | 0.0000 | 0.0000 | 0.0000 | 0.0000 |
| Comp Mole Frac (n-C24) | 0.0000 | 0.0000 | 0.0000 | 0.0000 | 0.0000 | 0.0000 | 0.0000 |
| Comp Mole Frac (n-C23) | 0.0000 | 0.0000 | 0.0000 | 0.0000 | 0.0000 | 0.0000 | 0.0000 |
| Comp Mole Frac (Nitrogen) | 0.0500 | 0.0000 | 0.0160 | 0.0160 | 0.0160 | 0.0000 | 0.0177 |
| Name | S-200 | S-206 | S-205 | S-207 | S-204 | S-202 | S-201 |
| Comp Mole Frac (Methane) | 0.0076 | 0.0834 | 0.0072 | 0.0000 | 0.0365 | 0.0085 | 0.0365 |
| Comp Mole Frac (Ethane) | 0.0000 | 0.1395 | 0.0543 | 0.0000 | 0.0636 | 0.0219 | 0.0636 |
| Comp Mole Frac (n-Octane) | 0.0000 | 0.0003 | 0.0728 | 0.0000 | 0.0044 | 0.0090 | 0.0044 |
| Comp Mole Frac (n-Hexane) | 0.0000 | 0.0035 | 0.1137 | 0.0000 | 0.0082 | 0.0096 | 0.0082 |
| Comp Mole Frac (n-Nonane) | 0.0000 | 0.0001 | 0.0554 | 0.0000 | 0.0033 | 0.0088 | 0.0033 |
| Comp Mole Frac (n-Heptane) | 0.0000 | 0.0010 | 0.0921 | 0.0000 | 0.0059 | 0.0091 | 0.0059 |
| Comp Mole Frac (n-Decane) | 0.0000 | 0.0000 | 0.0447 | 0.0000 | 0.0026 | 0.0093 | 0.0026 |
| Comp Mole Frac (n-C22) | 0.0000 | 0.0000 | 0.0023 | 0.0000 | 0.0001 | 0.0089 | 0.0001 |

126

| Name | S-200 | S-206 | S-205 | S-207 | S-204 | S-202 | S-201 |
|------|-------|-------|-------|-------|-------|-------|-------|
| Comp Mole Frac (n-C21) | 0.0000 | 0.0000 | 0.0029 | 0.0000 | 0.0002 | 0.0092 | 0.0002 |
| Comp Mole Frac (n-C20) | 0.0000 | 0.0000 | 0.0038 | 0.0000 | 0.0002 | 0.0094 | 0.0002 |
| Comp Mole Frac (n-C19) | 0.0000 | 0.0000 | 0.0048 | 0.0000 | 0.0003 | 0.0095 | 0.0003 |
| Comp Mole Frac (n-C18) | 0.0000 | 0.0000 | 0.0062 | 0.0000 | 0.0004 | 0.0096 | 0.0004 |
| Comp Mole Frac (n-C17) | 0.0000 | 0.0000 | 0.0079 | 0.0000 | 0.0005 | 0.0096 | 0.0005 |
| Comp Mole Frac (n-C16) | 0.0000 | 0.0000 | 0.0102 | 0.0000 | 0.0006 | 0.0094 | 0.0006 |
| Comp Mole Frac (n-C15) | 0.0000 | 0.0000 | 0.0130 | 0.0000 | 0.0008 | 0.0097 | 0.0008 |
| Comp Mole Frac (n-C14) | 0.0000 | 0.0000 | 0.0167 | 0.0000 | 0.0010 | 0.0099 | 0.0010 |
| Comp Mole Frac (n-C13) | 0.0000 | 0.0000 | 0.0213 | 0.0000 | 0.0013 | 0.0096 | 0.0013 |
| Comp Mole Frac (n-C12) | 0.0000 | 0.0000 | 0.0273 | 0.0000 | 0.0016 | 0.0095 | 0.0016 |
| Comp Mole Frac (n-C11) | 0.0000 | 0.0000 | 0.0350 | 0.0000 | 0.0021 | 0.0093 | 0.0021 |
| Comp Mole Frac (n-Butane) | 0.0000 | 0.0345 | 0.1315 | 0.0000 | 0.0227 | 0.0147 | 0.0227 |
| Comp Mole Frac (Propane) | 0.0000 | 0.0808 | 0.0988 | 0.0000 | 0.0408 | 0.0192 | 0.0408 |
| Comp Mole Frac (i-Butane) | 0.0000 | 0.0000 | 0.0000 | 0.0000 | 0.0000 | 0.0000 | 0.0000 |
| Comp Mole Frac (i-Pentane) | 0.0000 | 0.0000 | 0.0000 | 0.0000 | 0.0000 | 0.0000 | 0.0000 |
| Comp Mole Frac (H2O) | 0.0034 | 0.0043 | 0.0009 | 0.9999 | 0.5099 | 0.1487 | 0.5099 |
| Comp Mole Frac (Oxygen) | 0.0000 | 0.0000 | 0.0000 | 0.0000 | 0.0000 | 0.0000 | 0.0000 |
| Comp Mole Frac (Hydrogen) | 0.6478 | 0.0000 | 0.0000 | 0.0000 | 0.0000 | 0.0000 | 0.0000 |
| Comp Mole Frac (CO2) | 0.0000 | 0.0000 | 0.0000 | 0.0000 | 0.0000 | 0.0000 | 0.0000 |
| Comp Mole Frac (CO) | 0.3230 | 0.3638 | 0.0135 | 0.0000 | 0.1583 | 0.0270 | 0.1583 |
| Comp Mole Frac (1-Butene) | 0.0000 | 0.0000 | 0.0000 | 0.0000 | 0.0000 | 0.0000 | 0.0000 |
| Comp Mole Frac (n-Pentane) | 0.0000 | 0.0116 | 0.1317 | 0.0000 | 0.0128 | 0.0111 | 0.0128 |
| Comp Mole Frac (n-C30) | 0.0000 | 0.0000 | 0.0165 | 0.0000 | 0.0010 | 0.5116 | 0.0010 |
| Comp Mole Frac (n-C29) | 0.0000 | 0.0000 | 0.0004 | 0.0000 | 0.0000 | 0.0069 | 0.0000 |
| Comp Mole Frac (n-C28) | 0.0000 | 0.0000 | 0.0005 | 0.0000 | 0.0000 | 0.0077 | 0.0000 |
| Comp Mole Frac (n-C27) | 0.0000 | 0.0000 | 0.0007 | 0.0000 | 0.0000 | 0.0082 | 0.0000 |
| Comp Mole Frac (n-C26) | 0.0000 | 0.0000 | 0.0009 | 0.0000 | 0.0001 | 0.0083 | 0.0001 |

| Name | S-200 | S-206 | S-205 | S-207 | S-204 | S-202 | S-201 |
|---|---|---|---|---|---|---|---|
| Comp Mole Frac (n-C25) | 0.0000 | 0.0000 | 0.0011 | 0.0000 | 0.0001 | 0.0083 | 0.0001 |
| Comp Mole Frac (n-C24) | 0.0000 | 0.0000 | 0.0014 | 0.0000 | 0.0001 | 0.0087 | 0.0001 |
| Comp Mole Frac (n-C23) | 0.0000 | 0.0000 | 0.0018 | 0.0000 | 0.0001 | 0.0089 | 0.0001 |
| Comp Mole Frac (Nitrogen) | 0.0181 | 0.2773 | 0.0088 | 0.0001 | 0.1206 | 0.0210 | 0.1206 |
| Name | S-203 | S-209 | S-210 | S-211 | S-300 | S-302 | Purge |
| Comp Mole Frac (Methane) | 0.0365 | 0.0835 | 0.0835 | 0.0835 | 0.0000 | 0.0069 | 0.0834 |
| Comp Mole Frac (Ethane) | 0.0636 | 0.1394 | 0.1394 | 0.1394 | 0.0000 | 0.0525 | 0.1395 |
| Comp Mole Frac (n-Octane) | 0.0044 | 0.0003 | 0.0003 | 0.0003 | 0.0000 | 0.0704 | 0.0003 |
| Comp Mole Frac (n-Hexane) | 0.0082 | 0.0035 | 0.0035 | 0.0035 | 0.0000 | 0.1099 | 0.0035 |
| Comp Mole Frac (n-Nonane) | 0.0033 | 0.0001 | 0.0001 | 0.0001 | 0.0000 | 0.0536 | 0.0001 |
| Comp Mole Frac (n-Heptane) | 0.0059 | 0.0010 | 0.0010 | 0.0010 | 0.0000 | 0.0890 | 0.0010 |
| Comp Mole Frac (n-Decane) | 0.0026 | 0.0000 | 0.0000 | 0.0000 | 0.0000 | 0.0432 | 0.0000 |
| Comp Mole Frac (n-C22) | 0.0001 | 0.0000 | 0.0000 | 0.0000 | 0.0000 | 0.0022 | 0.0000 |
| Comp Mole Frac (n-C21) | 0.0002 | 0.0000 | 0.0000 | 0.0000 | 0.0000 | 0.0028 | 0.0000 |
| Comp Mole Frac (n-C20) | 0.0002 | 0.0000 | 0.0000 | 0.0000 | 0.0000 | 0.0036 | 0.0000 |
| Comp Mole Frac (n-C19) | 0.0003 | 0.0000 | 0.0000 | 0.0000 | 0.0000 | 0.0047 | 0.0000 |
| Comp Mole Frac (n-C18) | 0.0004 | 0.0000 | 0.0000 | 0.0000 | 0.0000 | 0.0060 | 0.0000 |
| Comp Mole Frac (n-C17) | 0.0005 | 0.0000 | 0.0000 | 0.0000 | 0.0000 | 0.0077 | 0.0000 |
| Comp Mole Frac (n-C16) | 0.0006 | 0.0000 | 0.0000 | 0.0000 | 0.0000 | 0.0098 | 0.0000 |
| Comp Mole Frac (n-C15) | 0.0008 | 0.0000 | 0.0000 | 0.0000 | 0.0000 | 0.0126 | 0.0000 |
| Comp Mole Frac (n-C14) | 0.0010 | 0.0000 | 0.0000 | 0.0000 | 0.0000 | 0.0161 | 0.0000 |
| Comp Mole Frac (n-C13) | 0.0013 | 0.0000 | 0.0000 | 0.0000 | 0.0000 | 0.0206 | 0.0000 |
| Comp Mole Frac (n-C12) | 0.0016 | 0.0000 | 0.0000 | 0.0000 | 0.0000 | 0.0264 | 0.0000 |
| Comp Mole Frac (n-C11) | 0.0021 | 0.0000 | 0.0000 | 0.0000 | 0.0000 | 0.0338 | 0.0000 |
| Comp Mole Frac (n-Butane) | 0.0227 | 0.0345 | 0.0345 | 0.0345 | 0.0000 | 0.1271 | 0.0345 |
| Comp Mole Frac (Propane) | 0.0408 | 0.0808 | 0.0808 | 0.0808 | 0.0000 | 0.0955 | 0.0808 |

| Name | S-203 | S-209 | S-210 | S-211 | S-300 | S-302 | Purge |
|---|---|---|---|---|---|---|---|
| Comp Mole Frac (i-Butane) | 0.0000 | 0.0000 | 0.0000 | 0.0000 | 0.0000 | 0.0000 | 0.0000 |
| Comp Mole Frac (i-Pentane) | 0.0000 | 0.0000 | 0.0000 | 0.0000 | 0.0000 | 0.0000 | 0.0000 |
| Comp Mole Frac (H2O) | 0.5099 | 0.0043 | 0.0043 | 0.0043 | 0.0000 | 0.0009 | 0.0043 |
| Comp Mole Frac (Oxygen) | 0.0000 | 0.0000 | 0.0000 | 0.0000 | 0.0000 | 0.0000 | 0.0000 |
| Comp Mole Frac (Hydrogen) | 0.0000 | 0.0000 | 0.0000 | 0.0000 | 1.0000 | 0.0332 | 0.0000 |
| Comp Mole Frac (CO2) | 0.0000 | 0.0000 | 0.0000 | 0.0000 | 0.0000 | 0.0000 | 0.0000 |
| Comp Mole Frac (CO) | 0.1583 | 0.3637 | 0.3637 | 0.3637 | 0.0000 | 0.0130 | 0.3638 |
| Comp Mole Frac (1-Butene) | 0.0000 | 0.0000 | 0.0000 | 0.0000 | 0.0000 | 0.0000 | 0.0000 |
| Comp Mole Frac (n-Pentane) | 0.0128 | 0.0116 | 0.0116 | 0.0116 | 0.0000 | 0.1273 | 0.0116 |
| Comp Mole Frac (n-C30) | 0.0010 | 0.0000 | 0.0000 | 0.0000 | 0.0000 | 0.0160 | 0.0000 |
| Comp Mole Frac (n-C29) | 0.0000 | 0.0000 | 0.0000 | 0.0000 | 0.0000 | 0.0004 | 0.0000 |
| Comp Mole Frac (n-C28) | 0.0000 | 0.0000 | 0.0000 | 0.0000 | 0.0000 | 0.0005 | 0.0000 |
| Comp Mole Frac (n-C27) | 0.0000 | 0.0000 | 0.0000 | 0.0000 | 0.0000 | 0.0006 | 0.0000 |
| Comp Mole Frac (n-C26) | 0.0001 | 0.0000 | 0.0000 | 0.0000 | 0.0000 | 0.0008 | 0.0000 |
| Comp Mole Frac (n-C25) | 0.0001 | 0.0000 | 0.0000 | 0.0000 | 0.0000 | 0.0010 | 0.0000 |
| Comp Mole Frac (n-C24) | 0.0001 | 0.0000 | 0.0000 | 0.0000 | 0.0000 | 0.0014 | 0.0000 |
| Comp Mole Frac (n-C23) | 0.0001 | 0.0000 | 0.0000 | 0.0000 | 0.0000 | 0.0017 | 0.0000 |
| Comp Mole Frac (Nitrogen) | 0.1206 | 0.2774 | 0.2774 | 0.2774 | 0.0000 | 0.0085 | 0.2773 |
| Name | S-303 | S-304 | S-305 | S-306 | S-307 | S-308 | S-208 |
| Comp Mole Frac (Methane) | 0.0069 | 0.0069 | 0.0069 | 0.0069 | 0.0069 | 0.0069 | 0.0834 |
| Comp Mole Frac (Ethane) | 0.0525 | 0.0525 | 0.0525 | 0.0525 | 0.0525 | 0.0525 | 0.1395 |
| Comp Mole Frac (n-Octane) | 0.0704 | 0.0704 | 0.0704 | 0.0704 | 0.0704 | 0.0704 | 0.0003 |
| Comp Mole Frac (n-Hexane) | 0.1099 | 0.1099 | 0.1100 | 0.1099 | 0.1099 | 0.1099 | 0.0035 |
| Comp Mole Frac (n-Nonane) | 0.0536 | 0.0536 | 0.0536 | 0.0536 | 0.0536 | 0.0536 | 0.0001 |
| Comp Mole Frac (n-Heptane) | 0.0890 | 0.0890 | 0.0890 | 0.0890 | 0.0890 | 0.0890 | 0.0010 |
| Comp Mole Frac (n-Decane) | 0.0432 | 0.0454 | 0.0454 | 0.0454 | 0.0454 | 0.0454 | 0.0000 |

| Name | S-303 | S-304 | S-305 | S-306 | S-307 | S-308 | S-208 |
|------|-------|-------|-------|-------|-------|-------|-------|
| Comp Mole Frac (n-C22) | 0.0022 | 0.0006 | 0.0006 | 0.0006 | 0.0006 | 0.0006 | 0.0000 |
| Comp Mole Frac (n-C21) | 0.0028 | 0.0007 | 0.0007 | 0.0007 | 0.0007 | 0.0007 | 0.0000 |
| Comp Mole Frac (n-C20) | 0.0036 | 0.0036 | 0.0036 | 0.0036 | 0.0036 | 0.0036 | 0.0000 |
| Comp Mole Frac (n-C19) | 0.0047 | 0.0047 | 0.0047 | 0.0047 | 0.0047 | 0.0047 | 0.0000 |
| Comp Mole Frac (n-C18) | 0.0060 | 0.0060 | 0.0060 | 0.0060 | 0.0060 | 0.0060 | 0.0000 |
| Comp Mole Frac (n-C17) | 0.0077 | 0.0077 | 0.0076 | 0.0077 | 0.0077 | 0.0077 | 0.0000 |
| Comp Mole Frac (n-C16) | 0.0098 | 0.0098 | 0.0098 | 0.0098 | 0.0098 | 0.0098 | 0.0000 |
| Comp Mole Frac (n-C15) | 0.0126 | 0.0368 | 0.0368 | 0.0368 | 0.0368 | 0.0368 | 0.0000 |
| Comp Mole Frac (n-C14) | 0.0161 | 0.0176 | 0.0176 | 0.0176 | 0.0176 | 0.0176 | 0.0000 |
| Comp Mole Frac (n-C13) | 0.0206 | 0.0231 | 0.0231 | 0.0231 | 0.0231 | 0.0231 | 0.0000 |
| Comp Mole Frac (n-C12) | 0.0264 | 0.0305 | 0.0305 | 0.0305 | 0.0305 | 0.0305 | 0.0000 |
| Comp Mole Frac (n-C11) | 0.0338 | 0.0406 | 0.0406 | 0.0406 | 0.0406 | 0.0406 | 0.0000 |
| Comp Mole Frac (n-Butane) | 0.1271 | 0.1271 | 0.1271 | 0.1271 | 0.1271 | 0.1271 | 0.0345 |
| Comp Mole Frac (Propane) | 0.0955 | 0.0955 | 0.0955 | 0.0955 | 0.0955 | 0.0955 | 0.0808 |
| Comp Mole Frac (i-Butane) | 0.0000 | 0.0000 | 0.0000 | 0.0000 | 0.0000 | 0.0000 | 0.0000 |
| Comp Mole Frac (i-Pentane) | 0.0000 | 0.0000 | 0.0000 | 0.0000 | 0.0000 | 0.0000 | 0.0000 |
| Comp Mole Frac (H2O) | 0.0009 | 0.0009 | 0.0009 | 0.0009 | 0.0009 | 0.0009 | 0.0043 |
| Comp Mole Frac (Oxygen) | 0.0000 | 0.0000 | 0.0000 | 0.0000 | 0.0000 | 0.0000 | 0.0000 |
| Comp Mole Frac (Hydrogen) | 0.0332 | 0.0125 | 0.0125 | 0.0125 | 0.0125 | 0.0125 | 0.0000 |
| Comp Mole Frac (CO2) | 0.0000 | 0.0000 | 0.0000 | 0.0000 | 0.0000 | 0.0000 | 0.0000 |
| Comp Mole Frac (CO) | 0.0130 | 0.0130 | 0.0130 | 0.0130 | 0.0130 | 0.0130 | 0.3638 |
| Comp Mole Frac (1-Butene) | 0.0000 | 0.0000 | 0.0000 | 0.0000 | 0.0000 | 0.0000 | 0.0000 |
| Comp Mole Frac (n-Pentane) | 0.1273 | 0.1273 | 0.1274 | 0.1273 | 0.1273 | 0.1273 | 0.0116 |
| Comp Mole Frac (n-C30) | 0.0160 | 0.0040 | 0.0040 | 0.0040 | 0.0040 | 0.0040 | 0.0000 |
| Comp Mole Frac (n-C29) | 0.0004 | 0.0001 | 0.0001 | 0.0001 | 0.0001 | 0.0001 | 0.0000 |
| Comp Mole Frac (n-C28) | 0.0005 | 0.0001 | 0.0001 | 0.0001 | 0.0001 | 0.0001 | 0.0000 |
| Comp Mole Frac (n-C27) | 0.0006 | 0.0002 | 0.0002 | 0.0002 | 0.0002 | 0.0002 | 0.0000 |

| Name | S-303 | S-304 | S-305 | S-306 | S-307 | S-308 | S-208 |
|------|-------|-------|-------|-------|-------|-------|-------|
| Comp Mole Frac (n-C26) | 0.0008 | 0.0002 | 0.0002 | 0.0002 | 0.0002 | 0.0002 | 0.0000 |
| Comp Mole Frac (n-C25) | 0.0010 | 0.0003 | 0.0003 | 0.0003 | 0.0003 | 0.0003 | 0.0000 |
| Comp Mole Frac (n-C24) | 0.0014 | 0.0003 | 0.0003 | 0.0003 | 0.0003 | 0.0003 | 0.0000 |
| Comp Mole Frac (n-C23) | 0.0017 | 0.0004 | 0.0004 | 0.0004 | 0.0004 | 0.0004 | 0.0000 |
| Comp Mole Frac (Nitrogen) | 0.0085 | 0.0085 | 0.0085 | 0.0085 | 0.0085 | 0.0085 | 0.2773 |

| Name | S-106 | S-108 | S-111 | S-112 | Oxygen | S-301 | S-309 |
|------|-------|-------|-------|-------|--------|-------|-------|
| Comp Mole Frac (Methane) | 0.0067 | 0.0067 | 0.0000 | 0.0076 | 0.0000 | 0.0072 | 0.0218 |
| Comp Mole Frac (Ethane) | 0.0000 | 0.0000 | 0.0000 | 0.0000 | 0.0000 | 0.0543 | 0.1654 |
| Comp Mole Frac (n-Octane) | 0.0000 | 0.0000 | 0.0000 | 0.0000 | 0.0000 | 0.0728 | 0.0000 |
| Comp Mole Frac (n-Hexane) | 0.0000 | 0.0000 | 0.0000 | 0.0000 | 0.0000 | 0.1137 | 0.0000 |
| Comp Mole Frac (n-Nonane) | 0.0000 | 0.0000 | 0.0000 | 0.0000 | 0.0000 | 0.0554 | 0.0000 |
| Comp Mole Frac (n-Heptane) | 0.0000 | 0.0000 | 0.0000 | 0.0000 | 0.0000 | 0.0921 | 0.0000 |
| Comp Mole Frac (n-Decane) | 0.0000 | 0.0000 | 0.0000 | 0.0000 | 0.0000 | 0.0447 | 0.0000 |
| Comp Mole Frac (n-C22) | 0.0000 | 0.0000 | 0.0000 | 0.0000 | 0.0000 | 0.0023 | 0.0000 |
| Comp Mole Frac (n-C21) | 0.0000 | 0.0000 | 0.0000 | 0.0000 | 0.0000 | 0.0029 | 0.0000 |
| Comp Mole Frac (n-C20) | 0.0000 | 0.0000 | 0.0000 | 0.0000 | 0.0000 | 0.0038 | 0.0000 |
| Comp Mole Frac (n-C19) | 0.0000 | 0.0000 | 0.0000 | 0.0000 | 0.0000 | 0.0048 | 0.0000 |
| Comp Mole Frac (n-C18) | 0.0000 | 0.0000 | 0.0000 | 0.0000 | 0.0000 | 0.0062 | 0.0000 |
| Comp Mole Frac (n-C17) | 0.0000 | 0.0000 | 0.0000 | 0.0000 | 0.0000 | 0.0079 | 0.0000 |
| Comp Mole Frac (n-C16) | 0.0000 | 0.0000 | 0.0000 | 0.0000 | 0.0000 | 0.0102 | 0.0000 |
| Comp Mole Frac (n-C15) | 0.0000 | 0.0000 | 0.0000 | 0.0000 | 0.0000 | 0.0130 | 0.0000 |
| Comp Mole Frac (n-C14) | 0.0000 | 0.0000 | 0.0000 | 0.0000 | 0.0000 | 0.0167 | 0.0000 |
| Comp Mole Frac (n-C13) | 0.0000 | 0.0000 | 0.0000 | 0.0000 | 0.0000 | 0.0213 | 0.0000 |
| Comp Mole Frac (n-C12) | 0.0000 | 0.0000 | 0.0000 | 0.0000 | 0.0000 | 0.0273 | 0.0000 |
| Comp Mole Frac (n-C11) | 0.0000 | 0.0000 | 0.0000 | 0.0000 | 0.0000 | 0.0350 | 0.0000 |
| Comp Mole Frac (n-Butane) | 0.0000 | 0.0000 | 0.0000 | 0.0000 | 0.0000 | 0.1315 | 0.4002 |

| Name | S-106 | S-108 | S-111 | S-112 | Oxygen | S-301 | S-309 |
|---|---|---|---|---|---|---|---|
| Comp Mole Frac (Propane) | 0.0000 | 0.0000 | 0.0000 | 0.0000 | 0.0000 | 0.0988 | 0.3007 |
| Comp Mole Frac (i-Butane) | 0.0000 | 0.0000 | 0.0000 | 0.0000 | 0.0000 | 0.0000 | 0.0000 |
| Comp Mole Frac (i-Pentane) | 0.0000 | 0.0000 | 0.0000 | 0.0000 | 0.0000 | 0.0000 | 0.0000 |
| Comp Mole Frac (H2O) | 0.0969 | 0.0969 | 0.0000 | 0.0034 | 0.0000 | 0.0009 | 0.0027 |
| Comp Mole Frac (Oxygen) | 0.0000 | 0.0000 | 0.0000 | 0.0000 | 1.0000 | 0.0000 | 0.0000 |
| Comp Mole Frac (Hydrogen) | 0.5728 | 0.5728 | 0.0000 | 0.6478 | 0.0000 | 0.0000 | 0.0394 |
| Comp Mole Frac (CO2) | 0.0219 | 0.0219 | 1.0000 | 0.0000 | 0.0000 | 0.0000 | 0.0000 |
| Comp Mole Frac (CO) | 0.2856 | 0.2856 | 0.0000 | 0.3230 | 0.0000 | 0.0135 | 0.0410 |
| Comp Mole Frac (1-Butene) | 0.0000 | 0.0000 | 0.0000 | 0.0000 | 0.0000 | 0.0000 | 0.0000 |
| Comp Mole Frac (n-Pentane) | 0.0000 | 0.0000 | 0.0000 | 0.0000 | 0.0000 | 0.1317 | 0.0022 |
| Comp Mole Frac (n-C30) | 0.0000 | 0.0000 | 0.0000 | 0.0000 | 0.0000 | 0.0165 | 0.0000 |
| Comp Mole Frac (n-C29) | 0.0000 | 0.0000 | 0.0000 | 0.0000 | 0.0000 | 0.0004 | 0.0000 |
| Comp Mole Frac (n-C28) | 0.0000 | 0.0000 | 0.0000 | 0.0000 | 0.0000 | 0.0005 | 0.0000 |
| Comp Mole Frac (n-C27) | 0.0000 | 0.0000 | 0.0000 | 0.0000 | 0.0000 | 0.0007 | 0.0000 |
| Comp Mole Frac (n-C26) | 0.0000 | 0.0000 | 0.0000 | 0.0000 | 0.0000 | 0.0009 | 0.0000 |
| Comp Mole Frac (n-C25) | 0.0000 | 0.0000 | 0.0000 | 0.0000 | 0.0000 | 0.0011 | 0.0000 |
| Comp Mole Frac (n-C24) | 0.0000 | 0.0000 | 0.0000 | 0.0000 | 0.0000 | 0.0014 | 0.0000 |
| Comp Mole Frac (n-C23) | 0.0000 | 0.0000 | 0.0000 | 0.0000 | 0.0000 | 0.0018 | 0.0000 |
| Comp Mole Frac (Nitrogen) | 0.0160 | 0.0160 | 0.0000 | 0.0181 | 0.0000 | 0.0088 | 0.0266 |
| Name | S-310 | S-311 | S-312 | S-313 | S-100 | S-101 | S-102 |
| Comp Mole Frac (Methane) | 0.0000 | 0.0000 | 0.0000 | 0.0000 | 0.9200 | 0.7700 | 0.7700 |
| Comp Mole Frac (Ethane) | 0.0000 | 0.0000 | 0.0000 | 0.0000 | 0.0300 | 0.0001 | 0.0001 |
| Comp Mole Frac (n-Octane) | 0.1032 | 0.1339 | 0.0031 | 0.0000 | 0.0000 | 0.0000 | 0.0000 |
| Comp Mole Frac (n-Hexane) | 0.1611 | 0.2099 | 0.0020 | 0.0000 | 0.0000 | 0.0000 | 0.0000 |
| Comp Mole Frac (n-Nonane) | 0.0786 | 0.1015 | 0.0038 | 0.0000 | 0.0000 | 0.0000 | 0.0000 |
| Comp Mole Frac (n-Heptane) | 0.1305 | 0.1697 | 0.0025 | 0.0000 | 0.0000 | 0.0000 | 0.0000 |

| Name | S-310 | S-311 | S-312 | S-313 | S-100 | S-101 | S-102 |
|---|---|---|---|---|---|---|---|
| Comp Mole Frac (n-Decane) | 0.0665 | 0.0851 | 0.0059 | 0.0000 | 0.0000 | 0.0000 | 0.0000 |
| Comp Mole Frac (n-C22) | 0.0008 | 0.0000 | 0.0002 | 0.0675 | 0.0000 | 0.0000 | 0.0000 |
| Comp Mole Frac (n-C21) | 0.0010 | 0.0000 | 0.0005 | 0.0815 | 0.0000 | 0.0000 | 0.0000 |
| Comp Mole Frac (n-C20) | 0.0053 | 0.0000 | 0.0162 | 0.1504 | 0.0000 | 0.0000 | 0.0000 |
| Comp Mole Frac (n-C19) | 0.0069 | 0.0000 | 0.0302 | 0.0102 | 0.0000 | 0.0000 | 0.0000 |
| Comp Mole Frac (n-C18) | 0.0087 | 0.0000 | 0.0392 | 0.0003 | 0.0000 | 0.0000 | 0.0000 |
| Comp Mole Frac (n-C17) | 0.0112 | 0.0000 | 0.0503 | 0.0000 | 0.0000 | 0.0000 | 0.0000 |
| Comp Mole Frac (n-C16) | 0.0144 | 0.0000 | 0.0646 | 0.0000 | 0.0000 | 0.0000 | 0.0000 |
| Comp Mole Frac (n-C15) | 0.0540 | 0.0000 | 0.2420 | 0.0000 | 0.0000 | 0.0000 | 0.0000 |
| Comp Mole Frac (n-C14) | 0.0258 | 0.0000 | 0.1159 | 0.0000 | 0.0000 | 0.0000 | 0.0000 |
| Comp Mole Frac (n-C13) | 0.0339 | 0.0000 | 0.1519 | 0.0000 | 0.0000 | 0.0000 | 0.0000 |
| Comp Mole Frac (n-C12) | 0.0447 | 0.0003 | 0.1995 | 0.0000 | 0.0000 | 0.0000 | 0.0000 |
| Comp Mole Frac (n-C11) | 0.0595 | 0.0575 | 0.0692 | 0.0000 | 0.0000 | 0.0000 | 0.0000 |
| Comp Mole Frac (n-Butane) | 0.0000 | 0.0000 | 0.0000 | 0.0000 | 0.0000 | 0.0000 | 0.0000 |
| Comp Mole Frac (Propane) | 0.0000 | 0.0000 | 0.0000 | 0.0000 | 0.0000 | 0.0000 | 0.0000 |
| Comp Mole Frac (i-Butane) | 0.0000 | 0.0000 | 0.0000 | 0.0000 | 0.0000 | 0.0000 | 0.0000 |
| Comp Mole Frac (i-Pentane) | 0.0000 | 0.0000 | 0.0000 | 0.0000 | 0.0000 | 0.0000 | 0.0000 |
| Comp Mole Frac (H2O) | 0.0000 | 0.0000 | 0.0000 | 0.0000 | 0.0000 | 0.1261 | 0.1261 |
| Comp Mole Frac (Oxygen) | 0.0000 | 0.0000 | 0.0000 | 0.0000 | 0.0000 | 0.0000 | 0.0000 |
| Comp Mole Frac (Hydrogen) | 0.0000 | 0.0000 | 0.0000 | 0.0000 | 0.0000 | 0.0459 | 0.0459 |
| Comp Mole Frac (CO2) | 0.0000 | 0.0000 | 0.0000 | 0.0000 | 0.0000 | 0.0170 | 0.0170 |
| Comp Mole Frac (CO) | 0.0000 | 0.0000 | 0.0000 | 0.0000 | 0.0000 | 0.0006 | 0.0006 |
| Comp Mole Frac (1-Butene) | 0.0000 | 0.0000 | 0.0000 | 0.0000 | 0.0000 | 0.0000 | 0.0000 |
| Comp Mole Frac (n-Pentane) | 0.1856 | 0.2421 | 0.0014 | 0.0000 | 0.0000 | 0.0000 | 0.0000 |
| Comp Mole Frac (n-C30) | 0.0059 | 0.0000 | 0.0011 | 0.4909 | 0.0000 | 0.0000 | 0.0000 |
| Comp Mole Frac (n-C29) | 0.0001 | 0.0000 | 0.0000 | 0.0115 | 0.0000 | 0.0000 | 0.0000 |
| Comp Mole Frac (n-C28) | 0.0002 | 0.0000 | 0.0000 | 0.0155 | 0.0000 | 0.0000 | 0.0000 |

| Name | S-310 | S-311 | S-312 | S-313 | S-100 | S-101 | S-102 |
|------|-------|-------|-------|-------|-------|-------|-------|
| Comp Mole Frac (n-C27) | 0.0002 | 0.0000 | 0.0000 | 0.0197 | 0.0000 | 0.0000 | 0.0000 |
| Comp Mole Frac (n-C26) | 0.0003 | 0.0000 | 0.0001 | 0.0256 | 0.0000 | 0.0000 | 0.0000 |
| Comp Mole Frac (n-C25) | 0.0004 | 0.0000 | 0.0001 | 0.0319 | 0.0000 | 0.0000 | 0.0000 |
| Comp Mole Frac (n-C24) | 0.0005 | 0.0000 | 0.0001 | 0.0415 | 0.0000 | 0.0000 | 0.0000 |
| Comp Mole Frac (n-C23) | 0.0006 | 0.0000 | 0.0001 | 0.0534 | 0.0000 | 0.0000 | 0.0000 |
| Comp Mole Frac (Nitrogen) | 0.0000 | 0.0000 | 0.0000 | 0.0000 | 0.0500 | 0.0402 | 0.0402 |

| Name | S-103 | ** New ** |
|------|-------|-----------|
| Comp Mole Frac (Methane) | 0.7700 | |
| Comp Mole Frac (Ethane) | 0.0001 | |
| Comp Mole Frac (n-Octane) | 0.0000 | |
| Comp Mole Frac (n-Hexane) | 0.0000 | |
| Comp Mole Frac (n-Nonane) | 0.0000 | |
| Comp Mole Frac (n-Heptane) | 0.0000 | |
| Comp Mole Frac (n-Decane) | 0.0000 | |
| Comp Mole Frac (n-C22) | 0.0000 | |
| Comp Mole Frac (n-C21) | 0.0000 | |
| Comp Mole Frac (n-C20) | 0.0000 | |
| Comp Mole Frac (n-C19) | 0.0000 | |
| Comp Mole Frac (n-C18) | 0.0000 | |
| Comp Mole Frac (n-C17) | 0.0000 | |
| Comp Mole Frac (n-C16) | 0.0000 | |
| Comp Mole Frac (n-C15) | 0.0000 | |
| Comp Mole Frac (n-C14) | 0.0000 | |
| Comp Mole Frac (n-C13) | 0.0000 | |
| Comp Mole Frac (n-C12) | 0.0000 | |
| Comp Mole Frac (n-C11) | 0.0000 | |

| Name | S-103 | ** New ** |
|---|---|---|
| Comp Mole Frac (n-Butane) | 0.0000 | |
| Comp Mole Frac (Propane) | 0.0000 | |
| Comp Mole Frac (i-Butane) | 0.0000 | |
| Comp Mole Frac (i-Pentane) | 0.0000 | |
| Comp Mole Frac (H2O) | 0.1261 | |
| Comp Mole Frac (Oxygen) | 0.0000 | |
| Comp Mole Frac (Hydrogen) | 0.0459 | |
| Comp Mole Frac (CO2) | 0.0170 | |
| Comp Mole Frac (CO) | 0.0006 | |
| Comp Mole Frac (1-Butene) | 0.0000 | |
| Comp Mole Frac (n-Pentane) | 0.0000 | |
| Comp Mole Frac (n-C30) | 0.0000 | |
| Comp Mole Frac (n-C29) | 0.0000 | |
| Comp Mole Frac (n-C28) | 0.0000 | |
| Comp Mole Frac (n-C27) | 0.0000 | |
| Comp Mole Frac (n-C26) | 0.0000 | |
| Comp Mole Frac (n-C25) | 0.0000 | |
| Comp Mole Frac (n-C24) | 0.0000 | |
| Comp Mole Frac (n-C23) | 0.0000 | |
| Comp Mole Frac (Nitrogen) | 0.0402 | |

**APPENDIX D:** Low Temperature Fischer Tropsch Simulation
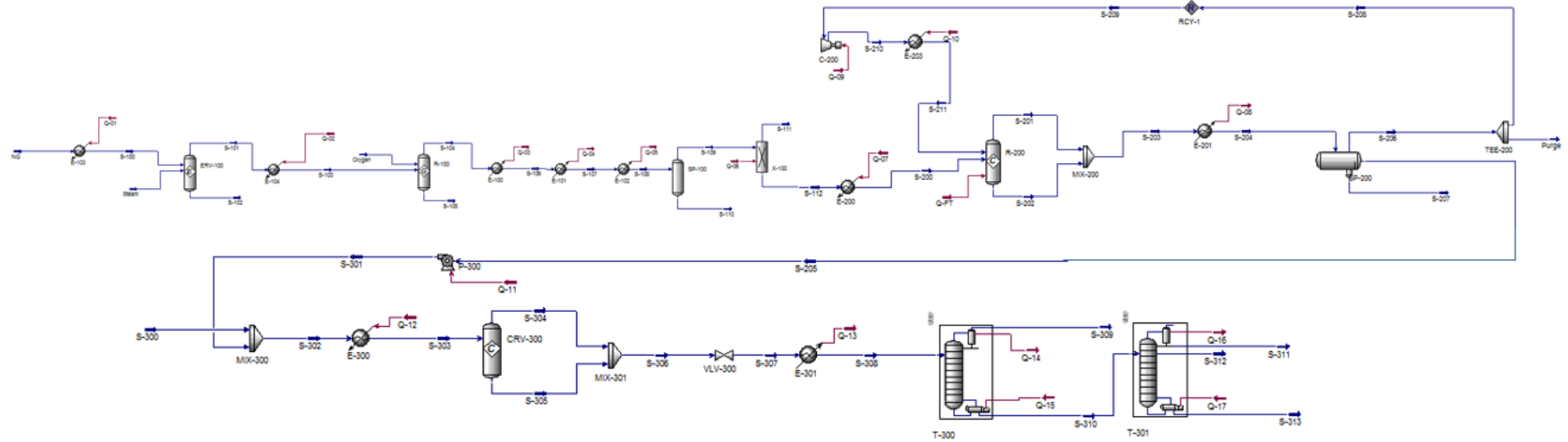
# APPENDIX D: Low Temperature Fischer Tropsch material stream

Table D 1: Low temperature Fischer Tropsch material stream.

| Name | NG | Steam | S-104 | S-105 | S-107 | S-110 | S-109 | S-200 |
|---|---|---|---|---|---|---|---|---|
| Vapour Fraction | 1 | 1 | 1 | 0 | 1 | 0 | 1 | 1 |
| Temperature [C] | 25 | 500 | 1143.687 | 1143.687 | 293.6869 | 38 | 38 | 240 |
| Pressure [kPa] | 100 | 2500 | 2500 | 2500 | 2400 | 2300 | 2300 | 2000 |
| Molar Flow [kgmole/h] | 37540 | 7508 | 117401.6 | 0 | 117401.6 | 10913.02 | 106488.6 | 104030 |
| Mass Flow [kg/h] | 640515.6 | 135257.4 | 1454067 | 0 | 1454067 | 196648.3 | 1257418 | 1149215 |
| Liquid Volume Flow [m3/h] | 2011.056 | 135.5303 | 3561.089 | 0 | 3561.089 | 197.0714 | 3364.018 | 3232.915 |
| Heat Flow [Mkcal/h] | -641.235 | -404.37 | -773.082 | 0 | -1559.94 | -743.835 | -1145.65 | -767.206 |
| Name | S-206 | S-205 | S-207 | S-204 | S-202 | S-201 | S-203 | S-209 |
| Vapour Fraction | 1 | 0 | 0 | 0.41757 | 0 | 1 | 0.988952 | 1 |
| Temperature [C] | 38 | 38 | 38 | 38 | 240 | 240 | 240 | 38 |
| Pressure [kPa] | 1800 | 1800 | 1800 | 1800 | 2000 | 2000 | 2000 | 1800 |
| Molar Flow [kgmole/h] | 24673.57 | 2377.394 | 32037.53 | 59088.5 | 652.7825 | 58435.71 | 59088.5 | 18478.81 |
| Mass Flow [kg/h] | 608338.6 | 419203.2 | 577178.8 | 1604721 | 208185.4 | 1396535 | 1604721 | 455548.9 |
| Liquid Volume Flow [m3/h] | 1055.972 | 557.2235 | 578.361 | 2191.556 | 259.7204 | 1931.836 | 2191.556 | 790.6109 |
| Heat Flow [Mkcal/h] | -343.403 | -201.746 | -2183.53 | -2728.68 | -69.8889 | -2164.13 | -2234.02 | -257.159 |
| Name | S-210 | S-211 | S-300 | S-302 | Purge | S-304 | S-305 | S-306 |
| Vapour Fraction | 1 | 1 | 1 | 0.186889 | 1 | 1 | 0 | 0 |
| Temperature [C] | 48.46641 | 240 | 320 | 41.02892 | 38 | 363.2401 | 363.2401 | 363.2401 |
| Pressure [kPa] | 2000 | 2000 | 2000 | 2000 | 1800 | 8000 | 8000 | 8000 |
| Molar Flow [kgmole/h] | 18478.81 | 18478.81 | 450 | 2827.394 | 6168.392 | 0 | 2827.394 | 2827.394 |
| Mass Flow [kg/h] | 455548.9 | 455548.9 | 907.2 | 420110.4 | 152084.7 | 0 | 420113.5 | 420113.5 |
| Liquid Volume Flow [m3/h] | 790.6109 | 790.6109 | 12.98614 | 570.2096 | 263.9929 | 0 | 570.8779 | 570.8779 |

| Name | S-210 | S-211 | S-300 | S-302 | Purge | S-304 | S-305 | S-306 |
|---|---|---|---|---|---|---|---|---|
| Heat Flow [Mkcal/h] | -255.56 | -222.436 | 0.915518 | -200.795 | -85.8508 | 0 | -111.357 | -111.357 |

| Name | S-307 | S-208 | S-106 | S-108 | S-111 | S-112 | Oxygen | S-301 |
|---|---|---|---|---|---|---|---|---|
| Vapour Fraction | 0.981423 | 1 | 1 | 0.907045 | 1 | 0.999903 | 1 | 0 |
| Temperature [C] | 305.8604 | 38 | 693.6869 | 38 | 38 | 38 | 144 | 38.04486 |
| Pressure [kPa] | 101 | 1800 | 2500 | 2300 | 2300 | 2300 | 2500 | 2000 |
| Molar Flow [kgmole/h] | 2827.394 | 18505.18 | 117401.6 | 117401.6 | 2458.633 | 104030 | 21196.88 | 2377.394 |
| Mass Flow [kg/h] | 420113.5 | 456254 | 1454067 | 1454067 | 108203.7 | 1149215 | 678300 | 419203.2 |
| Liquid Volume Flow [m3/h] | 570.8779 | 791.9788 | 3561.089 | 3561.089 | 131.1028 | 3232.915 | 596.2133 | 557.2235 |
| Heat Flow [Mkcal/h] | -111.357 | -257.552 | -1202.29 | -1889.48 | -231.677 | -914.405 | 17.3478 | -201.71 |

| Name | S-309 | S-311 | S-312 | S-310 | S-308 | S-313 | S-303 | S-100 |
|---|---|---|---|---|---|---|---|---|
| Vapour Fraction | 0.996599 | 2.76E-05 | 1.58E-06 | 1.19E-04 | 0.189797 | 0 | 0.124703 | 1 |
| Temperature [C] | -22.0461 | 82.02535 | 266.3027 | 131.8092 | 70 | 400.9093 | 345 | 455 |
| Pressure [kPa] | 100 | 100 | 150 | 150 | 101 | 150 | 8000 | 100 |
| Molar Flow [kgmole/h] | 468.0047 | 1087.421 | 1111.608 | 2359.389 | 2827.394 | 160.3603 | 2827.394 | 37540 |
| Mass Flow [kg/h] | 15559.31 | 120813.2 | 227159.5 | 404554.2 | 420113.5 | 56581.54 | 420110.4 | 640515.6 |
| Liquid Volume Flow [m3/h] | 31.88417 | 172.4571 | 296.1074 | 538.9938 | 570.8779 | 70.42921 | 570.2096 | 2011.056 |
| Heat Flow [Mkcal/h] | -8.99435 | -59.5314 | -75.5671 | -174.393 | -196.639 | -11.313 | -111.357 | -458.228 |

| Name | S-101 | S-102 | S-103 | ** New ** |
|---|---|---|---|---|
| Vapour Fraction | 1 | 0 | 1 | |
| Temperature [C] | 379.5768 | 379.5768 | 500 | |
| Pressure [kPa] | 100 | 100 | 2500 | |
| Molar Flow [kgmole/h] | 48023.83 | 0 | 48023.83 | |
| Mass Flow [kg/h] | 775773.7 | 0 | 775773.7 | |
| Liquid Volume Flow [m3/h] | 2254.631 | 0 | 2254.631 | |
| Heat Flow [Mkcal/h] | -862.59 | 0 | -790.43 | |

## APPENDIX D: Low Temperature Fischer Tropsch stream composition

Table D 2: Low temperature Fischer Tropsch stream composition.

| Name | NG | Steam | S-104 | S-105 | S-107 | S-110 | S-109 | S-200 |
|---|---|---|---|---|---|---|---|---|
| Comp Mole Frac (Methane) | 0.9200 | 0.0000 | 0.0052 | 0.0052 | 0.0052 | 0.0000 | 0.0057 | 0.0059 |
| Comp Mole Frac (Ethane) | 0.0300 | 0.0000 | 0.0000 | 0.0000 | 0.0000 | 0.0000 | 0.0000 | 0.0000 |
| Comp Mole Frac (n-Octane) | 0.0000 | 0.0000 | 0.0000 | 0.0000 | 0.0000 | 0.0000 | 0.0000 | 0.0000 |
| Comp Mole Frac (n-Hexane) | 0.0000 | 0.0000 | 0.0000 | 0.0000 | 0.0000 | 0.0000 | 0.0000 | 0.0000 |
| Comp Mole Frac (n-Nonane) | 0.0000 | 0.0000 | 0.0000 | 0.0000 | 0.0000 | 0.0000 | 0.0000 | 0.0000 |
| Comp Mole Frac (n-Heptane) | 0.0000 | 0.0000 | 0.0000 | 0.0000 | 0.0000 | 0.0000 | 0.0000 | 0.0000 |
| Comp Mole Frac (n-Decane) | 0.0000 | 0.0000 | 0.0000 | 0.0000 | 0.0000 | 0.0000 | 0.0000 | 0.0000 |
| Comp Mole Frac (n-C22) | 0.0000 | 0.0000 | 0.0000 | 0.0000 | 0.0000 | 0.0000 | 0.0000 | 0.0000 |
| Comp Mole Frac (n-C21) | 0.0000 | 0.0000 | 0.0000 | 0.0000 | 0.0000 | 0.0000 | 0.0000 | 0.0000 |
| Comp Mole Frac (n-C20) | 0.0000 | 0.0000 | 0.0000 | 0.0000 | 0.0000 | 0.0000 | 0.0000 | 0.0000 |
| Comp Mole Frac (n-C19) | 0.0000 | 0.0000 | 0.0000 | 0.0000 | 0.0000 | 0.0000 | 0.0000 | 0.0000 |
| Comp Mole Frac (n-C18) | 0.0000 | 0.0000 | 0.0000 | 0.0000 | 0.0000 | 0.0000 | 0.0000 | 0.0000 |
| Comp Mole Frac (n-C17) | 0.0000 | 0.0000 | 0.0000 | 0.0000 | 0.0000 | 0.0000 | 0.0000 | 0.0000 |
| Comp Mole Frac (n-C16) | 0.0000 | 0.0000 | 0.0000 | 0.0000 | 0.0000 | 0.0000 | 0.0000 | 0.0000 |
| Comp Mole Frac (n-C15) | 0.0000 | 0.0000 | 0.0000 | 0.0000 | 0.0000 | 0.0000 | 0.0000 | 0.0000 |
| Comp Mole Frac (n-C14) | 0.0000 | 0.0000 | 0.0000 | 0.0000 | 0.0000 | 0.0000 | 0.0000 | 0.0000 |
| Comp Mole Frac (n-C13) | 0.0000 | 0.0000 | 0.0000 | 0.0000 | 0.0000 | 0.0000 | 0.0000 | 0.0000 |
| Comp Mole Frac (n-C12) | 0.0000 | 0.0000 | 0.0000 | 0.0000 | 0.0000 | 0.0000 | 0.0000 | 0.0000 |
| Comp Mole Frac (n-C11) | 0.0000 | 0.0000 | 0.0000 | 0.0000 | 0.0000 | 0.0000 | 0.0000 | 0.0000 |
| Comp Mole Frac (n-Butane) | 0.0000 | 0.0000 | 0.0000 | 0.0000 | 0.0000 | 0.0000 | 0.0000 | 0.0000 |
| Comp Mole Frac (Propane) | 0.0000 | 0.0000 | 0.0000 | 0.0000 | 0.0000 | 0.0000 | 0.0000 | 0.0000 |
| Comp Mole Frac (i-Butane) | 0.0000 | 0.0000 | 0.0000 | 0.0000 | 0.0000 | 0.0000 | 0.0000 | 0.0000 |
| Comp Mole Frac (i-Pentane) | 0.0000 | 0.0000 | 0.0000 | 0.0000 | 0.0000 | 0.0000 | 0.0000 | 0.0000 |

| Name | NG | Steam | S-104 | S-105 | S-107 | S-110 | S-109 | S-200 |
|---|---|---|---|---|---|---|---|---|
| Comp Mole Frac (H2O) | 0.0000 | 1.0000 | 0.0959 | 0.0959 | 0.0959 | 0.9998 | 0.0033 | 0.0034 |
| Comp Mole Frac (Oxygen) | 0.0000 | 0.0000 | 0.0000 | 0.0000 | 0.0000 | 0.0000 | 0.0000 | 0.0000 |
| Comp Mole Frac (Hydrogen) | 0.0000 | 0.0000 | 0.5747 | 0.5747 | 0.5747 | 0.0000 | 0.6336 | 0.6486 |
| Comp Mole Frac (CO2) | 0.0000 | 0.0000 | 0.0210 | 0.0210 | 0.0210 | 0.0002 | 0.0231 | 0.0000 |
| Comp Mole Frac (CO) | 0.0000 | 0.0000 | 0.2872 | 0.2872 | 0.2872 | 0.0000 | 0.3166 | 0.3241 |
| Comp Mole Frac (1-Butene) | 0.0000 | 0.0000 | 0.0000 | 0.0000 | 0.0000 | 0.0000 | 0.0000 | 0.0000 |
| Comp Mole Frac (n-Pentane) | 0.0000 | 0.0000 | 0.0000 | 0.0000 | 0.0000 | 0.0000 | 0.0000 | 0.0000 |
| Comp Mole Frac (n-C30) | 0.0000 | 0.0000 | 0.0000 | 0.0000 | 0.0000 | 0.0000 | 0.0000 | 0.0000 |
| Comp Mole Frac (n-C29) | 0.0000 | 0.0000 | 0.0000 | 0.0000 | 0.0000 | 0.0000 | 0.0000 | 0.0000 |
| Comp Mole Frac (n-C28) | 0.0000 | 0.0000 | 0.0000 | 0.0000 | 0.0000 | 0.0000 | 0.0000 | 0.0000 |
| Comp Mole Frac (n-C27) | 0.0000 | 0.0000 | 0.0000 | 0.0000 | 0.0000 | 0.0000 | 0.0000 | 0.0000 |
| Comp Mole Frac (n-C26) | 0.0000 | 0.0000 | 0.0000 | 0.0000 | 0.0000 | 0.0000 | 0.0000 | 0.0000 |
| Comp Mole Frac (n-C25) | 0.0000 | 0.0000 | 0.0000 | 0.0000 | 0.0000 | 0.0000 | 0.0000 | 0.0000 |
| Comp Mole Frac (n-C24) | 0.0000 | 0.0000 | 0.0000 | 0.0000 | 0.0000 | 0.0000 | 0.0000 | 0.0000 |
| Comp Mole Frac (n-C23) | 0.0000 | 0.0000 | 0.0000 | 0.0000 | 0.0000 | 0.0000 | 0.0000 | 0.0000 |
| Comp Mole Frac (Nitrogen) | 0.0500 | 0.0000 | 0.0160 | 0.0160 | 0.0160 | 0.0000 | 0.0176 | 0.0180 |
| Name | S-206 | S-205 | S-207 | S-204 | S-202 | S-201 | S-203 | S-209 |
| Comp Mole Frac (Methane) | 0.1481 | 0.0118 | 0.0000 | 0.0623 | 0.0042 | 0.0630 | 0.0623 | 0.1480 |
| Comp Mole Frac (Ethane) | 0.0448 | 0.0158 | 0.0000 | 0.0193 | 0.0023 | 0.0195 | 0.0193 | 0.0448 |
| Comp Mole Frac (n-Octane) | 0.0002 | 0.0642 | 0.0000 | 0.0027 | 0.0046 | 0.0027 | 0.0027 | 0.0002 |
| Comp Mole Frac (n-Hexane) | 0.0024 | 0.0770 | 0.0000 | 0.0041 | 0.0031 | 0.0041 | 0.0041 | 0.0024 |
| Comp Mole Frac (n-Nonane) | 0.0001 | 0.0570 | 0.0000 | 0.0023 | 0.0060 | 0.0023 | 0.0023 | 0.0001 |
| Comp Mole Frac (n-Heptane) | 0.0008 | 0.0715 | 0.0000 | 0.0032 | 0.0037 | 0.0032 | 0.0032 | 0.0008 |
| Comp Mole Frac (n-Decane) | 0.0000 | 0.0503 | 0.0000 | 0.0020 | 0.0078 | 0.0020 | 0.0020 | 0.0000 |
| Comp Mole Frac (n-C22) | 0.0000 | 0.0110 | 0.0000 | 0.0004 | 0.0322 | 0.0001 | 0.0004 | 0.0000 |
| Comp Mole Frac (n-C21) | 0.0000 | 0.0125 | 0.0000 | 0.0005 | 0.0340 | 0.0001 | 0.0005 | 0.0000 |

| Name | S-206 | S-205 | S-207 | S-204 | S-202 | S-201 | S-203 | S-209 |
|---|---|---|---|---|---|---|---|---|
| Comp Mole Frac (n-C20) | 0.0000 | 0.0142 | 0.0000 | 0.0006 | 0.0350 | 0.0002 | 0.0006 | 0.0000 |
| Comp Mole Frac (n-C19) | 0.0000 | 0.0161 | 0.0000 | 0.0006 | 0.0334 | 0.0003 | 0.0006 | 0.0000 |
| Comp Mole Frac (n-C18) | 0.0000 | 0.0182 | 0.0000 | 0.0007 | 0.0325 | 0.0004 | 0.0007 | 0.0000 |
| Comp Mole Frac (n-C17) | 0.0000 | 0.0207 | 0.0000 | 0.0008 | 0.0302 | 0.0005 | 0.0008 | 0.0000 |
| Comp Mole Frac (n-C16) | 0.0000 | 0.0235 | 0.0000 | 0.0009 | 0.0269 | 0.0007 | 0.0009 | 0.0000 |
| Comp Mole Frac (n-C15) | 0.0000 | 0.0267 | 0.0000 | 0.0011 | 0.0235 | 0.0008 | 0.0011 | 0.0000 |
| Comp Mole Frac (n-C14) | 0.0000 | 0.0304 | 0.0000 | 0.0012 | 0.0206 | 0.0010 | 0.0012 | 0.0000 |
| Comp Mole Frac (n-C13) | 0.0000 | 0.0345 | 0.0000 | 0.0014 | 0.0161 | 0.0012 | 0.0014 | 0.0000 |
| Comp Mole Frac (n-C12) | 0.0000 | 0.0392 | 0.0000 | 0.0016 | 0.0126 | 0.0015 | 0.0016 | 0.0000 |
| Comp Mole Frac (n-C11) | 0.0000 | 0.0444 | 0.0000 | 0.0018 | 0.0100 | 0.0017 | 0.0018 | 0.0000 |
| Comp Mole Frac (n-Butane) | 0.0174 | 0.0606 | 0.0000 | 0.0097 | 0.0030 | 0.0098 | 0.0097 | 0.0173 |
| Comp Mole Frac (Propane) | 0.0320 | 0.0355 | 0.0000 | 0.0148 | 0.0029 | 0.0149 | 0.0148 | 0.0320 |
| Comp Mole Frac (i-Butane) | 0.0000 | 0.0000 | 0.0000 | 0.0000 | 0.0000 | 0.0000 | 0.0000 | 0.0000 |
| Comp Mole Frac (i-Pentane) | 0.0000 | 0.0000 | 0.0000 | 0.0000 | 0.0000 | 0.0000 | 0.0000 | 0.0000 |
| Comp Mole Frac (H2O) | 0.0043 | 0.0009 | 0.9999 | 0.5440 | 0.0536 | 0.5495 | 0.5440 | 0.0043 |
| Comp Mole Frac (Oxygen) | 0.0000 | 0.0000 | 0.0000 | 0.0000 | 0.0000 | 0.0000 | 0.0000 | 0.0000 |
| Comp Mole Frac (Hydrogen) | 0.1238 | 0.0020 | 0.0000 | 0.0518 | 0.0019 | 0.0523 | 0.0518 | 0.1238 |
| Comp Mole Frac (CO2) | 0.0000 | 0.0000 | 0.0000 | 0.0000 | 0.0000 | 0.0000 | 0.0000 | 0.0000 |
| Comp Mole Frac (CO) | 0.3197 | 0.0121 | 0.0000 | 0.1340 | 0.0060 | 0.1354 | 0.1340 | 0.3199 |
| Comp Mole Frac (1-Butene) | 0.0000 | 0.0000 | 0.0000 | 0.0000 | 0.0000 | 0.0000 | 0.0000 | 0.0000 |
| Comp Mole Frac (n-Pentane) | 0.0071 | 0.0754 | 0.0000 | 0.0060 | 0.0029 | 0.0060 | 0.0060 | 0.0071 |
| Comp Mole Frac (n-C30) | 0.0000 | 0.1177 | 0.0000 | 0.0047 | 0.4250 | 0.0000 | 0.0047 | 0.0000 |
| Comp Mole Frac (n-C29) | 0.0000 | 0.0045 | 0.0000 | 0.0002 | 0.0160 | 0.0000 | 0.0002 | 0.0000 |
| Comp Mole Frac (n-C28) | 0.0000 | 0.0051 | 0.0000 | 0.0002 | 0.0181 | 0.0000 | 0.0002 | 0.0000 |
| Comp Mole Frac (n-C27) | 0.0000 | 0.0058 | 0.0000 | 0.0002 | 0.0204 | 0.0000 | 0.0002 | 0.0000 |
| Comp Mole Frac (n-C26) | 0.0000 | 0.0066 | 0.0000 | 0.0003 | 0.0228 | 0.0000 | 0.0003 | 0.0000 |

| Name | S-206 | S-205 | S-207 | S-204 | S-202 | S-201 | S-203 | S-209 |
|---|---|---|---|---|---|---|---|---|
| Comp Mole Frac (n-C25) | 0.0000 | 0.0075 | 0.0000 | 0.0003 | 0.0252 | 0.0000 | 0.0003 | 0.0000 |
| Comp Mole Frac (n-C24) | 0.0000 | 0.0085 | 0.0000 | 0.0003 | 0.0277 | 0.0000 | 0.0003 | 0.0000 |
| Comp Mole Frac (n-C23) | 0.0000 | 0.0096 | 0.0000 | 0.0004 | 0.0302 | 0.0001 | 0.0004 | 0.0000 |
| Comp Mole Frac (Nitrogen) | 0.2992 | 0.0096 | 0.0001 | 0.1254 | 0.0056 | 0.1267 | 0.1254 | 0.2993 |
| Name | S-210 | S-211 | S-300 | S-302 | Purge | S-304 | S-305 | S-306 |
| Comp Mole Frac (Methane) | 0.1480 | 0.1480 | 0.0000 | 0.0099 | 0.1481 | 0.0099 | 0.0099 | 0.0099 |
| Comp Mole Frac (Ethane) | 0.0448 | 0.0448 | 0.0000 | 0.0133 | 0.0448 | 0.0133 | 0.0133 | 0.0133 |
| Comp Mole Frac (n-Octane) | 0.0002 | 0.0002 | 0.0000 | 0.0540 | 0.0002 | 0.0540 | 0.0540 | 0.0540 |
| Comp Mole Frac (n-Hexane) | 0.0024 | 0.0024 | 0.0000 | 0.0647 | 0.0024 | 0.0647 | 0.0647 | 0.0647 |
| Comp Mole Frac (n-Nonane) | 0.0001 | 0.0001 | 0.0000 | 0.0479 | 0.0001 | 0.0479 | 0.0479 | 0.0479 |
| Comp Mole Frac (n-Heptane) | 0.0008 | 0.0008 | 0.0000 | 0.0601 | 0.0008 | 0.0601 | 0.0601 | 0.0601 |
| Comp Mole Frac (n-Decane) | 0.0000 | 0.0000 | 0.0000 | 0.0423 | 0.0000 | 0.0501 | 0.0501 | 0.0501 |
| Comp Mole Frac (n-C22) | 0.0000 | 0.0000 | 0.0000 | 0.0092 | 0.0000 | 0.0023 | 0.0023 | 0.0023 |
| Comp Mole Frac (n-C21) | 0.0000 | 0.0000 | 0.0000 | 0.0105 | 0.0000 | 0.0026 | 0.0026 | 0.0026 |
| Comp Mole Frac (n-C20) | 0.0000 | 0.0000 | 0.0000 | 0.0119 | 0.0000 | 0.0119 | 0.0119 | 0.0119 |
| Comp Mole Frac (n-C19) | 0.0000 | 0.0000 | 0.0000 | 0.0135 | 0.0000 | 0.0135 | 0.0135 | 0.0135 |
| Comp Mole Frac (n-C18) | 0.0000 | 0.0000 | 0.0000 | 0.0153 | 0.0000 | 0.0153 | 0.0153 | 0.0153 |
| Comp Mole Frac (n-C17) | 0.0000 | 0.0000 | 0.0000 | 0.0174 | 0.0000 | 0.0174 | 0.0174 | 0.0174 |
| Comp Mole Frac (n-C16) | 0.0000 | 0.0000 | 0.0000 | 0.0198 | 0.0000 | 0.0198 | 0.0198 | 0.0198 |
| Comp Mole Frac (n-C15) | 0.0000 | 0.0000 | 0.0000 | 0.0224 | 0.0000 | 0.1738 | 0.1737 | 0.1737 |
| Comp Mole Frac (n-C14) | 0.0000 | 0.0000 | 0.0000 | 0.0255 | 0.0000 | 0.0385 | 0.0385 | 0.0385 |
| Comp Mole Frac (n-C13) | 0.0000 | 0.0000 | 0.0000 | 0.0290 | 0.0000 | 0.0457 | 0.0457 | 0.0457 |
| Comp Mole Frac (n-C12) | 0.0000 | 0.0000 | 0.0000 | 0.0329 | 0.0000 | 0.0544 | 0.0544 | 0.0544 |
| Comp Mole Frac (n-C11) | 0.0000 | 0.0000 | 0.0000 | 0.0373 | 0.0000 | 0.0651 | 0.0651 | 0.0651 |
| Comp Mole Frac (n-Butane) | 0.0173 | 0.0173 | 0.0000 | 0.0510 | 0.0174 | 0.0510 | 0.0510 | 0.0510 |
| Comp Mole Frac (Propane) | 0.0320 | 0.0320 | 0.0000 | 0.0298 | 0.0320 | 0.0298 | 0.0298 | 0.0298 |

| Name | S-210 | S-211 | S-300 | S-302 | Purge | S-304 | S-305 | S-306 |
|---|---|---|---|---|---|---|---|---|
| Comp Mole Frac (i-Butane) | 0.0000 | 0.0000 | 0.0000 | 0.0000 | 0.0000 | 0.0000 | 0.0000 | 0.0000 |
| Comp Mole Frac (i-Pentane) | 0.0000 | 0.0000 | 0.0000 | 0.0000 | 0.0000 | 0.0000 | 0.0000 | 0.0000 |
| Comp Mole Frac (H2O) | 0.0043 | 0.0043 | 0.0000 | 0.0007 | 0.0043 | 0.0007 | 0.0007 | 0.0007 |
| Comp Mole Frac (Oxygen) | 0.0000 | 0.0000 | 0.0000 | 0.0000 | 0.0000 | 0.0000 | 0.0000 | 0.0000 |
| Comp Mole Frac (Hydrogen) | 0.1238 | 0.1238 | 1.0000 | 0.1608 | 0.1238 | 0.0418 | 0.0418 | 0.0418 |
| Comp Mole Frac (CO2) | 0.0000 | 0.0000 | 0.0000 | 0.0000 | 0.0000 | 0.0000 | 0.0000 | 0.0000 |
| Comp Mole Frac (CO) | 0.3199 | 0.3199 | 0.0000 | 0.0102 | 0.3197 | 0.0102 | 0.0102 | 0.0102 |
| Comp Mole Frac (1-Butene) | 0.0000 | 0.0000 | 0.0000 | 0.0000 | 0.0000 | 0.0000 | 0.0000 | 0.0000 |
| Comp Mole Frac (n-Pentane) | 0.0071 | 0.0071 | 0.0000 | 0.0634 | 0.0071 | 0.0634 | 0.0634 | 0.0634 |
| Comp Mole Frac (n-C30) | 0.0000 | 0.0000 | 0.0000 | 0.0990 | 0.0000 | 0.0248 | 0.0247 | 0.0247 |
| Comp Mole Frac (n-C29) | 0.0000 | 0.0000 | 0.0000 | 0.0038 | 0.0000 | 0.0009 | 0.0009 | 0.0009 |
| Comp Mole Frac (n-C28) | 0.0000 | 0.0000 | 0.0000 | 0.0043 | 0.0000 | 0.0011 | 0.0011 | 0.0011 |
| Comp Mole Frac (n-C27) | 0.0000 | 0.0000 | 0.0000 | 0.0049 | 0.0000 | 0.0012 | 0.0012 | 0.0012 |
| Comp Mole Frac (n-C26) | 0.0000 | 0.0000 | 0.0000 | 0.0056 | 0.0000 | 0.0014 | 0.0014 | 0.0014 |
| Comp Mole Frac (n-C25) | 0.0000 | 0.0000 | 0.0000 | 0.0063 | 0.0000 | 0.0016 | 0.0016 | 0.0016 |
| Comp Mole Frac (n-C24) | 0.0000 | 0.0000 | 0.0000 | 0.0071 | 0.0000 | 0.0018 | 0.0018 | 0.0018 |
| Comp Mole Frac (n-C23) | 0.0000 | 0.0000 | 0.0000 | 0.0081 | 0.0000 | 0.0020 | 0.0020 | 0.0020 |
| Comp Mole Frac (Nitrogen) | 0.2993 | 0.2993 | 0.0000 | 0.0080 | 0.2992 | 0.0080 | 0.0080 | 0.0080 |

| Name | S-307 | S-208 | S-106 | S-108 | S-111 | S-112 | Oxygen | S-301 |
|---|---|---|---|---|---|---|---|---|
| Comp Mole Frac (Methane) | 0.0099 | 0.1481 | 0.0052 | 0.0052 | 0.0000 | 0.0059 | 0.0000 | 0.0118 |
| Comp Mole Frac (Ethane) | 0.0133 | 0.0448 | 0.0000 | 0.0000 | 0.0000 | 0.0000 | 0.0000 | 0.0158 |
| Comp Mole Frac (n-Octane) | 0.0540 | 0.0002 | 0.0000 | 0.0000 | 0.0000 | 0.0000 | 0.0000 | 0.0642 |
| Comp Mole Frac (n-Hexane) | 0.0647 | 0.0024 | 0.0000 | 0.0000 | 0.0000 | 0.0000 | 0.0000 | 0.0770 |
| Comp Mole Frac (n-Nonane) | 0.0479 | 0.0001 | 0.0000 | 0.0000 | 0.0000 | 0.0000 | 0.0000 | 0.0570 |
| Comp Mole Frac (n-Heptane) | 0.0601 | 0.0008 | 0.0000 | 0.0000 | 0.0000 | 0.0000 | 0.0000 | 0.0715 |
| Comp Mole Frac (n-Decane) | 0.0501 | 0.0000 | 0.0000 | 0.0000 | 0.0000 | 0.0000 | 0.0000 | 0.0503 |

| Name | S-307 | S-208 | S-106 | S-108 | S-111 | S-112 | Oxygen | S-301 |
|---|---|---|---|---|---|---|---|---|
| Comp Mole Frac (n-C22) | 0.0023 | 0.0000 | 0.0000 | 0.0000 | 0.0000 | 0.0000 | 0.0000 | 0.0110 |
| Comp Mole Frac (n-C21) | 0.0026 | 0.0000 | 0.0000 | 0.0000 | 0.0000 | 0.0000 | 0.0000 | 0.0125 |
| Comp Mole Frac (n-C20) | 0.0119 | 0.0000 | 0.0000 | 0.0000 | 0.0000 | 0.0000 | 0.0000 | 0.0142 |
| Comp Mole Frac (n-C19) | 0.0135 | 0.0000 | 0.0000 | 0.0000 | 0.0000 | 0.0000 | 0.0000 | 0.0161 |
| Comp Mole Frac (n-C18) | 0.0153 | 0.0000 | 0.0000 | 0.0000 | 0.0000 | 0.0000 | 0.0000 | 0.0182 |
| Comp Mole Frac (n-C17) | 0.0174 | 0.0000 | 0.0000 | 0.0000 | 0.0000 | 0.0000 | 0.0000 | 0.0207 |
| Comp Mole Frac (n-C16) | 0.0198 | 0.0000 | 0.0000 | 0.0000 | 0.0000 | 0.0000 | 0.0000 | 0.0235 |
| Comp Mole Frac (n-C15) | 0.1737 | 0.0000 | 0.0000 | 0.0000 | 0.0000 | 0.0000 | 0.0000 | 0.0267 |
| Comp Mole Frac (n-C14) | 0.0385 | 0.0000 | 0.0000 | 0.0000 | 0.0000 | 0.0000 | 0.0000 | 0.0304 |
| Comp Mole Frac (n-C13) | 0.0457 | 0.0000 | 0.0000 | 0.0000 | 0.0000 | 0.0000 | 0.0000 | 0.0345 |
| Comp Mole Frac (n-C12) | 0.0544 | 0.0000 | 0.0000 | 0.0000 | 0.0000 | 0.0000 | 0.0000 | 0.0392 |
| Comp Mole Frac (n-C11) | 0.0651 | 0.0000 | 0.0000 | 0.0000 | 0.0000 | 0.0000 | 0.0000 | 0.0444 |
| Comp Mole Frac (n-Butane) | 0.0510 | 0.0174 | 0.0000 | 0.0000 | 0.0000 | 0.0000 | 0.0000 | 0.0606 |
| Comp Mole Frac (Propane) | 0.0298 | 0.0320 | 0.0000 | 0.0000 | 0.0000 | 0.0000 | 0.0000 | 0.0355 |
| Comp Mole Frac (i-Butane) | 0.0000 | 0.0000 | 0.0000 | 0.0000 | 0.0000 | 0.0000 | 0.0000 | 0.0000 |
| Comp Mole Frac (i-Pentane) | 0.0000 | 0.0000 | 0.0000 | 0.0000 | 0.0000 | 0.0000 | 0.0000 | 0.0000 |
| Comp Mole Frac (H2O) | 0.0007 | 0.0043 | 0.0959 | 0.0959 | 0.0000 | 0.0034 | 0.0000 | 0.0009 |
| Comp Mole Frac (Oxygen) | 0.0000 | 0.0000 | 0.0000 | 0.0000 | 0.0000 | 0.0000 | 1.0000 | 0.0000 |
| Comp Mole Frac (Hydrogen) | 0.0418 | 0.1238 | 0.5747 | 0.5747 | 0.0000 | 0.6486 | 0.0000 | 0.0020 |
| Comp Mole Frac (CO2) | 0.0000 | 0.0000 | 0.0210 | 0.0210 | 1.0000 | 0.0000 | 0.0000 | 0.0000 |
| Comp Mole Frac (CO) | 0.0102 | 0.3197 | 0.2872 | 0.2872 | 0.0000 | 0.3241 | 0.0000 | 0.0121 |
| Comp Mole Frac (1-Butene) | 0.0000 | 0.0000 | 0.0000 | 0.0000 | 0.0000 | 0.0000 | 0.0000 | 0.0000 |
| Comp Mole Frac (n-Pentane) | 0.0634 | 0.0071 | 0.0000 | 0.0000 | 0.0000 | 0.0000 | 0.0000 | 0.0754 |
| Comp Mole Frac (n-C30) | 0.0247 | 0.0000 | 0.0000 | 0.0000 | 0.0000 | 0.0000 | 0.0000 | 0.1177 |
| Comp Mole Frac (n-C29) | 0.0009 | 0.0000 | 0.0000 | 0.0000 | 0.0000 | 0.0000 | 0.0000 | 0.0045 |
| Comp Mole Frac (n-C28) | 0.0011 | 0.0000 | 0.0000 | 0.0000 | 0.0000 | 0.0000 | 0.0000 | 0.0051 |

| Name | S-307 | S-208 | S-106 | S-108 | S-111 | S-112 | Oxygen | S-301 |
|---|---|---|---|---|---|---|---|---|
| Comp Mole Frac (n-C27) | 0.0012 | 0.0000 | 0.0000 | 0.0000 | 0.0000 | 0.0000 | 0.0000 | 0.0058 |
| Comp Mole Frac (n-C26) | 0.0014 | 0.0000 | 0.0000 | 0.0000 | 0.0000 | 0.0000 | 0.0000 | 0.0066 |
| Comp Mole Frac (n-C25) | 0.0016 | 0.0000 | 0.0000 | 0.0000 | 0.0000 | 0.0000 | 0.0000 | 0.0075 |
| Comp Mole Frac (n-C24) | 0.0018 | 0.0000 | 0.0000 | 0.0000 | 0.0000 | 0.0000 | 0.0000 | 0.0085 |
| Comp Mole Frac (n-C23) | 0.0020 | 0.0000 | 0.0000 | 0.0000 | 0.0000 | 0.0000 | 0.0000 | 0.0096 |
| Comp Mole Frac (Nitrogen) | 0.0080 | 0.2992 | 0.0160 | 0.0160 | 0.0000 | 0.0180 | 0.0000 | 0.0096 |
| Name | S-309 | S-311 | S-312 | S-310 | S-308 | S-313 | S-303 | S-100 |
| Comp Mole Frac (Methane) | 0.0598 | 0.0000 | 0.0000 | 0.0000 | 0.0099 | 0.0000 | 0.0099 | 0.9200 |
| Comp Mole Frac (Ethane) | 0.0802 | 0.0000 | 0.0000 | 0.0000 | 0.0133 | 0.0000 | 0.0133 | 0.0300 |
| Comp Mole Frac (n-Octane) | 0.0000 | 0.1391 | 0.0012 | 0.0647 | 0.0540 | 0.0000 | 0.0540 | 0.0000 |
| Comp Mole Frac (n-Hexane) | 0.0000 | 0.1676 | 0.0006 | 0.0775 | 0.0647 | 0.0000 | 0.0647 | 0.0000 |
| Comp Mole Frac (n-Nonane) | 0.0000 | 0.1230 | 0.0016 | 0.0575 | 0.0479 | 0.0000 | 0.0479 | 0.0000 |
| Comp Mole Frac (n-Heptane) | 0.0000 | 0.1555 | 0.0009 | 0.0721 | 0.0601 | 0.0000 | 0.0601 | 0.0000 |
| Comp Mole Frac (n-Decane) | 0.0000 | 0.1273 | 0.0030 | 0.0601 | 0.0501 | 0.0000 | 0.0423 | 0.0000 |
| Comp Mole Frac (n-C22) | 0.0000 | 0.0000 | 0.0004 | 0.0028 | 0.0023 | 0.0383 | 0.0092 | 0.0000 |
| Comp Mole Frac (n-C21) | 0.0000 | 0.0000 | 0.0004 | 0.0031 | 0.0026 | 0.0433 | 0.0105 | 0.0000 |
| Comp Mole Frac (n-C20) | 0.0000 | 0.0000 | 0.0026 | 0.0143 | 0.0119 | 0.1923 | 0.0119 | 0.0000 |
| Comp Mole Frac (n-C19) | 0.0000 | 0.0000 | 0.0145 | 0.0162 | 0.0135 | 0.1377 | 0.0135 | 0.0000 |
| Comp Mole Frac (n-C18) | 0.0000 | 0.0000 | 0.0378 | 0.0184 | 0.0153 | 0.0086 | 0.0153 | 0.0000 |
| Comp Mole Frac (n-C17) | 0.0000 | 0.0000 | 0.0442 | 0.0208 | 0.0174 | 0.0002 | 0.0174 | 0.0000 |
| Comp Mole Frac (n-C16) | 0.0000 | 0.0000 | 0.0504 | 0.0237 | 0.0198 | 0.0000 | 0.0198 | 0.0000 |
| Comp Mole Frac (n-C15) | 0.0000 | 0.0000 | 0.4419 | 0.2082 | 0.1737 | 0.0000 | 0.0224 | 0.0000 |
| Comp Mole Frac (n-C14) | 0.0000 | 0.0000 | 0.0979 | 0.0461 | 0.0385 | 0.0000 | 0.0255 | 0.0000 |
| Comp Mole Frac (n-C13) | 0.0000 | 0.0000 | 0.1162 | 0.0548 | 0.0457 | 0.0000 | 0.0290 | 0.0000 |
| Comp Mole Frac (n-C12) | 0.0000 | 0.0008 | 0.1376 | 0.0652 | 0.0544 | 0.0000 | 0.0329 | 0.0000 |
| Comp Mole Frac (n-C11) | 0.0000 | 0.1245 | 0.0438 | 0.0780 | 0.0651 | 0.0000 | 0.0373 | 0.0000 |

| Name | S-309 | S-311 | S-312 | S-310 | S-308 | S-313 | S-303 | S-100 |
|---|---|---|---|---|---|---|---|---|
| Comp Mole Frac (n-Butane) | 0.3078 | 0.0000 | 0.0000 | 0.0000 | 0.0510 | 0.0000 | 0.0510 | 0.0000 |
| Comp Mole Frac (Propane) | 0.1802 | 0.0000 | 0.0000 | 0.0000 | 0.0298 | 0.0000 | 0.0298 | 0.0000 |
| Comp Mole Frac (i-Butane) | 0.0000 | 0.0000 | 0.0000 | 0.0000 | 0.0000 | 0.0000 | 0.0000 | 0.0000 |
| Comp Mole Frac (i-Pentane) | 0.0000 | 0.0000 | 0.0000 | 0.0000 | 0.0000 | 0.0000 | 0.0000 | 0.0000 |
| Comp Mole Frac (H2O) | 0.0044 | 0.0000 | 0.0000 | 0.0000 | 0.0007 | 0.0000 | 0.0007 | 0.0000 |
| Comp Mole Frac (Oxygen) | 0.0000 | 0.0000 | 0.0000 | 0.0000 | 0.0000 | 0.0000 | 0.0000 | 0.0000 |
| Comp Mole Frac (Hydrogen) | 0.2524 | 0.0000 | 0.0000 | 0.0000 | 0.0418 | 0.0000 | 0.1608 | 0.0000 |
| Comp Mole Frac (CO2) | 0.0000 | 0.0000 | 0.0000 | 0.0000 | 0.0000 | 0.0000 | 0.0000 | 0.0000 |
| Comp Mole Frac (CO) | 0.0616 | 0.0000 | 0.0000 | 0.0000 | 0.0102 | 0.0000 | 0.0102 | 0.0000 |
| Comp Mole Frac (1-Butene) | 0.0000 | 0.0000 | 0.0000 | 0.0000 | 0.0000 | 0.0000 | 0.0000 | 0.0000 |
| Comp Mole Frac (n-Pentane) | 0.0051 | 0.1622 | 0.0004 | 0.0749 | 0.0634 | 0.0000 | 0.0634 | 0.0000 |
| Comp Mole Frac (n-C30) | 0.0000 | 0.0000 | 0.0034 | 0.0297 | 0.0247 | 0.4131 | 0.0990 | 0.0000 |
| Comp Mole Frac (n-C29) | 0.0000 | 0.0000 | 0.0001 | 0.0011 | 0.0009 | 0.0157 | 0.0038 | 0.0000 |
| Comp Mole Frac (n-C28) | 0.0000 | 0.0000 | 0.0001 | 0.0013 | 0.0011 | 0.0180 | 0.0043 | 0.0000 |
| Comp Mole Frac (n-C27) | 0.0000 | 0.0000 | 0.0002 | 0.0015 | 0.0012 | 0.0203 | 0.0049 | 0.0000 |
| Comp Mole Frac (n-C26) | 0.0000 | 0.0000 | 0.0002 | 0.0017 | 0.0014 | 0.0231 | 0.0056 | 0.0000 |
| Comp Mole Frac (n-C25) | 0.0000 | 0.0000 | 0.0002 | 0.0019 | 0.0016 | 0.0261 | 0.0063 | 0.0000 |
| Comp Mole Frac (n-C24) | 0.0000 | 0.0000 | 0.0003 | 0.0021 | 0.0018 | 0.0296 | 0.0071 | 0.0000 |
| Comp Mole Frac (n-C23) | 0.0000 | 0.0000 | 0.0003 | 0.0024 | 0.0020 | 0.0337 | 0.0081 | 0.0000 |
| Comp Mole Frac (Nitrogen) | 0.0486 | 0.0000 | 0.0000 | 0.0000 | 0.0080 | 0.0000 | 0.0080 | 0.0500 |

| Name | S-101 | S-102 | S-103 | ** New ** | | | | |
|---|---|---|---|---|---|---|---|---|
| Comp Mole Frac (Methane) | 0.7350 | 0.7350 | 0.7350 | | | | | |
| Comp Mole Frac (Ethane) | 0.0000 | 0.0000 | 0.0000 | | | | | |
| Comp Mole Frac (n-Octane) | 0.0000 | 0.0000 | 0.0000 | | | | | |
| Comp Mole Frac (n-Hexane) | 0.0000 | 0.0000 | 0.0000 | | | | | |
| Comp Mole Frac (n-Nonane) | 0.0000 | 0.0000 | 0.0000 | | | | | |

| Name | S-101 | S-102 | S-103 | ** New ** | Name | S-101 | S-102 |
|---|---|---|---|---|---|---|---|
| Comp Mole Frac (n-Heptane) | 0.0000 | 0.0000 | 0.0000 | | | | |
| Comp Mole Frac (n-Decane) | 0.0000 | 0.0000 | 0.0000 | | | | |
| Comp Mole Frac (n-C22) | 0.0000 | 0.0000 | 0.0000 | | | | |
| Comp Mole Frac (n-C21) | 0.0000 | 0.0000 | 0.0000 | | | | |
| Comp Mole Frac (n-C20) | 0.0000 | 0.0000 | 0.0000 | | | | |
| Comp Mole Frac (n-C19) | 0.0000 | 0.0000 | 0.0000 | | | | |
| Comp Mole Frac (n-C18) | 0.0000 | 0.0000 | 0.0000 | | | | |
| Comp Mole Frac (n-C17) | 0.0000 | 0.0000 | 0.0000 | | | | |
| Comp Mole Frac (n-C16) | 0.0000 | 0.0000 | 0.0000 | | | | |
| Comp Mole Frac (n-C15) | 0.0000 | 0.0000 | 0.0000 | | | | |
| Comp Mole Frac (n-C14) | 0.0000 | 0.0000 | 0.0000 | | | | |
| Comp Mole Frac (n-C13) | 0.0000 | 0.0000 | 0.0000 | | | | |
| Comp Mole Frac (n-C12) | 0.0000 | 0.0000 | 0.0000 | | | | |
| Comp Mole Frac (n-C11) | 0.0000 | 0.0000 | 0.0000 | | | | |
| Comp Mole Frac (n-Butane) | 0.0000 | 0.0000 | 0.0000 | | | | |
| Comp Mole Frac (Propane) | 0.0000 | 0.0000 | 0.0000 | | | | |
| Comp Mole Frac (i-Butane) | 0.0000 | 0.0000 | 0.0000 | | | | |
| Comp Mole Frac (i-Pentane) | 0.0000 | 0.0000 | 0.0000 | | | | |
| Comp Mole Frac (H2O) | 0.0962 | 0.0962 | 0.0962 | | | | |
| Comp Mole Frac (Oxygen) | 0.0000 | 0.0000 | 0.0000 | | | | |
| Comp Mole Frac (Hydrogen) | 0.0986 | 0.0986 | 0.0986 | | | | |
| Comp Mole Frac (CO2) | 0.0291 | 0.0291 | 0.0291 | | | | |
| Comp Mole Frac (CO) | 0.0019 | 0.0019 | 0.0019 | | | | |
| Comp Mole Frac (1-Butene) | 0.0000 | 0.0000 | 0.0000 | | | | |
| Comp Mole Frac (n-Pentane) | 0.0000 | 0.0000 | 0.0000 | | | | |
| Comp Mole Frac (n-C30) | 0.0000 | 0.0000 | 0.0000 | | | | |

| Name | S-101 | S-102 | S-103 | ** New ** |
|---|---|---|---|---|
| Comp Mole Frac (n-C29) | 0.0000 | 0.0000 | 0.0000 | |
| Comp Mole Frac (n-C28) | 0.0000 | 0.0000 | 0.0000 | |
| Comp Mole Frac (n-C27) | 0.0000 | 0.0000 | 0.0000 | |
| Comp Mole Frac (n-C26) | 0.0000 | 0.0000 | 0.0000 | |
| Comp Mole Frac (n-C25) | 0.0000 | 0.0000 | 0.0000 | |
| Comp Mole Frac (n-C24) | 0.0000 | 0.0000 | 0.0000 | |
| Comp Mole Frac (n-C23) | 0.0000 | 0.0000 | 0.0000 | |
| Comp Mole Frac (Nitrogen) | 0.0391 | 0.0391 | 0.0391 | |

**APPENDIX E:** Methanol to Gasoline Simulation
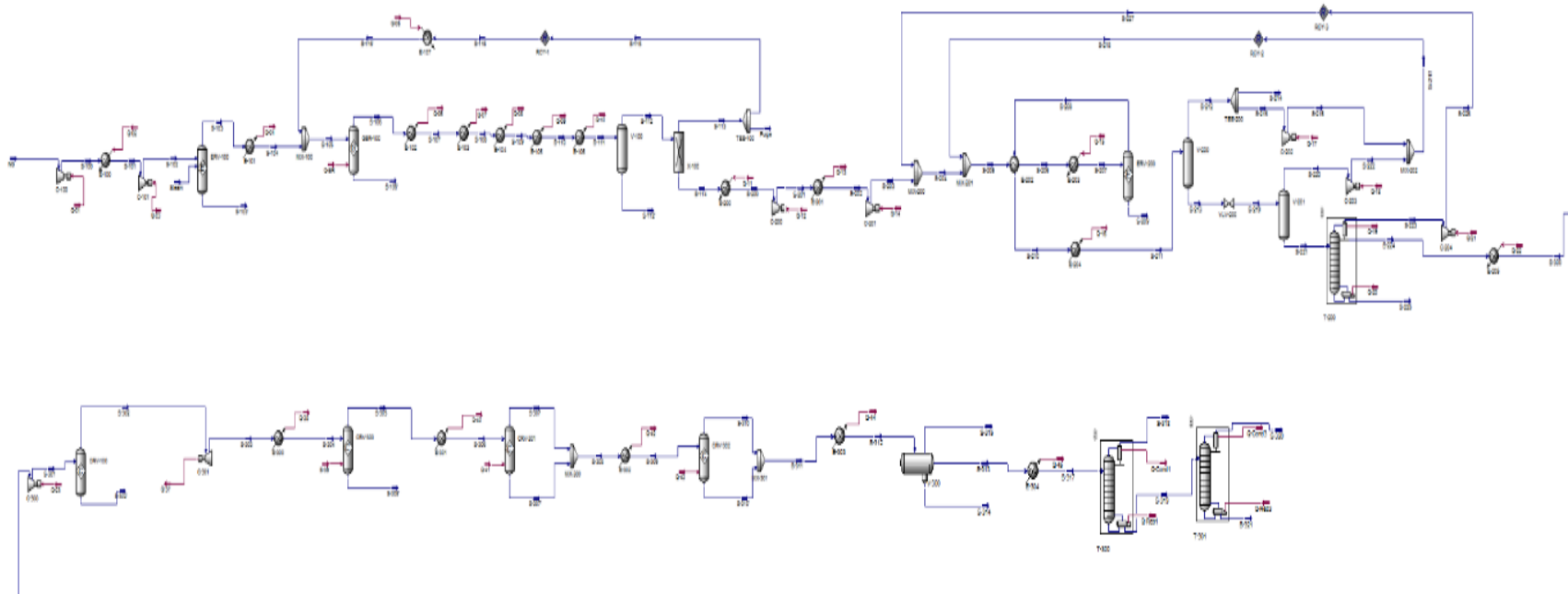
# APPENDIX E: Methanol to Gasoline Simulation

Table E 1: Methanol to Gasoline material stream.

| Name | NG | S-100 | S-101 | S-102 | Steam | S-106 | *S-106'* | *S-107* |
|---|---|---|---|---|---|---|---|---|
| Vapour Fraction | 1 | 1 | 1 | 1 | 1 | 1 | 0 | 1 |
| Temperature [C] | 25 | 110.2313 | 268.7 | 345.0003 | 345 | 950 | 950 | 550 |
| Pressure [bar] | 6.6 | 16.06 | 16.06 | 30 | 30 | 30 | 30 | 30 |
| Molar Flow [MMSCFD] | 753.7081 | 753.7081 | 753.7081 | 753.7081 | 2261.124 | 6789.027 | 0 | 6789.027 |
| Mass Flow [kg/h] | 618879.1 | 618879.1 | 618879.1 | 618879.1 | 2028861 | 3030850 | 0 | 3030850 |
| Liquid Volume Flow [m3/h] | 2048.263 | 2048.263 | 2048.263 | 2048.263 | 2032.955 | 9484.427 | 0 | 9484.427 |
| Heat Flow [kJ/h] | -2.8E+09 | -2.7E+09 | -2.4E+09 | -2.3E+09 | -2.6E+10 | -1.5E+10 | 0 | -1.9E+10 |
| Name | S-108 | S-109 | S-110 | S-111 | S-112 | S-112' | S-200 | S-201 |
| Vapour Fraction | 1 | 1 | 0.781397 | 0.772552 | 1 | 0 | 1 | 1 |
| Temperature [C] | 350 | 170 | 70 | 10 | 10 | 10 | 160 | 321.5094 |
| Pressure [bar] | 30 | 30 | 30 | 30 | 30 | 30 | 30 | 75 |
| Molar Flow [MMSCFD] | 6789.027 | 6789.027 | 6789.027 | 6789.027 | 5244.875 | 1544.152 | 1886.197 | 1886.197 |
| Mass Flow [kg/h] | 3030850 | 3030850 | 3030850 | 3030850 | 1644368 | 1386482 | 1131774 | 1131774 |
| Liquid Volume Flow [m3/h] | 9484.427 | 9484.427 | 9484.427 | 9484.427 | 8094.767 | 1389.66 | 3119.068 | 3119.068 |
| Heat Flow [kJ/h] | -2.2E+10 | -2.3E+10 | -2.8E+10 | -2.9E+10 | -6.4E+09 | -2.2E+10 | -4.5E+09 | -4E+09 |
| Name | S-113 | S-114 | S-103 | S-103' | S-104 | S-115 | Purge | S-116 |
| Vapour Fraction | 1 | 0.99918 | 1 | 0 | 1 | 1 | 1 | 1 |
| Temperature [C] | 10.63849 | 10.64242 | 321.087 | 321.087 | 345 | 10.63849 | 10.63849 | 10.63833 |
| Pressure [bar] | 30 | 30 | 30 | 30 | 30 | 30 | 30 | 30 |
| Molar Flow [MMSCFD] | 3358.678 | 1886.197 | 3061.207 | 0 | 3061.207 | 2519.009 | 839.6696 | 2508.275 |

| Name | S-113 | S-114 | S-103 | S-103' | S-104 | S-115 | Purge | S-116 |
|---|---|---|---|---|---|---|---|---|
| Mass Flow [kg/h] | 512594.3 | 1131774 | 2647740 | 0 | 2647740 | 384445.8 | 128148.6 | 383083.6 |
| Liquid Volume Flow [m3/h] | 4975.699 | 3119.068 | 4165.115 | 0 | 4165.115 | 3731.774 | 1243.925 | 3715.818 |
| Heat Flow [kJ/h] | -1.6E+09 | -4.9E+09 | -2.8E+10 | 0 | -2.8E+10 | -1.2E+09 | -3.9E+08 | -1.2E+09 |

| Name | S-105 | S-116' | S-300 | S-302 | S-302' | S-304 | S-301 | S-303 |
|---|---|---|---|---|---|---|---|---|
| Vapour Fraction | 1 | 1 | 1 | 1 | 0 | 1 | 1 | 1 |
| Temperature [C] | 342.1039 | 345 | 149.9 | 434.4513 | 434.4513 | 350 | 309.9599 | 412.8161 |
| Pressure [bar] | 30 | 30 | 5 | 27 | 27 | 19 | 27 | 19 |
| Molar Flow [MMSCFD] | 5569.482 | 2508.275 | 426.4879 | 426.4879 | 0 | 426.4879 | 426.4879 | 426.4879 |
| Mass Flow [kg/h] | 3030824 | 383083.6 | 681988.8 | 681991.9 | 0 | 681991.9 | 681988.8 | 681991.9 |
| Liquid Volume Flow [m3/h] | 7880.933 | 3715.818 | 857.2038 | 923.0879 | 0 | 923.0879 | 857.2038 | 923.0879 |
| Heat Flow [kJ/h] | -2.8E+10 | 63049746 | -4.2E+09 | -4E+09 | 0 | -4.1E+09 | -4E+09 | -4E+09 |

| Name | S-202 | S-203 | S-204 | S-205 | S-206 | S-207 | S-208 | S-209 |
|---|---|---|---|---|---|---|---|---|
| Vapour Fraction | 1 | 1 | 1 | 1 | 1 | 1 | 1 | 0 |
| Temperature [C] | 60 | 110.3049 | 110.315 | 58.30504 | 145 | 150 | 321.7798 | 321.7798 |
| Pressure [bar] | 75 | 110 | 110 | 110 | 110 | 110 | 110 | 110 |
| Molar Flow [MMSCFD] | 1886.197 | 1886.197 | 1886.228 | 7211.014 | 7211.014 | 7211.014 | 6356.186 | 0 |
| Mass Flow [kg/h] | 1131774 | 1131774 | 1131810 | 5102385 | 5102385 | 5102385 | 5102364 | 0 |
| Liquid Volume Flow [m3/h] | 3119.068 | 3119.068 | 3119.14 | 13177.38 | 13177.38 | 13177.38 | 12028.43 | 0 |
| Heat Flow [kJ/h] | -4.7E+09 | -4.6E+09 | -4.6E+09 | -2.4E+10 | -2.3E+10 | -2.3E+10 | -2.3E+10 | 0 |

| Name | S-210 | S-211 | S-212 | S-213 | S-214 | S-215 | S-216 | S-217 |
|---|---|---|---|---|---|---|---|---|
| Vapour Fraction | 1 | 0.923723 | 1 | 0 | 1 | 1 | 1 | 1 |
| Temperature [C] | 236.3566 | 38 | 38 | 38 | 38 | 38 | 38 | 42.18652 |
| Pressure [bar] | 110 | 110 | 110 | 110 | 110 | 110 | 110 | 110 |
| Molar Flow [MMSCFD] | 6356.186 | 6356.186 | 5871.353 | 484.8336 | 557.7785 | 5313.574 | 5313.574 | 5347.158 |

| Name | S-210 | S-211 | S-212 | S-213 | S-214 | S-215 | S-216 | S-217 |
|---|---|---|---|---|---|---|---|---|
| Mass Flow [kg/h] | 5102364 | 5102364 | 4348193 | 754171.5 | 413078.3 | 3935114 | 3935114 | 3984775 |
| Liquid Volume Flow [m3/h] | 12028.43 | 12028.43 | 11067.73 | 960.699 | 1051.435 | 10016.3 | 10016.3 | 10097.02 |
| Heat Flow [kJ/h] | -2.4E+10 | -2.7E+10 | -2.1E+10 | -5.9E+09 | -2E+09 | -1.9E+10 | -1.9E+10 | -2E+10 |

| Name | S-218 | S-219 | S-220 | S-221 | S-222 | S-223 | S-224 | S-225 |
|---|---|---|---|---|---|---|---|---|
| Vapour Fraction | 1 | 6.93E-02 | 1 | 0 | 1 | 1 | 0 | 0 |
| Temperature [C] | 42.13349 | 36.45472 | 36.45472 | 36.45472 | 505.9505 | -24.778 | -24.778 | 108.8581 |
| Pressure [bar] | 110 | 2 | 2 | 2 | 110 | 1 | 1 | 1.4 |
| Molar Flow [MMSCFD] | 5324.786 | 484.8336 | 33.5836 | 451.25 | 33.5836 | 3.12E-02 | 426.4879 | 24.73097 |
| Mass Flow [kg/h] | 3970576 | 754171.5 | 49660.87 | 704510.6 | 49660.87 | 36.04618 | 681988.8 | 22485.79 |
| Liquid Volume Flow [m3/h] | 10058.24 | 960.699 | 80.71974 | 879.9793 | 80.71974 | 7.25E-02 | 857.2038 | 22.70292 |
| Heat Flow [kJ/h] | -2E+10 | -5.9E+09 | -3.7E+08 | -5.5E+09 | -3.4E+08 | -245335 | -5.3E+09 | -3.4E+08 |

| Name | S-226 | S-227 | S-305 | S-305' | S-306 | S-309 | S-310 | S-310' |
|---|---|---|---|---|---|---|---|---|
| Vapour Fraction | 1 | 1 | 1 | 0 | 1 | 5.68E-03 | 1 | 0 |
| Temperature [C] | 536.7985 | 536.8699 | 350 | 350 | 350 | 330 | 330 | 330 |
| Pressure [bar] | 110 | 110 | 19 | 19 | 19 | 19 | 19 | 19 |
| Molar Flow [MMSCFD] | 3.12E-02 | 3.12E-02 | 497.0979 | 0 | 497.0979 | 497.0979 | 1.4122 | 496.5791 |
| Mass Flow [kg/h] | 36.04618 | 36.03661 | 681992.5 | 0 | 681992.5 | 681991.3 | 4507.583 | 677484.2 |
| Liquid Volume Flow [m3/h] | 7.25E-02 | 7.25E-02 | 834.1016 | 0 | 834.1016 | 833.8122 | 5.634479 | 823.27 |
| Heat Flow [kJ/h] | -209181 | -209169 | -4.8E+09 | 0 | -4.8E+09 | 8.4E+13 | 4.2E+13 | -5E+09 |

| Name | S-307 | S-307' | S-312 | S-315 | S-313 | S-314 | S-311 | S-317 |
|---|---|---|---|---|---|---|---|---|
| Vapour Fraction | 1 | 0 | 2.84E-03 | 1 | 0 | 0 | 0.997171 | 0 |
| Temperature [C] | 350 | 350 | 440 | 440 | 440 | 440 | 1938.85 | 40 |
| Pressure [bar] | 19 | 19 | 17 | 17 | 17 | 17 | 19 | 20.7 |
| Molar Flow [MMSCFD] | 2.8244 | 494.2735 | 497.9913 | 1.4122 | 95.114 | 401.4651 | 497.9913 | 95.114 |

| Name | S-307 | S-307' | S-312 | S-315 | S-313 | S-314 | S-311 | S-317 |
|---|---|---|---|---|---|---|---|---|
| Mass Flow [kg/h] | 9015.166 | 672976.1 | 681991.8 | 4507.583 | 317257.8 | 360226.4 | 681991.8 | 317257.8 |
| Liquid Volume Flow [m3/h] | 11.26896 | 822.5432 | 828.9045 | 5.634479 | 462.3166 | 360.9534 | 828.9045 | 462.3166 |
| Heat Flow [kJ/h] | 8.54E+13 | -4.9E+09 | 4.32E+13 | 4.32E+13 | -2.7E+08 | -4.5E+09 | 4.2E+13 | -6.7E+08 |
| Name | S-318 | S-319 | S-320 | S-321 | S-308 | ** New ** | | |
| Vapour Fraction | 1 | 0 | 1 | 0 | 2.96E-06 | | | |
| Temperature [C] | -56.6845 | 101.065 | 44.97607 | 138.592 | 1944.446 | | | |
| Pressure [bar] | 11.4 | 11.8 | 7.58423 | 7.58423 | 19 | | | |
| Molar Flow [MMSCFD] | 5.84309 | 89.27091 | 35.03002 | 54.24089 | 497.0979 | | | |
| Mass Flow [kg/h] | 8388.012 | 308869.8 | 86182.19 | 222687.6 | 681991.3 | | | |
| Liquid Volume Flow [m3/h] | 15.68563 | 446.631 | 136.8234 | 309.8076 | 833.8122 | | | |
| Heat Flow [kJ/h] | -6.3E+07 | -5.6E+08 | -2.4E+08 | -2.8E+08 | 8.54E+13 | | | |

## APPENDIX E: Methanol to Gasoline Simulation

Table E 2: Methanol to Gasoline stream composition.

| Name | NG | S-100 | S-101 | S-102 | Steam | S-106 | S-106' | S-107 |
|---|---|---|---|---|---|---|---|---|
| Comp Mole Frac (Methane) | 0.968421 | 0.968421 | 0.968421 | 0.968421 | 0 | 2.74E-02 | 2.74E-02 | 2.74E-02 |
| Comp Mole Frac (Ethane) | 3.16E-02 | 3.16E-02 | 3.16E-02 | 3.16E-02 | 0 | 1.31E-06 | 1.31E-06 | 1.31E-06 |
| Comp Mole Frac (Ethylene) | 0 | 0 | 0 | 0 | 0 | 8.20E-49 | 8.20E-49 | 8.20E-49 |
| Comp Mole Frac (H2O) | 0 | 0 | 0 | 0 | 1 | 0.227709595 | 0.227709595 | 0.227709595 |
| Comp Mole Frac (Oxygen) | 0 | 0 | 0 | 0 | 0 | 8.20E-49 | 8.20E-49 | 8.20E-49 |
| Comp Mole Frac (Hydrogen) | 0 | 0 | 0 | 0 | 0 | 0.644465478 | 0.644465478 | 0.644465478 |
| Comp Mole Frac (CO2) | 0 | 0 | 0 | 0 | 0 | 1.93E-02 | 1.93E-02 | 1.93E-02 |
| Comp Mole Frac (CO) | 0 | 0 | 0 | 0 | 0 | 8.11E-02 | 8.11E-02 | 8.11E-02 |
| Comp Mole Frac (1-Butene) | 0 | 0 | 0 | 0 | 0 | 8.20E-49 | 8.20E-49 | 8.20E-49 |
| Comp Mole Frac (1-Hexene) | 0 | 0 | 0 | 0 | 0 | 8.20E-49 | 8.20E-49 | 8.20E-49 |
| Comp Mole Frac (Cyclopentane) | 0 | 0 | 0 | 0 | 0 | 8.20E-49 | 8.20E-49 | 8.20E-49 |
| Comp Mole Frac (Cyclononane) | 0 | 0 | 0 | 0 | 0 | 8.20E-49 | 8.20E-49 | 8.20E-49 |
| Comp Mole Frac (Cyclooctane) | 0 | 0 | 0 | 0 | 0 | 8.20E-49 | 8.20E-49 | 8.20E-49 |
| Comp Mole Frac (Cycloheptane) | 0 | 0 | 0 | 0 | 0 | 8.20E-49 | 8.20E-49 | 8.20E-49 |
| Comp Mole Frac (Propene) | 0 | 0 | 0 | 0 | 0 | 8.20E-49 | 8.20E-49 | 8.20E-49 |
| Comp Mole Frac (Methanol) | 0 | 0 | 0 | 0 | 0 | 8.20E-49 | 8.20E-49 | 8.20E-49 |
| Comp Mole Frac (Nitrogen) | 0 | 0 | 0 | 0 | 0 | 8.20E-49 | 8.20E-49 | 8.20E-49 |
| Comp Mole Frac (diM-Ether) | 0 | 0 | 0 | 0 | 0 | 8.20E-49 | 8.20E-49 | 8.20E-49 |
| Comp Mole Frac (n-Hexane) | 0 | 0 | 0 | 0 | 0 | 8.20E-49 | 8.20E-49 | 8.20E-49 |
| Comp Mole Frac (2Norbornene) | 0 | 0 | 0 | 0 | 0 | 8.20E-49 | 8.20E-49 | 8.20E-49 |
| Comp Mole Frac (i-Pentane) | 0 | 0 | 0 | 0 | 0 | 8.20E-49 | 8.20E-49 | 8.20E-49 |
| Comp Mole Frac (n-Pentane) | 0 | 0 | 0 | 0 | 0 | 8.20E-49 | 8.20E-49 | 8.20E-49 |

| Name | NG | S-100 | S-101 | S-102 | Steam | S-106 | S-106' | S-107 |
|---|---|---|---|---|---|---|---|---|
| Comp Mole Frac (n-Butane) | 0 | 0 | 0 | 0 | 0 | 8.20E-49 | 8.20E-49 | 8.20E-49 |
| Comp Mole Frac (1245-M-BZ) | 0 | 0 | 0 | 0 | 0 | 8.20E-49 | 8.20E-49 | 8.20E-49 |
| Comp Mole Frac (Toluene) | 0 | 0 | 0 | 0 | 0 | 8.20E-49 | 8.20E-49 | 8.20E-49 |
| Comp Mole Frac (Naphthalene) | 0 | 0 | 0 | 0 | 0 | 8.20E-49 | 8.20E-49 | 8.20E-49 |
| Comp Mole Frac (p-Xylene) | 0 | 0 | 0 | 0 | 0 | 8.20E-49 | 8.20E-49 | 8.20E-49 |
| Comp Mole Frac (Benzene) | 0 | 0 | 0 | 0 | 0 | 8.20E-49 | 8.20E-49 | 8.20E-49 |
| Comp Mole Frac (Propane) | 0 | 0 | 0 | 0 | 0 | 8.20E-49 | 8.20E-49 | 8.20E-49 |
| Comp Mole Frac (i-Butane) | 0 | 0 | 0 | 0 | 0 | 8.20E-49 | 8.20E-49 | 8.20E-49 |
| Comp Mole Frac (Biacetylene) | 0 | 0 | 0 | 0 | 0 | 8.20E-49 | 8.20E-49 | 8.20E-49 |

| Name | S-108 | S-109 | S-110 | S-111 | S-112 | S-112' | S-200 | S-201 |
|---|---|---|---|---|---|---|---|---|
| Comp Mole Frac (Methane) | 2.74E-02 | 2.74E-02 | 2.74E-02 | 2.74E-02 | 3.54E-02 | 2.06E-09 | 6.90E-02 | 6.90E-02 |
| Comp Mole Frac (Ethane) | 1.31E-06 | 1.31E-06 | 1.31E-06 | 1.31E-06 | 1.70E-06 | 1.28E-15 | 4.73E-06 | 4.73E-06 |
| Comp Mole Frac (Ethylene) | 8.20E-49 | 8.20E-49 | 8.20E-49 | 8.20E-49 | 0 | 0 | 0 | 0 |
| Comp Mole Frac (H2O) | 0.22771 | 0.22771 | 0.22771 | 0.22771 | 4.86E-04 | 0.999497161 | 1.35E-03 | 1.35E-03 |
| Comp Mole Frac (Oxygen) | 8.20E-49 | 8.20E-49 | 8.20E-49 | 8.20E-49 | 0 | 0 | 0 | 0 |
| Comp Mole Frac (Hydrogen) | 0.644465 | 0.644465 | 0.644465 | 0.644465 | 0.834199 | 1.70E-05 | 0.603102251 | 0.603102251 |
| Comp Mole Frac (CO2) | 1.93E-02 | 1.93E-02 | 1.93E-02 | 1.93E-02 | 2.49E-02 | 4.83E-04 | 3.46E-02 | 3.46E-02 |
| Comp Mole Frac (CO) | 8.11E-02 | 8.11E-02 | 8.11E-02 | 8.11E-02 | 0.105001 | 3.27E-06 | 0.291972023 | 0.291972023 |
| Comp Mole Frac (1-Butene) | 8.20E-49 | 8.20E-49 | 8.20E-49 | 8.20E-49 | 0 | 0 | 0 | 0 |
| Comp Mole Frac (1-Hexene) | 8.20E-49 | 8.20E-49 | 8.20E-49 | 8.20E-49 | 0 | 0 | 0 | 0 |
| Comp Mole Frac (Cyclopentane) | 8.20E-49 | 8.20E-49 | 8.20E-49 | 8.20E-49 | 0 | 0 | 0 | 0 |
| Comp Mole Frac (Cyclononane) | 8.20E-49 | 8.20E-49 | 8.20E-49 | 8.20E-49 | 0 | 0 | 0 | 0 |
| Comp Mole Frac (Cyclooctane) | 8.20E-49 | 8.20E-49 | 8.20E-49 | 8.20E-49 | 0 | 0 | 0 | 0 |
| Comp Mole Frac (Cycloheptane) | 8.20E-49 | 8.20E-49 | 8.20E-49 | 8.20E-49 | 0 | 0 | 0 | 0 |
| Comp Mole Frac (Propene) | 8.20E-49 | 8.20E-49 | 8.20E-49 | 8.20E-49 | 0 | 0 | 0 | 0 |
| Comp Mole Frac (Methanol) | 8.20E-49 | 8.20E-49 | 8.20E-49 | 8.20E-49 | 0 | 0 | 0 | 0 |

| Name | S-108 | S-109 | S-110 | S-111 | S-112 | S-112' | S-200 | S-201 |
|---|---|---|---|---|---|---|---|---|
| Comp Mole Frac (Nitrogen) | 8.20E-49 | 8.20E-49 | 8.20E-49 | 8.20E-49 | 0 | 0 | 0 | 0 |
| Comp Mole Frac (diM-Ether) | 8.20E-49 | 8.20E-49 | 8.20E-49 | 8.20E-49 | 0 | 0 | 0 | 0 |
| Comp Mole Frac (n-Hexane) | 8.20E-49 | 8.20E-49 | 8.20E-49 | 8.20E-49 | 0 | 0 | 0 | 0 |
| Comp Mole Frac (2Norbornene) | 8.20E-49 | 8.20E-49 | 8.20E-49 | 8.20E-49 | 0 | 0 | 0 | 0 |
| Comp Mole Frac (i-Pentane) | 8.20E-49 | 8.20E-49 | 8.20E-49 | 8.20E-49 | 0 | 0 | 0 | 0 |
| Comp Mole Frac (n-Pentane) | 8.20E-49 | 8.20E-49 | 8.20E-49 | 8.20E-49 | 0 | 0 | 0 | 0 |
| Comp Mole Frac (n-Butane) | 8.20E-49 | 8.20E-49 | 8.20E-49 | 8.20E-49 | 0 | 0 | 0 | 0 |
| Comp Mole Frac (1245-M-BZ) | 8.20E-49 | 8.20E-49 | 8.20E-49 | 8.20E-49 | 0 | 0 | 0 | 0 |
| Comp Mole Frac (Toluene) | 8.20E-49 | 8.20E-49 | 8.20E-49 | 8.20E-49 | 0 | 0 | 0 | 0 |
| Comp Mole Frac (Naphthalene) | 8.20E-49 | 8.20E-49 | 8.20E-49 | 8.20E-49 | 0 | 0 | 0 | 0 |
| Comp Mole Frac (p-Xylene) | 8.20E-49 | 8.20E-49 | 8.20E-49 | 8.20E-49 | 0 | 0 | 0 | 0 |
| Comp Mole Frac (1,4-Pentadiyne*) | 8.20E-49 | 8.20E-49 | 8.20E-49 | 8.20E-49 | 0 | 0 | 0 | 0 |
| Comp Mole Frac (Benzene) | 8.20E-49 | 8.20E-49 | 8.20E-49 | 8.20E-49 | 0 | 0 | 0 | 0 |
| Comp Mole Frac (Propane) | 8.20E-49 | 8.20E-49 | 8.20E-49 | 8.20E-49 | 0 | 0 | 0 | 0 |
| Comp Mole Frac (i-Butane) | 8.20E-49 | 8.20E-49 | 8.20E-49 | 8.20E-49 | 0 | 0 | 0 | 0 |
| Comp Mole Frac (Biacetylene) | 8.20E-49 | 8.20E-49 | 8.20E-49 | 8.20E-49 | 0 | 0 | 0 | 0 |
| Name | S-113 | S-114 | S-103 | S-103' | S-104 | S-115 | Purge | S-116 |
| Comp Mole Frac (Methane) | 1.66E-02 | 6.90E-02 | 0.246408 | 4.35E-03 | 0.246408 | 1.66E-02 | 1.66E-02 | 1.65E-02 |
| Comp Mole Frac (Ethane) | 0 | 4.73E-06 | 2.91E-06 | 3.89E-08 | 2.91E-06 | 0 | 0 | 0 |
| Comp Mole Frac (Ethylene) | 0 | 0 | 0 | 0 | 0 | 0 | 0 | 0 |
| Comp Mole Frac (H2O) | 0 | 1.35E-03 | 0.723497 | 0.994421 | 0.723497 | 0 | 0 | 0 |
| Comp Mole Frac (Oxygen) | 0 | 0 | 0 | 0 | 0 | 0 | 0 | 0 |
| Comp Mole Frac (Hydrogen) | 0.96398 | 0.603102 | 2.25E-02 | 7.22E-04 | 2.25E-02 | 0.963979732 | 0.963979732 | 0.963996618 |
| Comp Mole Frac (CO2) | 1.94E-02 | 3.46E-02 | 7.57E-03 | 5.07E-04 | 7.57E-03 | 1.94E-02 | 1.94E-02 | 1.95E-02 |
| Comp Mole Frac (CO) | 0 | 0.291972 | 7.81E-06 | 2.35E-07 | 7.81E-06 | 0 | 0 | 0 |
| Comp Mole Frac (1-Butene) | 0 | 0 | 0 | 0 | 0 | 0 | 0 | 0 |

| Name | S-113 | S-114 | S-103 | S-103' | S-104 | S-115 | Purge | S-116 |
|---|---|---|---|---|---|---|---|---|
| Comp Mole Frac (1-Hexene) | 0 | 0 | 0 | 0 | 0 | 0 | 0 | 0 |
| Comp Mole Frac (Cyclopentane) | 0 | 0 | 0 | 0 | 0 | 0 | 0 | 0 |
| Comp Mole Frac (Cyclononane) | 0 | 0 | 0 | 0 | 0 | 0 | 0 | 0 |
| Comp Mole Frac (Cyclooctane) | 0 | 0 | 0 | 0 | 0 | 0 | 0 | 0 |
| Comp Mole Frac (Cycloheptane) | 0 | 0 | 0 | 0 | 0 | 0 | 0 | 0 |
| Comp Mole Frac (Propene) | 0 | 0 | 0 | 0 | 0 | 0 | 0 | 0 |
| Comp Mole Frac (Methanol) | 0 | 0 | 0 | 0 | 0 | 0 | 0 | 0 |
| Comp Mole Frac (Nitrogen) | 0 | 0 | 0 | 0 | 0 | 0 | 0 | 0 |
| Comp Mole Frac (diM-Ether) | 0 | 0 | 0 | 0 | 0 | 0 | 0 | 0 |
| Comp Mole Frac (n-Hexane) | 0 | 0 | 0 | 0 | 0 | 0 | 0 | 0 |
| Comp Mole Frac (i-Pentane) | 0 | 0 | 0 | 0 | 0 | 0 | 0 | 0 |
| Comp Mole Frac (n-Pentane) | 0 | 0 | 0 | 0 | 0 | 0 | 0 | 0 |
| Comp Mole Frac (n-Butane) | 0 | 0 | 0 | 0 | 0 | 0 | 0 | 0 |
| Comp Mole Frac (1245-M-BZ) | 0 | 0 | 0 | 0 | 0 | 0 | 0 | 0 |
| Comp Mole Frac (Toluene) | 0 | 0 | 0 | 0 | 0 | 0 | 0 | 0 |
| Comp Mole Frac (Naphthalene) | 0 | 0 | 0 | 0 | 0 | 0 | 0 | 0 |
| Comp Mole Frac (p-Xylene) | 0 | 0 | 0 | 0 | 0 | 0 | 0 | 0 |
| Comp Mole Frac (1,4-Pentadiyne*) | 0 | 0 | 0 | 0 | 0 | 0 | 0 | 0 |
| Comp Mole Frac (Benzene) | 0 | 0 | 0 | 0 | 0 | 0 | 0 | 0 |
| Comp Mole Frac (Propane) | 0 | 0 | 0 | 0 | 0 | 0 | 0 | 0 |
| Comp Mole Frac (i-Butane) | 0 | 0 | 0 | 0 | 0 | 0 | 0 | 0 |
| Comp Mole Frac (Biacetylene) | 0 | 0 | 0 | 0 | 0 | 0 | 0 | 0 |

| Name | S-105 | S-116' | S-300 | S-302 | S-302' | S-304 | S-301 | S-303 |
|---|---|---|---|---|---|---|---|---|
| Comp Mole Frac (Methane) | 0.142867 | 1.65E-02 | 5.39E-04 | 5.39E-04 | 5.39E-04 | 5.39E-04 | 5.39E-04 | 5.39E-04 |
| Comp Mole Frac (Ethane) | 1.60E-06 | 0 | 2.51E-07 | 2.51E-07 | 2.51E-07 | 2.51E-07 | 2.51E-07 | 2.51E-07 |
| Comp Mole Frac (Ethylene) | 0 | 0 | 0 | 0 | 0 | 0 | 0 | 0 |

| Name | S-105 | S-116' | S-300 | S-302 | S-302' | S-304 | S-301 | S-303 |
|---|---|---|---|---|---|---|---|---|
| Comp Mole Frac (H2O) | 0.397662 | 0 | 1.26E-09 | 0.496685 | 0.496685 | 0.496684772 | 1.26E-09 | 0.496684772 |
| Comp Mole Frac (Oxygen) | 0 | 0 | 0 | 0 | 0 | 0 | 0 | 0 |
| Comp Mole Frac (Hydrogen) | 0.446523 | 0.963997 | 8.97E-06 | 8.97E-06 | 8.97E-06 | 8.97E-06 | 8.97E-06 | 8.97E-06 |
| Comp Mole Frac (CO2) | 1.29E-02 | 1.95E-02 | 6.06E-03 | 6.06E-03 | 6.06E-03 | 6.06E-03 | 6.06E-03 | 6.06E-03 |
| Comp Mole Frac (CO) | 4.29E-06 | 0 | 1.79E-05 | 1.79E-05 | 1.79E-05 | 1.79E-05 | 1.79E-05 | 1.79E-05 |
| Comp Mole Frac (1-Butene) | 0 | 0 | 0 | 0 | 0 | 0 | 0 | 0 |
| Comp Mole Frac (1-Hexene) | 0 | 0 | 0 | 0 | 0 | 0 | 0 | 0 |
| Comp Mole Frac (Cyclopentane) | 0 | 0 | 0 | 0 | 0 | 0 | 0 | 0 |
| Comp Mole Frac (Cyclononane) | 0 | 0 | 0 | 0 | 0 | 0 | 0 | 0 |
| Comp Mole Frac (Cyclooctane) | 0 | 0 | 0 | 0 | 0 | 0 | 0 | 0 |
| Comp Mole Frac (Cycloheptane) | 0 | 0 | 0 | 0 | 0 | 0 | 0 | 0 |
| Comp Mole Frac (Propene) | 0 | 0 | 0 | 0 | 0 | 0 | 0 | 0 |
| Comp Mole Frac (Methanol) | 0 | 0 | 0.99337 | 0 | 0 | 0 | 0.993369542 | 0 |
| Comp Mole Frac (Nitrogen) | 0 | 0 | 0 | 0 | 0 | 0 | 0 | 0 |
| Comp Mole Frac (diM-Ether) | 0 | 0 | 0 | 0.496685 | 0.496685 | 0.496684771 | 0 | 0.496684771 |
| Comp Mole Frac (Methylene*) | 0 | 0 | 0 | 0 | 0 | 0 | 0 | 0 |
| Comp Mole Frac (n-Hexane) | 0 | 0 | 0 | 0 | 0 | 0 | 0 | 0 |
| Comp Mole Frac (i-Pentane) | 0 | 0 | 0 | 0 | 0 | 0 | 0 | 0 |
| Comp Mole Frac (n-Pentane) | 0 | 0 | 0 | 0 | 0 | 0 | 0 | 0 |
| Comp Mole Frac (n-Butane) | 0 | 0 | 0 | 0 | 0 | 0 | 0 | 0 |
| Comp Mole Frac (1245-M-BZ) | 0 | 0 | 0 | 0 | 0 | 0 | 0 | 0 |
| Comp Mole Frac (Toluene) | 0 | 0 | 0 | 0 | 0 | 0 | 0 | 0 |
| Comp Mole Frac (Naphthalene) | 0 | 0 | 0 | 0 | 0 | 0 | 0 | 0 |
| Comp Mole Frac (p-Xylene) | 0 | 0 | 0 | 0 | 0 | 0 | 0 | 0 |
| Comp Mole Frac (1,4-Pentadiyne*) | 0 | 0 | 0 | 0 | 0 | 0 | 0 | 0 |
| Comp Mole Frac (Benzene) | 0 | 0 | 0 | 0 | 0 | 0 | 0 | 0 |

| Name | S-105 | S-116' | S-300 | S-302 | S-302' | S-304 | S-301 | S-303 |
|---|---|---|---|---|---|---|---|---|
| Comp Mole Frac (Propane) | 0 | 0 | 0 | 0 | 0 | 0 | 0 | 0 |
| Comp Mole Frac (i-Butane) | 0 | 0 | 0 | 0 | 0 | 0 | 0 | 0 |
| Comp Mole Frac (Biacetylene) | 0 | 0 | 0 | 0 | 0 | 0 | 0 | 0 |
| Name | S-202 | S-203 | S-204 | S-205 | S-206 | S-207 | S-208 | S-209 |
| Comp Mole Frac (Methane) | 6.90E-02 | 6.90E-02 | 6.90E-02 | 0.188697 | 0.188697 | 0.188696645 | 0.21407398 | 0.214074014 |
| Comp Mole Frac (Ethane) | 4.73E-06 | 4.73E-06 | 4.73E-06 | 1.18E-05 | 1.18E-05 | 1.18E-05 | 1.34E-05 | 1.34E-05 |
| Comp Mole Frac (Ethylene) | 0 | 0 | 0 | 0 | 0 | 0 | 0 | 0 |
| Comp Mole Frac (H2O) | 1.35E-03 | 1.35E-03 | 1.35E-03 | 3.92E-04 | 3.92E-04 | 3.92E-04 | 3.87E-03 | 3.87E-03 |
| Comp Mole Frac (Oxygen) | 0 | 0 | 0 | 0 | 0 | 0 | 0 | 0 |
| Comp Mole Frac (Hydrogen) | 0.603102 | 0.603102 | 0.603095 | 0.482182 | 0.482182 | 0.482182365 | 0.409116211 | 0.409116098 |
| Comp Mole Frac (CO2) | 3.46E-02 | 3.46E-02 | 3.46E-02 | 6.07E-02 | 6.07E-02 | 6.07E-02 | 6.54E-02 | 6.54E-02 |
| Comp Mole Frac (CO) | 0.291972 | 0.291972 | 0.29197 | 0.262816 | 0.262816 | 0.262815808 | 0.234343674 | 0.23434364 |
| Comp Mole Frac (1-Butene) | 0 | 0 | 0 | 0 | 0 | 0 | 0 | 0 |
| Comp Mole Frac (1-Hexene) | 0 | 0 | 0 | 0 | 0 | 0 | 0 | 0 |
| Comp Mole Frac (Cyclopentane) | 0 | 0 | 0 | 0 | 0 | 0 | 0 | 0 |
| Comp Mole Frac (Cyclononane) | 0 | 0 | 0 | 0 | 0 | 0 | 0 | 0 |
| Comp Mole Frac (Cyclooctane) | 0 | 0 | 0 | 0 | 0 | 0 | 0 | 0 |
| Comp Mole Frac (Cycloheptane) | 0 | 0 | 0 | 0 | 0 | 0 | 0 | 0 |
| Comp Mole Frac (Propene) | 0 | 0 | 0 | 0 | 0 | 0 | 0 | 0 |
| Comp Mole Frac (Methanol) | 0 | 0 | 7.77E-08 | 5.20E-03 | 5.20E-03 | 5.20E-03 | 7.31E-02 | 7.31E-02 |
| Comp Mole Frac (Nitrogen) | 0 | 0 | 0 | 0 | 0 | 0 | 0 | 0 |
| Comp Mole Frac (diM-Ether) | 0 | 0 | 0 | 0 | 0 | 0 | 0 | 0 |
| Comp Mole Frac (n-Hexane) | 0 | 0 | 0 | 0 | 0 | 0 | 0 | 0 |
| Comp Mole Frac (i-Pentane) | 0 | 0 | 0 | 0 | 0 | 0 | 0 | 0 |
| Comp Mole Frac (n-Pentane) | 0 | 0 | 0 | 0 | 0 | 0 | 0 | 0 |
| Comp Mole Frac (n-Butane) | 0 | 0 | 0 | 0 | 0 | 0 | 0 | 0 |

| Name | S-202 | S-203 | S-204 | S-205 | S-206 | S-207 | S-208 | S-209 |
|---|---|---|---|---|---|---|---|---|
| Comp Mole Frac (1245-M-BZ) | 0 | 0 | 0 | 0 | 0 | 0 | 0 | 0 |
| Comp Mole Frac (Toluene) | 0 | 0 | 0 | 0 | 0 | 0 | 0 | 0 |
| Comp Mole Frac (Naphthalene) | 0 | 0 | 0 | 0 | 0 | 0 | 0 | 0 |
| Comp Mole Frac (p-Xylene) | 0 | 0 | 0 | 0 | 0 | 0 | 0 | 0 |
| Comp Mole Frac (1,4-Pentadiyne*) | 0 | 0 | 0 | 0 | 0 | 0 | 0 | 0 |
| Comp Mole Frac (Benzene) | 0 | 0 | 0 | 0 | 0 | 0 | 0 | 0 |
| Comp Mole Frac (Propane) | 0 | 0 | 0 | 0 | 0 | 0 | 0 | 0 |
| Comp Mole Frac (i-Butane) | 0 | 0 | 0 | 0 | 0 | 0 | 0 | 0 |
| Comp Mole Frac (Biacetylene) | 0 | 0 | 0 | 0 | 0 | 0 | 0 | 0 |

| Name | S-210 | S-211 | S-212 | S-213 | S-214 | S-215 | S-216 | S-217 |
|---|---|---|---|---|---|---|---|---|
| Comp Mole Frac (Methane) | 0.214074 | 0.214074 | 0.230084 | 2.02E-02 | 0.230084 | 0.230083958 | 0.230083958 | 0.230424362 |
| Comp Mole Frac (Ethane) | 1.34E-05 | 1.34E-05 | 1.42E-05 | 3.09E-06 | 1.42E-05 | 1.42E-05 | 1.42E-05 | 1.44E-05 |
| Comp Mole Frac (Ethylene) | 0 | 0 | 0 | 0 | 0 | 0 | 0 | 0 |
| Comp Mole Frac (H2O) | 3.87E-03 | 3.87E-03 | 4.50E-05 | 5.02E-02 | 4.50E-05 | 4.50E-05 | 4.50E-05 | 5.11E-05 |
| Comp Mole Frac (Oxygen) | 0 | 0 | 0 | 0 | 0 | 0 | 0 | 0 |
| Comp Mole Frac (Hydrogen) | 0.409116 | 0.409116 | 0.442396 | 6.10E-03 | 0.442396 | 0.44239584 | 0.44239584 | 0.440168591 |
| Comp Mole Frac (CO2) | 6.54E-02 | 6.54E-02 | 6.79E-02 | 3.51E-02 | 6.79E-02 | 6.79E-02 | 6.79E-02 | 7.02E-02 |
| Comp Mole Frac (CO) | 0.234344 | 0.234344 | 0.25328 | 5.02E-03 | 0.25328 | 0.253280194 | 0.253280194 | 0.252142503 |
| Comp Mole Frac (1-Butene) | 0 | 0 | 0 | 0 | 0 | 0 | 0 | 0 |
| Comp Mole Frac (1-Hexene) | 0 | 0 | 0 | 0 | 0 | 0 | 0 | 0 |
| Comp Mole Frac (Cyclopentane) | 0 | 0 | 0 | 0 | 0 | 0 | 0 | 0 |
| Comp Mole Frac (Cyclononane) | 0 | 0 | 0 | 0 | 0 | 0 | 0 | 0 |
| Comp Mole Frac (Cyclooctane) | 0 | 0 | 0 | 0 | 0 | 0 | 0 | 0 |
| Comp Mole Frac (Cycloheptane) | 0 | 0 | 0 | 0 | 0 | 0 | 0 | 0 |
| Comp Mole Frac (Propene) | 0 | 0 | 0 | 0 | 0 | 0 | 0 | 0 |
| Comp Mole Frac (Methanol) | 7.31E-02 | 7.31E-02 | 6.24E-03 | 0.883398 | 6.24E-03 | 6.24E-03 | 6.24E-03 | 6.99E-03 |

| Name | S-210 | S-211 | S-212 | S-213 | S-214 | S-215 | S-216 | S-217 |
|---|---|---|---|---|---|---|---|---|
| Comp Mole Frac (Nitrogen) | 0 | 0 | 0 | 0 | 0 | 0 | 0 | 0 |
| Comp Mole Frac (diM-Ether) | 0 | 0 | 0 | 0 | 0 | 0 | 0 | 0 |
| Comp Mole Frac (n-Hexane) | 0 | 0 | 0 | 0 | 0 | 0 | 0 | 0 |
| Comp Mole Frac (i-Pentane) | 0 | 0 | 0 | 0 | 0 | 0 | 0 | 0 |
| Comp Mole Frac (n-Pentane) | 0 | 0 | 0 | 0 | 0 | 0 | 0 | 0 |
| Comp Mole Frac (n-Butane) | 0 | 0 | 0 | 0 | 0 | 0 | 0 | 0 |
| Comp Mole Frac (1245-M-BZ) | 0 | 0 | 0 | 0 | 0 | 0 | 0 | 0 |
| Comp Mole Frac (Toluene) | 0 | 0 | 0 | 0 | 0 | 0 | 0 | 0 |
| Comp Mole Frac (Naphthalene) | 0 | 0 | 0 | 0 | 0 | 0 | 0 | 0 |
| Comp Mole Frac (p-Xylene) | 0 | 0 | 0 | 0 | 0 | 0 | 0 | 0 |
| Comp Mole Frac (1,4-Pentadiyne*) | 0 | 0 | 0 | 0 | 0 | 0 | 0 | 0 |
| Comp Mole Frac (Benzene) | 0 | 0 | 0 | 0 | 0 | 0 | 0 | 0 |
| Comp Mole Frac (Propane) | 0 | 0 | 0 | 0 | 0 | 0 | 0 | 0 |
| Comp Mole Frac (i-Butane) | 0 | 0 | 0 | 0 | 0 | 0 | 0 | 0 |
| Comp Mole Frac (Biacetylene) | 0 | 0 | 0 | 0 | 0 | 0 | 0 | 0 |
| Name | S-218 | S-219 | S-220 | S-221 | S-222 | S-223 | S-224 | S-225 |
| Comp Mole Frac (Methane) | 0.231095 | 2.02E-02 | 0.284283 | 5.38E-04 | 0.284283 | 0.408749751 | 5.39E-04 | 1.04E-30 |
| Comp Mole Frac (Ethane) | 1.43E-05 | 3.09E-06 | 4.14E-05 | 2.40E-07 | 4.14E-05 | 3.89E-05 | 2.51E-07 | 1.05E-30 |
| Comp Mole Frac (Ethylene) | 0 | 0 | 0 | 0 | 0 | 0 | 0 | 0 |
| Comp Mole Frac (H2O) | 5.22E-05 | 5.02E-02 | 1.01E-03 | 5.39E-02 | 1.01E-03 | 3.88E-13 | 1.26E-09 | 0.982914939 |
| Comp Mole Frac (Oxygen) | 0 | 0 | 0 | 0 | 0 | 0 | 0 | 0 |
| Comp Mole Frac (Hydrogen) | 0.439351 | 6.10E-03 | 8.78E-02 | 2.01E-05 | 8.78E-02 | 0.167778364 | 8.97E-06 | 1.01E-30 |
| Comp Mole Frac (CO2) | 7.00E-02 | 3.51E-02 | 0.429144 | 5.75E-03 | 0.429144 | 0.276634982 | 6.06E-03 | 1.01E-30 |
| Comp Mole Frac (CO) | 0.252489 | 5.02E-03 | 7.21E-02 | 2.67E-05 | 7.21E-02 | 0.142114197 | 1.79E-05 | 1.01E-30 |
| Comp Mole Frac (1-Butene) | 0 | 0 | 0 | 0 | 0 | 0 | 0 | 0 |
| Comp Mole Frac (1-Hexene) | 0 | 0 | 0 | 0 | 0 | 0 | 0 | 0 |

| Name | S-218 | S-219 | S-220 | S-221 | S-222 | S-223 | S-224 | S-225 |
|---|---|---|---|---|---|---|---|---|
| Comp Mole Frac (Cyclopentane) | 0 | 0 | 0 | 0 | 0 | 0 | 0 | 0 |
| Comp Mole Frac (Cyclononane) | 0 | 0 | 0 | 0 | 0 | 0 | 0 | 0 |
| Comp Mole Frac (Cyclooctane) | 0 | 0 | 0 | 0 | 0 | 0 | 0 | 0 |
| Comp Mole Frac (Cycloheptane) | 0 | 0 | 0 | 0 | 0 | 0 | 0 | 0 |
| Comp Mole Frac (Propene) | 0 | 0 | 0 | 0 | 0 | 0 | 0 | 0 |
| Comp Mole Frac (Methanol) | 7.05E-03 | 0.883398 | 0.125611 | 0.939795 | 0.125611 | 4.68E-03 | 0.993369542 | 1.71E-02 |
| Comp Mole Frac (Nitrogen) | 0 | 0 | 0 | 0 | 0 | 0 | 0 | 0 |
| Comp Mole Frac (diM-Ether) | 0 | 0 | 0 | 0 | 0 | 0 | 0 | 0 |
| Comp Mole Frac (n-Hexane) | 0 | 0 | 0 | 0 | 0 | 0 | 0 | 0 |
| Comp Mole Frac (i-Pentane) | 0 | 0 | 0 | 0 | 0 | 0 | 0 | 0 |
| Comp Mole Frac (n-Pentane) | 0 | 0 | 0 | 0 | 0 | 0 | 0 | 0 |
| Comp Mole Frac (n-Butane) | 0 | 0 | 0 | 0 | 0 | 0 | 0 | 0 |
| Comp Mole Frac (1245-M-BZ) | 0 | 0 | 0 | 0 | 0 | 0 | 0 | 0 |
| Comp Mole Frac (Toluene) | 0 | 0 | 0 | 0 | 0 | 0 | 0 | 0 |
| Comp Mole Frac (Naphthalene) | 0 | 0 | 0 | 0 | 0 | 0 | 0 | 0 |
| Comp Mole Frac (p-Xylene) | 0 | 0 | 0 | 0 | 0 | 0 | 0 | 0 |
| Comp Mole Frac (1,4-Pentadiyne*) | 0 | 0 | 0 | 0 | 0 | 0 | 0 | 0 |
| Comp Mole Frac (Benzene) | 0 | 0 | 0 | 0 | 0 | 0 | 0 | 0 |
| Comp Mole Frac (Propane) | 0 | 0 | 0 | 0 | 0 | 0 | 0 | 0 |
| Comp Mole Frac (i-Butane) | 0 | 0 | 0 | 0 | 0 | 0 | 0 | 0 |
| Comp Mole Frac (Biacetylene) | 0 | 0 | 0 | 0 | 0 | 0 | 0 | 0 |
| Name | S-226 | S-227 | S-305 | S-305' | S-306 | S-309 | S-310 | S-310' |
| Comp Mole Frac (Methane) | 0.40875 | 0.40863 | -4.41E-19 | 0 | -4.41E-19 | 0 | 6.05E-103 | 6.31E-03 |
| Comp Mole Frac (Ethane) | 3.89E-05 | 3.89E-05 | 2.15E-07 | 2.15E-07 | 2.15E-07 | 2.15E-07 | 2.07E-107 | 2.15E-07 |
| Comp Mole Frac (Ethylene) | 0 | 0 | 0 | 0 | 0 | 0 | 8.89E-105 | 9.27E-05 |
| Comp Mole Frac (H2O) | 3.88E-13 | 4.03E-13 | 0.79568 | 0.795673 | 0.79568 | 0.795680476 | 7.76E-101 | 0.80846152 |

| Name | S-226 | S-227 | S-305 | S-305' | S-306 | S-309 | S-310 | S-310' |
|---|---|---|---|---|---|---|---|---|
| Comp Mole Frac (Oxygen) | 0 | 0 | 0 | 0 | 0 | 0 | 0 | 0 |
| Comp Mole Frac (Hydrogen) | 0.167778 | 0.167741 | 7.69E-06 | 7.69E-06 | 7.69E-06 | 7.69E-06 | 7.39E-106 | 7.70E-06 |
| Comp Mole Frac (CO2) | 0.276635 | 0.276826 | 5.20E-03 | 5.20E-03 | 5.20E-03 | 5.20E-03 | 5.00E-103 | 5.21E-03 |
| Comp Mole Frac (CO) | 0.142114 | 0.142065 | 1.53E-05 | 1.53E-05 | 1.53E-05 | 1.53E-05 | 1.47E-105 | 1.54E-05 |
| Comp Mole Frac (1-Butene) | 0 | 0 | 2.86E-02 | 2.86E-02 | 2.86E-02 | 4.30E-03 | 6.58E-103 | 6.86E-03 |
| Comp Mole Frac (1-Hexene) | 0 | 0 | 5.66E-02 | 5.66E-02 | 5.66E-02 | 1.13E-02 | 7.95E-103 | 8.28E-03 |
| Comp Mole Frac (Cyclopentane) | 0 | 0 | 5.68E-02 | 5.68E-02 | 5.68E-02 | 3.41E-02 | 3.27E-102 | 3.41E-02 |
| Comp Mole Frac (Cyclononane) | 0 | 0 | 0 | 0 | 0 | 0 | 0 | 0 |
| Comp Mole Frac (Cyclooctane) | 0 | 0 | 0 | 0 | 0 | 0 | 0 | 0 |
| Comp Mole Frac (Cycloheptane) | 0 | 0 | 0 | 0 | 0 | 0 | 0 | 0 |
| Comp Mole Frac (Propene) | 0 | 0 | 0 | 0 | 0 | 0 | 3.51E-103 | 3.66E-03 |
| Comp Mole Frac (Methanol) | 4.68E-03 | 4.70E-03 | 0 | 0 | 0 | 0 | 0 | 0 |
| Comp Mole Frac (Nitrogen) | 0 | 0 | 0 | 0 | 0 | 0 | 0 | 0 |
| Comp Mole Frac (diM-Ether) | 0 | 0 | 5.66E-02 | 5.66E-02 | 5.66E-02 | 5.66E-02 | 4.29E-102 | 4.47E-02 |
| Comp Mole Frac (n-Hexane) | 0 | 0 | 0 | 0 | 0 | 3.40E-02 | 3.26E-102 | 3.40E-02 |
| Comp Mole Frac (i-Pentane) | 0 | 0 | 0 | 0 | 0 | 1.70E-02 | 1.39E-102 | 1.45E-02 |
| Comp Mole Frac (n-Pentane) | 0 | 0 | 0 | 0 | 0 | 0 | 0 | 0 |
| Comp Mole Frac (n-Butane) | 0 | 0 | 0 | 0 | 0 | 1.83E-02 | 1.40E-102 | 1.46E-02 |
| Comp Mole Frac (1245-M-BZ) | 0 | 0 | 0 | 0 | 0 | 0 | 2.92E-103 | 3.05E-03 |
| Comp Mole Frac (Toluene) | 0 | 0 | 0 | 0 | 0 | 0 | 2.73E-103 | 2.84E-03 |
| Comp Mole Frac (Naphthalene) | 0 | 0 | 0 | 0 | 0 | 0 | 1.40E-103 | 1.46E-03 |
| Comp Mole Frac (p-Xylene) | 0 | 0 | 0 | 0 | 0 | 0 | 7.57E-103 | 7.89E-03 |
| Comp Mole Frac (1,4-Pentadiyne*) | 0 | 0 | 0 | 0 | 0 | 5.68E-03 | 1 | 2.31E-99 |
| Comp Mole Frac (Benzene) | 0 | 0 | 0 | 0 | 0 | 1.13E-02 | 3.07E-103 | 3.20E-03 |
| Comp Mole Frac (Propane) | 0 | 0 | 4.63E-04 | 4.63E-04 | 4.63E-04 | 4.63E-04 | 3.56E-104 | 3.71E-04 |
| Comp Mole Frac (i-Butane) | 0 | 0 | 0 | 0 | 0 | 0 | 0 | 0 |

| Name | S-307 | S-307' | S-312 | S-315 | S-313 | S-314 | S-311 | S-317 |
|---|---|---|---|---|---|---|---|---|
| Comp Mole Frac (Biacetylene) | 0 | 0 | 0 | 0 | 0 | 6.09E-03 | 3.51E-104 | 3.66E-04 |
| Comp Mole Frac (Methane) | 0 | 0 | 6.29E-03 | 3.16E-102 | 3.29E-02 | 2.86E-29 | 6.29E-03 | 3.29E-02 |
| Comp Mole Frac (Ethane) | 2.08E-107 | 2.16E-07 | 2.15E-07 | 1.08E-106 | 1.12E-06 | 7.91E-41 | 2.15E-07 | 1.12E-06 |
| Comp Mole Frac (Ethylene) | 0 | 0 | 9.24E-05 | 4.64E-104 | 4.84E-04 | 4.21E-31 | 9.24E-05 | 4.84E-04 |
| Comp Mole Frac (H2O) | 7.68E-101 | 0.800227 | 0.806169 | 9.59E-101 | 1.56E-67 | 1 | 0.806168891 | 1.56E-67 |
| Comp Mole Frac (Oxygen) | 0 | 0 | 0 | 0 | 0 | 0 | 0 | 0 |
| Comp Mole Frac (Hydrogen) | 7.42E-106 | 7.74E-06 | 7.68E-06 | 3.86E-105 | 4.02E-05 | 3.50E-32 | 7.68E-06 | 4.02E-05 |
| Comp Mole Frac (CO2) | 5.02E-103 | 5.23E-03 | 5.19E-03 | 2.61E-102 | 2.72E-02 | 2.36E-29 | 5.19E-03 | 2.72E-02 |
| Comp Mole Frac (CO) | 1.48E-105 | 1.54E-05 | 1.53E-05 | 7.69E-105 | 8.01E-05 | 6.97E-32 | 1.53E-05 | 8.01E-05 |
| Comp Mole Frac (1-Butene) | 4.14E-103 | 4.32E-03 | 6.84E-03 | 3.44E-102 | 3.58E-02 | 3.11E-29 | 6.84E-03 | 3.58E-02 |
| Comp Mole Frac (1-Hexene) | 1.09E-102 | 1.14E-02 | 8.26E-03 | 4.15E-102 | 4.32E-02 | 3.76E-29 | 8.26E-03 | 4.32E-02 |
| Comp Mole Frac (Cyclopentane) | 3.29E-102 | 3.43E-02 | 3.40E-02 | 1.71E-101 | 0.178169 | 1.55E-28 | 3.40E-02 | 0.178169363 |
| Comp Mole Frac (Cyclononane) | 0 | 0 | 0 | 0 | 0 | 0 | 0 | 0 |
| Comp Mole Frac (Cyclooctane) | 0 | 0 | 0 | 0 | 0 | 0 | 0 | 0 |
| Comp Mole Frac (Cycloheptane) | 0 | 0 | 0 | 0 | 0 | 0 | 0 | 0 |
| Comp Mole Frac (Propene) | 0 | 0 | 3.65E-03 | 1.83E-102 | 1.91E-02 | 1.66E-29 | 3.65E-03 | 1.91E-02 |
| Comp Mole Frac (Methanol) | 0 | 0 | 0 | 0 | 0 | 0 | 0 | 0 |
| Comp Mole Frac (Nitrogen) | 0 | 0 | 0 | 0 | 0 | 0 | 0 | 0 |
| Comp Mole Frac (diM-Ether) | 5.46E-102 | 5.69E-02 | 4.46E-02 | 2.24E-101 | 0.233351 | 2.03E-28 | 4.46E-02 | 0.233351041 |
| Comp Mole Frac (n-Hexane) | 3.28E-102 | 3.41E-02 | 3.39E-02 | 1.70E-101 | 0.177444 | 1.54E-28 | 3.39E-02 | 0.177443786 |
| Comp Mole Frac (i-Pentane) | 1.64E-102 | 1.71E-02 | 1.45E-02 | 7.26E-102 | 7.57E-02 | 6.58E-29 | 1.45E-02 | 7.57E-02 |
| Comp Mole Frac (n-Pentane) | 0 | 0 | 0 | 0 | 0 | 0 | 0 | 0 |
| Comp Mole Frac (n-Butane) | 1.76E-102 | 1.84E-02 | 1.46E-02 | 7.32E-102 | 7.63E-02 | 6.64E-29 | 1.46E-02 | 7.63E-02 |
| Comp Mole Frac (Toluene) | 0 | 0 | 2.84E-03 | 1.42E-102 | 1.48E-02 | 1.29E-29 | 2.84E-03 | 1.48E-02 |
| Comp Mole Frac (Naphthalene) | 0 | 0 | 1.46E-03 | 7.32E-103 | 7.63E-03 | 6.64E-30 | 1.46E-03 | 7.63E-03 |
| Comp Mole Frac (p-Xylene) | 0 | 0 | 7.87E-03 | 3.95E-102 | 4.12E-02 | 3.58E-29 | 7.87E-03 | 4.12E-02 |

| Name | S-307 | S-307' | S-312 | S-315 | S-313 | S-314 | S-311 | S-317 |
|---|---|---|---|---|---|---|---|---|
| Comp Mole Frac (1,4-Pentadiyne*) | 1 | 3.62E-99 | 2.84E-03 | 1 | 9.59E-101 | 6.15E-34 | 2.84E-03 | 9.59E-101 |
| Comp Mole Frac (Benzene) | 1.09E-102 | 1.14E-02 | 3.19E-03 | 1.60E-102 | 1.67E-02 | 1.45E-29 | 3.19E-03 | 1.67E-02 |
| Comp Mole Frac (Propane) | 4.46E-104 | 4.65E-04 | 3.70E-04 | 1.86E-103 | 1.93E-03 | 1.68E-30 | 3.70E-04 | 1.93E-03 |
| Comp Mole Frac (i-Butane) | 0 | 0 | 0 | 0 | 0 | 0 | 0 | 0 |
| Comp Mole Frac (Biacetylene) | 5.87E-103 | 6.12E-03 | 3.65E-04 | 1.83E-103 | 1.91E-03 | 1.66E-30 | 3.65E-04 | 1.91E-03 |

| Name | S-318 | S-319 | S-320 | S-321 | S-308 | ** New ** | | |
|---|---|---|---|---|---|---|---|---|
| Comp Mole Frac (Methane) | 0.536053 | 1.76E-25 | 4.50E-25 | 9.84E-31 | 0 | | | |
| Comp Mole Frac (Ethane) | 1.83E-05 | 1.51E-16 | 3.85E-16 | 1.00E-30 | 2.15E-07 | | | |
| Comp Mole Frac (Ethylene) | 7.87E-03 | 4.23E-17 | 1.08E-16 | 1.00E-30 | 0 | | | |
| Comp Mole Frac (H2O) | 1.56E-67 | 1.56E-67 | 1.56E-67 | 1.56E-67 | 0.79568 | | | |
| Comp Mole Frac (Oxygen) | 0 | 0 | 0 | 0 | 0 | | | |
| Comp Mole Frac (Hydrogen) | 6.55E-04 | 9.96E-31 | 2.53E-30 | 8.25E-33 | 7.69E-06 | | | |
| Comp Mole Frac (CO2) | 0.442611 | 2.59E-16 | 6.60E-16 | 1.00E-30 | 5.20E-03 | | | |
| Comp Mole Frac (CO) | 1.30E-03 | 9.93E-31 | 2.53E-30 | 3.00E-34 | 1.53E-05 | | | |
| Comp Mole Frac (1-Butene) | 2.19E-15 | 3.82E-02 | 9.72E-02 | 9.38E-10 | 4.30E-03 | | | |
| Comp Mole Frac (1-Hexene) | 9.99E-31 | 4.61E-02 | 1.98E-14 | 7.58E-02 | 1.13E-02 | | | |
| Comp Mole Frac (Cyclopentane) | 1.81E-29 | 0.189831 | 1.87E-08 | 0.312428 | 3.41E-02 | | | |
| Comp Mole Frac (Cyclononane) | 0 | 0 | 0 | 0 | 0 | | | |
| Comp Mole Frac (Cyclooctane) | 0 | 0 | 0 | 0 | 0 | | | |
| Comp Mole Frac (Cycloheptane) | 0 | 0 | 0 | 0 | 0 | | | |
| Comp Mole Frac (Propene) | 1.12E-02 | 1.96E-02 | 4.99E-02 | 5.44E-21 | 0 | | | |
| Comp Mole Frac (Methanol) | 0 | 0 | 0 | 0 | 0 | | | |
| Comp Mole Frac (Nitrogen) | 0 | 0 | 0 | 0 | 0 | | | |
| Comp Mole Frac (diM-Ether) | 4.47E-10 | 0.248625 | 0.633598 | 9.29E-15 | 5.66E-02 | | | |
| Comp Mole Frac (n-Hexane) | 9.99E-31 | 0.189058 | 5.39E-16 | 0.311156 | 3.40E-02 | | | |
| Comp Mole Frac (i-Pentane) | 4.51E-23 | 8.07E-02 | 1.54E-03 | 0.131787 | 1.70E-02 | | | |

| Name | S-318 | S-319 | S-320 | S-321 | S-308 | ** New ** |
|---|---|---|---|---|---|---|
| Comp Mole Frac (n-Pentane) | 0 | 0 | 0 | 0 | 0 | |
| Comp Mole Frac (n-Butane) | 1.83E-15 | 8.13E-02 | 0.207276 | 1.17E-07 | 1.83E-02 | |
| Comp Mole Frac (1245-M-BZ) | 9.99E-31 | 1.69E-02 | 1.03E-30 | 2.79E-02 | 0 | |
| Comp Mole Frac (Toluene) | 1.00E-30 | 1.58E-02 | 2.36E-26 | 2.60E-02 | 0 | |
| Comp Mole Frac (Naphthalene) | 9.99E-31 | 8.13E-03 | 1.03E-30 | 1.34E-02 | 0 | |
| Comp Mole Frac (p-Xylene) | 1.00E-30 | 4.39E-02 | 1.00E-30 | 7.22E-02 | 0 | |
| Comp Mole Frac (1,4-Pentadiyne*) | 9.59E-101 | 9.59E-101 | 9.59E-101 | 9.59E-101 | 5.68E-03 | |
| Comp Mole Frac (Benzene) | 9.98E-31 | 1.78E-02 | 8.99E-18 | 2.93E-02 | 1.13E-02 | |
| Comp Mole Frac (Propane) | 2.40E-04 | 2.05E-03 | 5.21E-03 | 1.52E-20 | 4.63E-04 | |
| Comp Mole Frac (i-Butane) | 0 | 0 | 0 | 0 | 0 | |
| Comp Mole Frac (Biacetylene) | 3.39E-19 | 2.03E-03 | 5.18E-03 | 7.95E-08 | 6.09E-03 | |